Chem Soc Rev

Enantiotopic Discrimination in the NMR Spectrum of Prochiral Solutes in Chiral Liquid Crystals

Journal:	*Chemical Society Reviews*
Manuscript ID:	CS-REV-07-2014-000260
Article Type:	Review Article
Date Submitted by the Author:	29-Jul-2014
Complete List of Authors:	Lesot, Phillippe; Universite Paris Sud (Paris XI), LRMN, ICMMO, UMR 8182 Aroulanda, Christie; Universite Paris Sud (Paris XI), LRMN, ICMMO, UMR 8182 Zimmermann, Herbert; Abteilung Biophysik, Max-Planck-Institut für Medizinische Forschung, Luz, Zeev; Weizmann Institute of Science, Department of Chemical Physics

Enantiotopic Discrimination in the NMR Spectrum of Prochiral Solutes in Chiral Liquid Crystals

Philippe Lesot*[,a], Christie Aroulanda[a], Herbert Zimmermann[b] and Zeev Luz[c]

[a] Laboratoire de RMN en Milieu Orienté CNRS UMR 8182, ICMMO, Bât. 410, Université de Paris-Sud, 91405 Orsay cedex, France.

[b]Abteilung Biophysik, Max-Planck-Institut für Medizinische Forschung, Jahnstrasse 29, 69120 Heidelberg, Germany.

[c] Weizmann Institute of Science, Department of Chemical Physics, Rehovot 76100, Israel.

Corresponding author: Philippe Lesot: philippe.lesot@u-psud.fr

Keywords: Prochirality,
Enantiotopic sites,
NMR,
Chiral Liquid Crystals,
Dynamics.

Type of article: (comprehensive) review

Abstract

The splitting of signals in the NMR spectra originating from enantiotopic sites in prochiral molecules when dissolved in chiral solvents is referred to as spectral enantiotopic discrimination. The phenomenon is particularly noticeable in chiral liquid crystals (CLC) due to the combined effect of the anisotropic magnetic interactions and the ordering of the solute in the mesophase. The enantiorecognition mechanisms are different for rigid and flexible solutes. For the former, discrimination results from symmetry breaking and is restricted to solutes whose point groups belong to one of the following four ("allowed") symmetries, C_s, C_{2v}, D_{2d} and S_4. The nature of the symmetry breaking for each one of these groups is discussed and experimental examples, using mainly ^{2}H 1D/2D-NMR in chiral polypeptide lyotropic mesophases are presented and analyzed.

When flexible optically active solutes undergo fast (on the NMR timescale) racemization their spectrum corresponds to that of an average prochiral molecule and may exhibit enantiotopic sites. In CLC, such sites will become discriminated, irrespective of their average (improper) symmetry. This enantiodiscrimination results mainly from the different ordering of the interchanging enantiomers. Several examples of such flexible molecules, including solutes with average axial and planar symmetries are commented.

Dynamic processes in solution that are not accompanied by modulation of magnetic interactions remain "NMR blind". This is sometimes the case for interconversion of enantiomers (racemization) or exchange of enantiotopic sites in isotropic solvents. The limitation can be lifted by using CLC. In such solvents, non-equivalence between enantiomers or between enantiotopic sites is induced by the chiral environment, thus providing the necessary interactions to be modulated by the dynamic processes. Illustrative examples involving exchange of both, enantiotopic sites and enantiomers are examined.

In this comprehensive review, various important aspects of enantiodiscrimination by NMR are presented. Thus the possibility to reveal enantiotopic recognition using residual dipolar couplings or to determine the absolute configuration of enantiotopic NMR signals are discussed. The various kinds of chiral mesophases able to reveal enantiotopic discrimination in guest prochiral molecules are also described and compared each other. Finally to illustrate the high analytical potentialities of NMR in CLC, several analytical applications involving the enantiodiscrimination phenomenon are described. A strategy for assigning the NMR signals of meso compound in a meso/threo mixture of cyclic molecules is first discussed. This is followed by a description of advantages of the method for the determination of (D/H) natural isotopic fractionation in biocompounds.

INDEX

1. Introduction

NMR spectroscopy proved to be a powerful tool in the study of chiral and prochiral compounds.[1,2] A major tool in these studies involves the spectral splitting observed when such compounds are dissolved in chiral solvents.[1,2,3] We refer to this splitting effect as chiral discrimination or enantiodiscrimination. Two types of spectral enantiodifferentiation can be distinguished. The first, referred to as enantiomeric discrimination, concerns the splitting of the NMR spectrum of racemates or other mixtures of optically active isomers, into subspectra corresponding to the two enantiomeric constituents.[2,3] The second type, referred to as enantiotopic discrimination, corresponds to spectral doubling resulting from the lifting of degeneracy of enantiotopic sites in prochiral molecules when dissolved in chiral solvents. In the term enantiotopic sites, we include atoms and group of atoms, as well as internuclear bonds and molecular faces that are related (only) by symmetry elements of the second kind (i.e. reflection planes and improper rotation axes).[2]

Enantiomeric discrimination using proton NMR in isotropic chiral solvents was first observed by Pirkle et al in the 1960's and was used by them to determine enantiomeric excess in mixtures of optically active isomers (see **Figure 1a**).[4] This approach and related methods based on the same concept were since extended to a variety of chiral compounds having polar groups and applied for the investigation of asymmetric synthesis employing a multitude of other magnetic nuclei as ^{13}C or ^{31}P. Numerous key articles[5,6,7,8,9] or well-documented reviews[10,11,12,13,14,15,16] on the subject can be found in the literature, [5,6,7,8,9,10,11,12,13,14,15,16], but periodically new enantiodiscriminating isotropic chiral solvents[17,18,19] or new original strategies[20] are still being proposed. Despite the obvious advantages of this application, its extent is quite limited. In particular, for majority of systems, it is restricted to solutes possessing a functional group (such as NH, OH, COOH or C=C) that can form with the auxiliary chiral compound distinguishable diastereomeric adducts. This method generally fails when applying to chiral guests lacking reactive

groups, such as chiral hydrocarbons or system of "weak" chirality, namely compounds which are chiral by virtue of the $^{1}H/^{2}H$ isotopic substitution. Other approaches, based, for example, on the use of chiral torus-shaped macromolecules such as α,β,γ-cyclodextrins (abbreviated α,β,γ-CD's) or chemically modified homologues have been proposed.[11] The enantioselective recognition within CD's originates from their ability to accommodate differently apolar enantiomers into the apolar cavities by virtue of hydrophobic attractive interactions, and then to produce short-lived diastereomeric solvates having anisochronous NMR resonances through differential shielding effects.

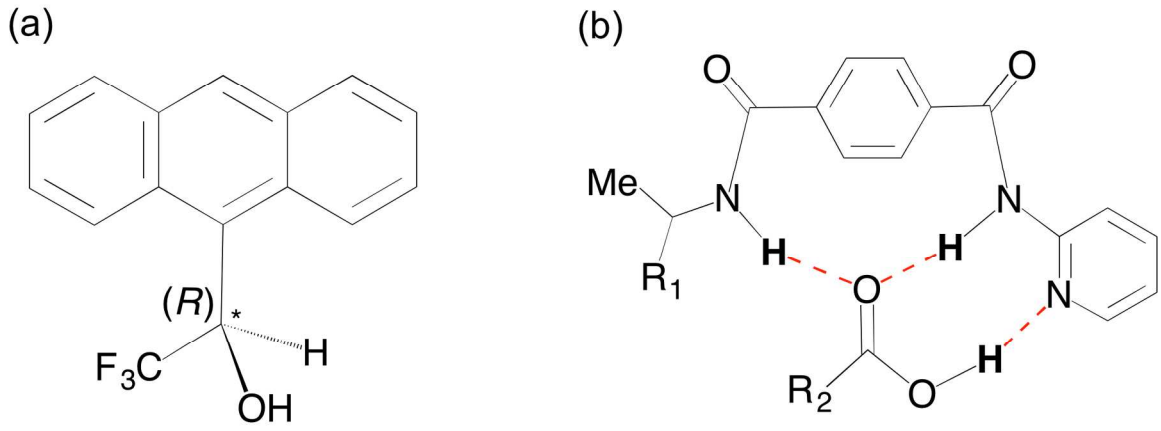

Fig. 1. Two examples of chiral solvating agent: (a) Proposed by Pirkle in 1977; (b) used to discriminate enantiotopic protons in prochiral carboxylic acid. Hydrogen bonds are shown in red. Adapted from refs. **4** and **23**.

In another domain, the NMR methodology using chiral isotropic solvents rarely succeeded in resolving signals of enantiotopic sites in prochiral solutes. The absence of (or, when observed, the very small) spectral enantiodiscrimination in such solvents reflects the generally weak (or rather the non-selective), solute-solvent interactions in these systems. To be resolved, the magnetic interactions (*i.e.* the isotropic chemical shift (cs) and the scalar spin-spin (J) coupling) in the two enantiotopic sites must be significantly different. Solute-solvent interactions are usually not sufficiently chiral selective to induce such dissimilarity. The chemical shift selectivity can, of course, be enhanced by

employing high magnetic NMR fields, or alternatively, using special chiral adducts, such as paramagnetic lanthanide shift reagents,[5,67] organometallic platinum,[14] or dirhodium complexes.[8,9] These methods are sometimes useful for discriminating enantiomers, but only rarely suitable for discriminating enantiotopic sites. A notable exception is the use of cryptand-type compounds (crown molecules) designed to accommodate certain classes of prochiral guest molecules.[21] However, again the approaches proposed so far remain quite specific.[21,22,23,24] One illustrative example is given in **Figure 1b**.

These limitations are largely removed when instead of isotropic solvents, chiral nematic liquid crystals are used.[25] In such solvents, the anisotropic magnetic interactions which average out to zero in isotropic environment are partially retained and expressed in the NMR spectra of the solutes.[25,26,27,28] The residual anisotropic observables include the chemical shift anisotropy ($\Delta\sigma_i$), the anisotropic indirect scalar (through bonds) (ΔJ_{ij}) and direct dipolar (D_{ij}) spin-spin coupling (through space) between pairs of magnetic nuclei and, for nuclei with spins $I \geq 1$, also the quadrupolar interaction ($\Delta\nu_{Qi}$).[26,28] These interactions can provide additional discrimination mechanisms that often dominate the effect. It is referred to in this review, as "discrimination by ordering".

The first experimental demonstration of this effect was reported by Sackmann, Meiboom and Snyder[25] in 1968 on a solution of racemic trichloroepoxypropane dissolved in a compensated mixture of thermotropic cholesteric liquid crystals, consisting of cholesteryl chloride and cholesteryl myristate. By compensated mixture is meant a mixture in which the cholesteric twist is cancelled, resulting in an (optically active) nematic, that allows high resolution NMR of the solutes to be observed. The method was subsequently repeated using similar solvents.[29,30] Such thermotropic chiral solvents are, however, quite viscous; the temperature range over which pitch cancellation occurs is narrow and their solubility power rather low. This last characteristic greatly limits the range of solutes that can be studied in such solvents.

Considerably more suitable ordered solvents are lyotropic liquid crystals consisting of a chiral mesogen dissolved in a suitable organic solvent. Examples of such lyo-mesogens include, *e.g.* homopolypeptides,[31,32,33] polysaccharides,[34,35,36] polyacethylenes,[37,38] polyguanidines[39] or polynucleotides.[40,41]

In the case of homopolypeptide polymer in solution, the mesogens form helical structures and the systems are weakly cholesteric. However, under the effect of strong enough magnetic field, B_0, of the NMR spectrometer, they undergo pitch unwinding to give well-aligned chiral nematic solvents with the director parallel to B_0.[31] Their viscosity and solubility power can be optimized by selecting suitable co-solvents and the strength of their chiral discrimination can to some extent be adjusted by the choice of the lyo-mesogen (type and concentration) and co-solvent polarity.[42] Although their ordering power on solutes is generally low, the relatively large anisotropic interactions result in overall large effect on the spectrum and in turn on the chiral discrimination.

The lyo-mesophases used for almost all studies involving enantiotopic discrimination (and discussed here) consist of solutions of poly-γ-benzyl-*L*-glutamate (PBLG) or poly-ε-carbobenzyloxy-*L*-lysine (PCBLL) in a variety of organic helicogenic solvents,[42,43,44], but oriented mixtures of those both homopolypeptides can be used as well (see also **Section 10**).[45] For simplicity, we refer to such lyotropic chiral solvents as chiral liquid crystals (CLC).

For analytical purposes or spectral comparisons, the NMR spectra of the same solutes are often also measured in corresponding achiral liquid crystals (ALC), where spectral enantiodiscriminations is absent.[46] Such solvents are prepared from the corresponding racemic mesogen (same total concentration). For example, the "corresponding" achiral "PBG" is prepared from an equimolar mixture of PBLG and its enantiomer PBDG (poly-γ-benzyl-*D*-glutamate) dissolved in the same co-solvent.[46]

The discrimination by the ordering mechanisms in CLC (and in all chiral oriented solvents) differs for enantiomeric mixtures (chiral solutes)[47,48,49] and for enantiotopic sites (prochiral solutes).[50,51,52] In both cases it appears that the effect of the chiral solvent on the geometry or the magnetic parameters of the solute is negligible, and consequently that the main effect arises *via* the ordering tensor, which is sensitive to the weak solute - (chiral) solvent interaction. In ALC the ordering of corresponding *R*- and *S*-enantiomers is identical, hence no discrimination occurs, while in CLC the ordering of such enantiomers is different leading to spectral discrimination. The origin of enantiotopic discrimination by ordering is different; in ALC the ordering of enantiotopic elements is identical due to their intrinsic (improper) symmetry, while the symmetry breaking effect of the CLC solvent may (or may not) render them dissimilar.[50,52] This type of discrimination is not general and applies to only special solute symmetries.[53] As it turns out, of the essentially infinite improper point groups only very few, referred to as the allowed groups, will exhibit enantiotopic discrimination in prochiral solutes.

In the present review, the background theory of enantiotopic-discrimination by ordering in CLC is discussed. We classify the rigid prochiral solutes according to their improper point group symmetry with emphasis on those groups that may show enantiotopic discrimination. The analysis of the NMR spectra of such molecules in CLC is described and the procedure demonstrated using illustrative examples.

Flexible chiral molecules undergoing fast (on the NMR timescale) conformational interconversion, exhibit NMR spectra, corresponding to some “average” molecular geometry. Their chiral properties depend on the nature of the dynamic processes. In a separate section of the review we analyze these effects and present examples for different types of reactions. In subsequent sections, the problem of the absolute assignment of the enantiotopic element is discussed and various analytical applications based on NMR discrimination in CLC are described. But first we start with a brief introduction to the

basic equations related to NMR in LC's, followed by the theory of enantiomeric and enantiotopic discrimination in CLC.

2. The spin Hamiltonian in nematic liquid crystals

Consider a nematic liquid crystals with positive anisotropic magnetic susceptibility ($\Delta\chi$), so that at equilibrium the director aligns parallel to the external magnetic field, B_0.[26] For liquid crystals consisting of helical homopolypeptides, $\Delta\chi$ is negative, but the unwinding effect of B_0 resultss in a nematic phase with positive $\Delta\chi$. The NMR spectra of solutes under these conditions are similar to those exhibited by isolated molecules in single crystals. They can be analyzed in terms of the following sum of spin interactions terms,[26]

$$\mathcal{H} = \sum_i \mathcal{H}_i^Z + \sum_i \mathcal{H}_i^{CS} + \sum_{i<j} \mathcal{H}_{i,j}^J + \sum_{i<j} \mathcal{H}_{i,j}^D + \sum_i \mathcal{H}_i^Q \qquad \textbf{(1)}$$

where the subscripts refer respectively to nuclei, i, or pairs of interacting nuclei, i, j, and the superscript to the nature of the interaction. Each of these interactions may consist of an isotropic and/or anisotropic terms and can be written as a dyadic of the form,[54]

$$\begin{aligned}\mathcal{H}^{\mathrm{k}} &= A^{\mathrm{k}} \cdot \left(l^{\mathrm{k}}\mathbf{1} + T^{\mathrm{k}}\right) \cdot B^{\mathrm{k}} =\cdot\, l^{\mathrm{k}} A^{\mathrm{k}} \cdot B^{\mathrm{k}} + A^{\mathrm{k}} \cdot T^{\mathrm{k}} \cdot B^{\mathrm{k}} \\ &= \mathcal{H}^{\mathrm{k}}(iso) + \mathcal{H}^{\mathrm{k}}(aniso)\end{aligned} \qquad \textbf{(2)}$$

where, for convenience we suppressed the nuclear indices. The labeling iso and aniso in this equation, refer to the isotropic and anisotropic parts of the Hamiltonian, the A^{k}'s and B^{k}'s are (row and column) vector operators, the l^{k}'s are isotropic (scalar) interactions and the T^{k}'s are corresponding anisotropic (second rank tensor) interaction.[26,24,28,54] The various H^{k} and their corresponding components in **Eq. 2** are defined in **Table 1**.

Table 1 (to insert here)

In the high-field approximation, namely when the Zeeman energy is much larger than the other interactions in **Eq. 1**, which always applies in the experiments described here, only the elements T^{k}_{ZZ} ($Z \| B_0$) of the anisotropic tensors affects the spectrum. They are related to the components $T^{k}_{\alpha\beta}$ in a molecule fixed axis system, α,β = a,b,c as follows,

$$T^{k}_{ZZ} = \sum_{\alpha,\beta=a,b,c} cos\,\theta^{\alpha}_{Z}\, cos\,\theta^{\beta}_{Z}\, T^{k}_{\alpha\beta} \quad \textbf{(3)}$$

where θ^{α}_{Z} is the angle between the molecular fixed axis α and B_0.

In the liquid crystalline solutions rapid (anisotropic) tumbling of the solute molecules averages the angular dependent terms in **Eq. 3** to yield the observable average anisotropic interactions,

$$\langle T^{k}_{ZZ}\rangle = \Delta T^{k} = \frac{2}{3} tr\left(S.T^{k}\right) = \sum_{\alpha,\beta=a,b,c} \frac{2}{3} S_{\alpha\beta} T^{k}_{\alpha\beta} \quad \textbf{(4)}$$

where,

$$S_{\alpha\beta} = \frac{1}{2}\langle 3cos\,\theta^{\alpha}_{Z}\, cos\,\theta^{\beta}_{Z} - \delta_{\alpha\beta}\rangle \quad \textbf{(5)}$$

are the elements of the Saupe ordering matrix, S, and $< \cdots >$ denotes ensemble or time averaging. Using the fact that both the T^{k}'s and S are real, symmetric and traceless, **Eq. 4** can be rearranged into the following form,

$$\Delta T^{k} = T^{k}_{aa} S_{aa} + \frac{1}{3}\left(T^{k}_{bb} - T^{k}_{cc}\right)\left(S_{bb} - S_{cc}\right) + \frac{4}{3}\left(T^{k}_{ab} S_{ab} + T^{k}_{ac} S_{ac} + T^{k}_{bc} S_{bc}\right) \quad \textbf{(6)}$$

If the principal values, T^{k}_{vv}, of the ΔT^{k} tensors and their respective principal directions, v = x, y, z, are known in a common molecular frame, α, β = a, b, c, then the elements $T^{k}_{\alpha\beta}$ can be calculated using an equation similar to **Eq. 3**,

$$T^{\mathrm{k}}_{\alpha\beta} = \sum_{\mathrm{v}=x,y,z} \cos\theta^{\alpha}_{\mathrm{v}} \cos\theta^{\beta}_{\mathrm{v}} T^{\mathrm{k}}_{\mathrm{vv}} \quad \textbf{(7)}$$

When the interaction is axially symmetric, as is the case for the dipolar interaction and often for the deuteron quadrupolar coupling in C-D bonds, $T^{\mathrm{k}}_{\mathrm{xx}} = T^{\mathrm{k}}_{yy} = -\frac{1}{2} T^{\mathrm{k}}_{zz}$. **Eq. 7** reduces to:

$$T^{\mathrm{k}}_{\alpha\beta} = \frac{1}{2}\left(3\cos\theta^{\alpha}_{Z}\cos\theta^{\beta}_{Z} - \delta_{\alpha\beta}\right) T^{\mathrm{k}}_{zz} \quad \textbf{(8)}$$

Otherwise, when T^{k} is biaxial, one usually defines an asymmetry parameter,

$$\eta = \frac{T^{\mathrm{k}}_{xx} - T^{\mathrm{k}}_{yy}}{T^{\mathrm{k}}_{zz}} \quad \textbf{(9)}$$

so that,

$$T^{\mathrm{k}}_{xx} = -\tfrac{1}{2} T^{\mathrm{k}}_{zz}(1-\eta) \text{ and } T^{\mathrm{k}}_{yy} = -\tfrac{1}{2} T^{\mathrm{k}}_{zz}(1+\eta) \quad \textbf{(10)}$$

The $T^{\mathrm{k}}_{\alpha\beta}$'s can then be computed from T^{k}_{zz} and η, using **Eqs. 7** and **9**. Expressions for T^{k}_{zz} for the various anisotropic tensors are included in **Table 1**.

Finally, using the definitions in **Table 1**, applying the high field approximations and transforming to the rotating frame (*i.e.* suppressing the Zeeman term), yields the equations for the various H^{k} interactions, as summarized in **Table 2**. These equations can readily be used to analyze experimental spectra of solutes in liquid crystalline solutions, and in turn (provided sufficient observables are measured) derive the elements of the Saupe ordering matrix. In the analysis the $T^{\mathrm{k}}_{\alpha\beta}$'s are calculated from the known (or computed) molecular geometry and the relevant interaction constants given in **Table 2**.

Table 2 (to insert here)

The five order parameters in **Eq. 6** can be understood in terms of three Euler angles relating an arbitrary coordinate system to the molecular fixed frame, (a, b, c), and two that measure the ordering of the molecular axes. In molecules possessing only the identity or

inversion symmetry (*resp.* C_1 and C_i point groups) these five order parameters are independent and at least five independent ΔT^k's need be measured for their determination. At the other end of the symmetry scale, cubic molecules do not align in nematic solvent ($S = 0$) and therefore do not exhibit discrimination by ordering.[55] For molecules with intermediate symmetry, the number of independent parameter can be reduced to, one, two, or three, by choosing the molecular axes according to the symmetry elements of the molecular point group. This effect is discussed in some more detail below.

3. Enantio-discrimination by ordering in chiral nematic solvents

As discussed in the introduction, chiral discrimination by ordering in CLC is brought about solely *via* the order parameters $S_{\alpha\beta}$; the molecular geometry and the magnetic interactions are assumed to be solvent independent, or at least chiral non selective.[53] This is so because, except for very specific cases, the solvent-solute interactions are too weak to affect the geometrical or electronic structure of the solute that would modify the l^k or T^k terms in the Hamiltonian. On the other hand, these interactions are clearly of the order of the forces that orient the molecules in liquid crystals. They are shape dependent and therefore chiral selective in CLC. The chiral discrimination by orientational ordering depends therefore only on the anisotropic, T^k, interactions. To observe the discrimination the ΔT^k's of at least one pair of equivalent sites in the enantiomers or of enantiotopic sites in prochiral solutes needs to be sufficiently dissimilar. The mechanism of the enantio-discrimination is, however, different for chiral and prochiral compounds and for the latter depends delicately on their symmetry.[53,54]

3.1 Principles of enantiomeric discrimination

Chiral compounds belong to one of the proper symmetry groups, namely point groups possessing only proper rotations. Excluding cubic compounds, they include the point

groups, C_n and D_n. Such compounds exhibit optical isomerism with pairs of enantiomers, (*R* and *S*) related to each other by reflection. Enantiomers thus have identical point group symmetry, but opposite chirality. While in ALC they exhibit identical ordering, $S^R = S^S$, in CLC, in general $S^R \neq S^S$, leading (see **Eq. 6**) to $\Delta T^{kR} \neq \Delta T^{kS}$ and consequently to enantiomeric discrimination,

$$\Delta T^{kR} = T^k_{aa}S^R_{aa} + \frac{1}{3}\left(T^k_{bb} - T^k_{cc}\right)\left(S^R_{bb} - S^R_{cc}\right) + \frac{4}{3}\left(T^k_{ab}S^R_{ab} + T^k_{ac}S^R_{ac} + T^k_{bc}S^R_{bc}\right) \quad \textbf{(11)}$$

and

$$\Delta T^{kS} = T^k_{aa}S^S_{aa} + \frac{1}{3}\left(T^k_{bb} - T^k_{cc}\right)\left(S^S_{bb} - S^S_{cc}\right) + \frac{4}{3}\left(T^k_{ab}S^S_{ab} + T^k_{ac}S^S_{ac} + T^k_{bc}S^S_{bc}\right) \quad \textbf{(12)}$$

As indicated above these expressions can be simplified for molecules possessing symmetry higher than C_1. Thus for molecules with C_2 symmetry, taking $C_2 \| a$, leads to $S_{ab} = S_{ac} = 0$, and only three independent order parameters remain to be determined.[53] For molecules with D_2 symmetry, taking a, b, c, to coincide with the three molecular C_2 axes renders all $S_{\alpha\beta}$ ($\alpha \neq \beta$) equal to 0, and hence only the two elements (S_{aa} and $S_{bb} - S_{cc}$) remain to be determined. All other proper groups (C_n, D_n, $n \geq 3$) possess a symmetry axis C_n ($n \geq 3$) and give rise to axial molecules, with S_{aa} as the only non-zero independent order parameter ($S_{bb} = S_{cc} = -\frac{1}{2}S_{aa}$). To analyze the spectra of chiral solutes and determine the ordering in CLC, one needs to identify their signals with the respective enantiomers and determine for each at least as many ΔT^k's as the number of independent $S_{\alpha\beta}$'s; five for C_1 molecules, three for C_2, two for D_2 and one for axial molecules. When more such interactions are available the order parameters are determined by best-fit procedures. For the special case of axial molecules the ratios of corresponding anisotropic splitting in the two enantiomers are independent of the nature of the magnetic interactions and depend only on the degree of their ordering,

$$\frac{\Delta T^{\mathrm{k}R}}{\Delta T^{\mathrm{k}S}} = \frac{T^{\mathrm{k}}_{aa} S^{R}_{aa}}{T^{\mathrm{k}}_{aa} S^{S}_{aa}} = \frac{S^{R}_{aa}}{S^{S}_{aa}} \qquad \textbf{(13)}$$

(independent of the interaction and the nuclei). Otherwise, there are no special symmetry considerations related to spectral splitting of enantiomers in CLC. We shall return to such symmetries when discussing flexible chiral molecules that are prochiral, on the average.

3.2 Principles of enantiotopic discrimination

The main topic of this review concerns enantiotopic discrimination in rigid and flexible prochiral molecules. Such molecules belong to improper point groups, namely groups that possess symmetry operations of the second kind (reflections and improper rotations). They are not chiral and do not exhibit enantiomeric isomerism. On the other hand, they may possess enantiotopic elements, namely atoms, groups of atoms, internuclear directions, molecular faces, that are solely related by reflection or improper rotations.[1,2] When such an element is replaced by a different group the molecule (having prostereogenic centers) becomes chiral, hence the term prochiral and the assignment of the enantiotopic elements (atoms or groups of atoms) as pro-*R* and pro-*S*.[1] For prochiral molecules having prostereogenic faces (see **Figure 9** in **Section 4.3.1**), the assignment of enantiotopic elements is usually denoted *Re* or *Si* according to the face they are belonging to.[1] For sake of simplicity, we will use the shorter notations, *r* and *s* in this review.

In achiral solvents enantiotopic sites are equivalent and in the NMR spectrum they exhibit identical magnetic interactions. However, when prochiral molecules are dissolved in chiral solvents their improper symmetry elements are quenched by the lower symmetry of the environment. Consequently their effective symmetry is reduced to that of the corresponding largest proper subgroup and at least in principle, enantiotopic pairs become dissimilar and should exhibit different NMR interactions. We refer to this effect as enantiotopic discrimination. This behavior should be contrasted with that of homotopic elements, namely elements that are related by symmetry operations of the first kind

(proper rotations). Such pairs remain equivalent in chiral solvents, and do not exhibit spectral discrimination.

As discussed in the **Introduction**, the solute–solvent interactions in isotropic solvents are in general not sufficient to enantio-selectively modify the geometrical and/or magnetic parameters of prochiral solute molecules to induce observable spectral discrimination between enantiotopic sites. A considerably more effective discrimination may be expected from the ordering mechanism in CLC. The reduction in symmetry of the ordering tensor in such solvents may result in different ordering of the enantiotopic sites, and hence in spectral discrimnation.[53]

For this to occur, the reduction in symmetry must be such that the restriction imposed on the orientation (or equivalence) of the principal axes of the Saupe ordering matrix in the ALC are relaxed when dissolved in CLC. Formally this effect manifests itself as an increase in the number of independent $S_{\alpha\beta}$ parameters on going from the improper group (applicable in ALC) to its corresponding proper subgroup (applicable in CLC). When the number of independent $S_{\alpha\beta}$ is the same for both solvents, no discrimination by ordering in CLC can be expected. It turns out that such a reduction in symmetry is limited to a small number of improper groups. In fact, only four groups fulfill this requirement. We refer to them, namely the symmetry groups in which enantiotopic discrimination by ordering in CLC is possible, as the "allowed groups". All other (non-cubic) improper groups are referred to as "forbidden" groups. Prochiral molecules with such symmetries will not exhibit enantiotopic discrimination by ordering.[54]

To obtain the list of allowed groups and derive expressions for enantiodiscrimination by ordering for these groups we use the entries in **Table 3**.[56] This table includes the relevant properties of the S and T^{k} tensors for all the non-cubic improper groups. In labeling the axes for these tensors, the following hierarchy was adopted: (i) if only one axis is defined by the molecular symmetry it is labeled a, if all three axes are defined, a is the main principal axis; (ii) if only a reflection plane is defined by the molecular symmetry

it is labeled the bc plane. In the table, under the row of the group's names, are indicated the number and identity of the independent ($\neq 0$) elements of the *Saupe* matrix in the group. We refer to this matrix as symmetric, $S^{ALC} = S(\text{sym})$, since it can be projected out from a general S matrix by the completely symmetric representation of the group (all characters being +1). In the next two lines of the table are indicated the names of the corresponding proper subgroups and number of independent elements associated with their S matrices (S^{CLC}).

Table 3 (to insert here)

The "forbidden" and "allowed" groups can now readily be determined by comparing these entries with those of $S(\text{sym})$ given in an upper row. Clearly the five families of axial molecules are forbidden since they possess a unique C_n ($n \geq 3$) axis leading to a single independent order parameter (S_{aa}) in both ALC and CLC. Likewise the three improper groups, C_i, C_{2h} and D_{2h} contain the same number of independent $S_{\alpha\beta}$ as their respective subgroups, C_1, C_2 and D_2 ($S^{ALC} = S^{CLC}$). Note that the latter improper groups contain an inversion operation that is independent of the coordinate system used. Such an improper element therefore does not modify the principal coordinate system on going from ALC to CLC. We are left with the four improper groups, C_s, C_{2v}, D_{2d} and S_4, for which the number of independent $S_{\alpha\beta}$ exceeds those in the corresponding proper groups. These four groups thus comprise the list of the allowed groups that may exhibit enantiotopic discrimination.[53,54] In the next line of **Table 3** are listed the extra $S_{\alpha\beta}$ that appear in the proper group and are missing in the improper one. We refer to this part of the S matrix as antisymmetric, $S(\text{anti})$, since it can be projected out from a general S matrix by the antisymmetric representation of the group (characters of the proper and improper operations being +1 and -1, respectively). Thus $S(\text{anti}) = S^{CLC} - S^{ALC}$. The changes in the principal axes systems (PAS) that take place on going from ALC (PAS^{ALC}) to CLC

(PAS^{CLC}) are presented in **Figure 2**. For the lowering of symmetry $C_s \rightarrow C_1$ two additional order parameters need be determined. They correspond to the angles β and γ, as α is already defined by fixing the PAS^{ALC}. For $C_{2v} \rightarrow C_2$ only one additional order parameter, corresponding to the angle α need be defined since the axis a $\| C_2$ remains fixed. For $D_{2d} \rightarrow D_2$ the loss of the σ_d planes in CLC renders the axes b and c nonequivalent ($S_{bb} - S_{cc} \neq 0$), but their orientation remains fixed. Finally, for $S_4 \rightarrow C_2$, the equivalence of the b and c axes is lost and their orientation is changed.

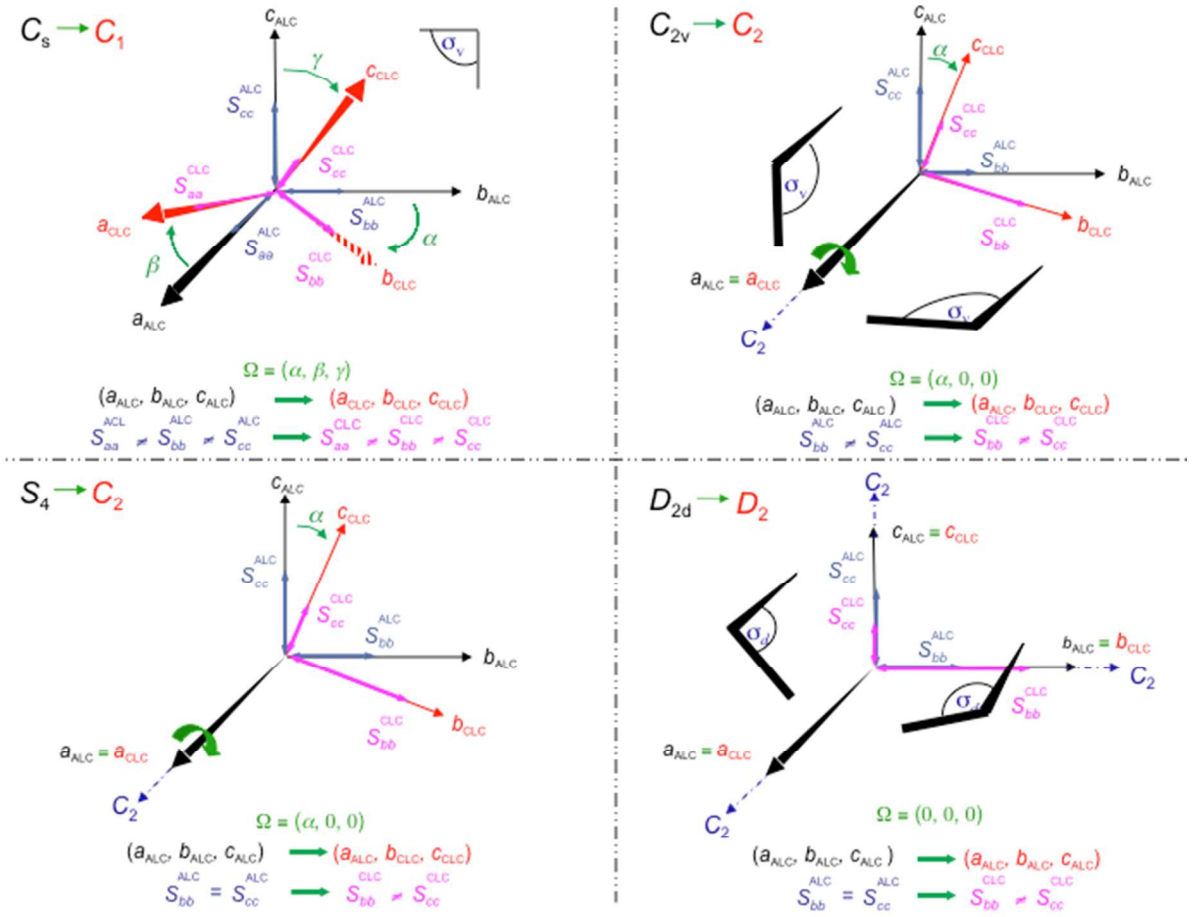

Fig. 2. Changes expected in the orientation and equivalence of the principal axes system (PAS) of the Saupe ordering tensor in the four allowed groups, on going from ACL to CLC. All panels follow the same color code. The variation of the length of the double arrows simulates the change in the magnitude of the $S_{\alpha\beta}$. Note that in the C_s group, the angle α is dependent on the angles β and γ.

To derive expressions for the enantiotopic discrimination it is convenient to partition the T^k matrices into their symmetric, T^k(sym), and antisymmetric, T^k(anti), parts, with indices $\alpha\beta$ defined as in the corresponding S(sym) and S(anti) matrices. The rest of the elements are irrelevant residue, T^k(res), which transform as other (than the sym and anti) representations of the group. Hence,

$$T^k = T^k(\text{sym}) + T^k(\text{anti}) + T^k(\text{res}) \quad \textbf{(14)}$$

Since there are no corresponding S(res) elements in S [S(res) = 0] and since in ALC S(anti) = 0, **Eq. 6** for the average anisotropic interaction, ΔT^{ki}, of a general site i in a solute dissolved in ALC becomes,

$$\Delta T^{ki}(ALC) = \frac{2}{3}\sum_{\alpha,\beta=a,b,c} S_{\alpha\beta}(\text{sym}) T^{ki}_{\alpha\beta}(\text{sym}) \quad \textbf{(15)}$$

while for the same solute in CLC, where S(anti) ≠ 0,

$$\Delta T^{ki}(\text{CLC}) = \frac{2}{3}\sum_{\alpha,\beta=a,b,c} S_{\alpha\beta}(\text{sym})\, T^{ki}_{\alpha\beta}(\text{sym}) + \frac{2}{3}\sum_{\alpha,\beta=a,b,c} S_{\alpha\beta}(\text{anti})\, T^{ki}_{\alpha\beta}(\text{anti}) \quad \textbf{(16)}$$

We note that by construction the elements $T^{ki}_{\alpha\beta}$(sym) of enantiotopic pairs, r, s, are equal, while those for $T^{ki}_{\alpha\beta}$(anti) are of opposite signs (see **Table 3**),

$$T^{kr}_{\alpha\beta}(\text{sym}) = T^{ks}_{\alpha\beta}(\text{sym}) \text{ and } T^{kr}_{\alpha\beta}(\text{anti}) = -T^{ks}_{\alpha\beta}(\text{anti}) \quad \textbf{(17)}$$

Hence for enantiotopic pair in ALC,

$$\Delta T^{kr}(\text{ALC}) = \Delta T^{ks}(\text{ALC}) = \Delta T^{ke}(\text{ALC}) = \frac{2}{3}\sum_{\alpha,\beta=a,b,c} S_{\alpha\beta}(\text{sym})\, T^{ke}_{\alpha\beta}(\text{sym}) \quad \textbf{(18)}$$

while we have in CLC:

$$\Delta T^{\mathrm{kr}}(\mathrm{CLC}) = \frac{2}{3}\sum_{\alpha,\beta=a,b,c} S_{\alpha\beta}(\mathrm{sym})\, T^{\mathrm{ke}}_{\alpha\beta}(\mathrm{sym}) + \frac{2}{3}\sum_{\alpha,\beta=a,b,c} S_{\alpha\beta}(\mathrm{anti})\, T^{\mathrm{ke}}_{\alpha\beta}(\mathrm{anti}) \quad \textbf{(19)}$$

$$T^{\mathrm{kr}}(\mathrm{CLC}) = \frac{2}{3}\sum_{\alpha,\beta=a,b,c} S_{\alpha\beta}(\mathrm{sym})\, T^{\mathrm{ke}}_{\alpha\beta}(\mathrm{sym}) - \frac{2}{3}\sum_{\alpha,\beta=a,b,c} S_{\alpha\beta}(\mathrm{anti})\, T^{\mathrm{ke}}_{\alpha\beta}(\mathrm{anti}) \quad \textbf{(20)}$$

As the indices of the enantiomers *r*, *s*, cannot be matched with the corresponding labels in the molecular formula, these indices can be we substituted on the right hand side (rhs) of the above equations by a neutral index, e, which could be either *r* or *s*. However, because of the different sign in front of the antisymmetric term, it should correspond to the same enantiotopic elements in both equations. Purely homotopic pairs, as well as diastereotopic sites, d, in prochiral compounds must lie on symmetry elements of the molecules. Their symmetric terms, $T^{\mathrm{kh}}_{\alpha\beta}$ (sym) are therefore pair wise equal, as for enantiotopic pairs, while their antisymmetric terms vanish. Consequently for such sites,

$$\Delta T^{\mathrm{kd}}(\mathrm{CLC}) = \Delta T^{\mathrm{kd}}(\mathrm{ALC}) = \frac{2}{3}\sum_{\alpha,\beta=a,b,c} S_{\alpha\beta}(\mathrm{sym})\, T^{\mathrm{kd}}_{\alpha\beta}(\mathrm{sym}) \quad \textbf{(21)}$$

The properties of the T^{k}(anti) tensors for enantiotopic and homotopic pairs in prochiral molecules are summarized in the last two lines in **Table 3**.

Analysis of the enantiotopic discrimination in terms of the solute ordering is best performed by factorizing **Eqs. 19,20** into their symmetric and antisymmetric parts. Taking (half) the sum and difference of these equations yields,

$$\Delta T^{\mathrm{ke}}(\mathrm{sym}) = \frac{1}{2}\left[\Delta T^{\mathrm{kr}}(CLC) + \Delta T^{\mathrm{ks}}(CLC)\right] = \frac{2}{3}\sum_{\alpha,\beta=a,b,c} S_{\alpha\beta}(\mathrm{sym})\, T^{\mathrm{ke}}_{\alpha\beta}(\mathrm{sym}) \quad \textbf{(22)}$$

and

$$\Delta T^{\mathrm{ke}}(\mathrm{anti}) = \tfrac{1}{2}\left[\Delta T^{\mathrm{kr}}(CLC) - \Delta T^{\mathrm{ks}}(CLC)\right] = \tfrac{2}{3}\sum_{\alpha,\beta=a,b,c} S_{\alpha\beta}(\mathrm{anti})\, T^{\mathrm{ke}}_{\alpha\beta}(\mathrm{anti}) \quad \textbf{(23)}$$

where $\Delta T^{\mathrm{ke}}(\mathrm{sym})$ corresponds to the average interaction of the enantiotopic pair, while $\Delta T^{\mathrm{ke}}(\mathrm{anti})$ to the extent of their discrimination. This factorization of the equations simplifies considerably the analysis of the spectra of prochiral solutes in CLC. In fact, it renders the complexity of the analysis of such spectra similar to that in ALC.[54] Data from homotopic (diastereotopic) sites (**Eq. 21**) are combined with those of the average splitting, $T^{\mathrm{ke}}(\mathrm{sym})$, of enantiotopic sites (**Eq. 22**) to solve for the elements $S(\mathrm{sym})$, as in ALC. The elements of $S(\mathrm{anti})$ are then solved separately using the observed discrimination, $\Delta T^{\mathrm{ke}}(\mathrm{anti})$, in the spectra of enantiotopic sites (**Eq. 23**). For the analysis, there should be at least as many observables as elements in the corresponding sub-matrix. When more observables are measured, the order parameters, $S_{\alpha\beta}$, are solved by optimization methods.

A special point in the derivation of the elements of $S(\mathrm{anti})$ concerns their signs. As already mentioned, matching the labeling, *r*/*s*, in the experimental spectra with the corresponding, *r*/*s*, labels in the molecular formula (and hence in the T^{kr}, T^{ks}) is not feasable, as they could equally well be reversed. Consequently the sign of the $\Delta T^{\mathrm{ke}}(\mathrm{anti})$'s cannot be determined. This is reflected in the absolute signs in **Eq. 23**. When $S(\mathrm{anti})$ consists of a single element (as for C_{2v} and D_{2d} symmetries) its absolute value (but not its sign) can thus be obtained from measurements of a single, or more, enantiotopic sites. However, when $S(\mathrm{anti})$ contains two independent terms (as for C_s and S_4), even their magnitude cannot directly be determined. As shown in two examples below, it is nevertheless still possible to determine the magnitude and relative signs of the $S_{\alpha\beta}(\mathrm{anti})$'s by a best-fit procedure, if at least three independent $\Delta T^{\mathrm{ke}}(\mathrm{anti})$'s are available, or if suitable correlation experiments can be performed.[54]

To complete this section we schematically demonstrate in **Figure 3** the effects of spectral enantio-discriminations by ordering for a pair of enantiotopic elements (*r*/*s*) or

enantiomeric objects (*R*/*S*), for several types of anisotropic interactions: (i) the ^{13}C chemical shift anisotropy, $\Delta\sigma_i$; (ii) the ^{13}C-^{1}H heteronuclear dipolar interaction, D_{ij}; (iii) the ^{2}H quadrupolar interaction, $\Delta\nu_{Qi}$.[28] The traces at the top correspond to isotropic (non chiral) solvents (absence of anisotropic interactions and of chiral discrimination). Those at the center correspond to ALC solvents (appearance of anisotropic interaction, but lack of chiral discrimination). Finally, at the bottom are displayed the spectra expected in CLC (exhibiting discrimination by ordering). Note here that the line positions, of an enantiotopic pair in ALC matches the average position ΔT^{ke}(sym) of the pair in CLC. This is consistent with the assumption that the $T_{\alpha\beta}^{ki}$'s are solvent independent, that the $S_{\alpha\beta}$(sym)'s are the same in the CLC and corresponding ALC and that the $S_{\alpha\beta}$(anti)'s vanish in the latter. Moreover, for a particular prochiral molecule dissolved in an enantiopure CLC, Dm or Lm, (here the polymer has a *D* or *L* absolute configuration), the $S_{\alpha\beta}$(anti)'s have opposite signs, namely $S_{\alpha\beta}$(anti)/Dm = -$S_{\alpha\beta}$(anti)/Lm).

In practice experiments are performed in lyotropic solutions consisting of a racemic lyomesophase [ALC = ½(Dm + Lm)] and in an identical solution (composition- and concentration-wise) except with an optically pure lyo-mesophase (Dm or Lm).[46] The equality, ΔT^{ke}(ALC) = ΔT^{ke}(sym), then applies if we can assume that $S_{\alpha\beta}$(anti) in a solvent mixture consisting of [pDm + (1 – p)Lm], is given (at least in the range p ~ ½) by,

$$\begin{aligned} S_{\alpha\beta}(\text{anti})/[\text{pDm} + (1-\text{p})\text{Lm}] &\approx \text{p}S_{\alpha\beta}(\text{anti})/\text{Dm} + (1-\text{p})S_{\alpha\beta}(\text{anti})/\text{Lm} \\ &= \text{p}S_{\alpha\beta}(\text{anti})/\text{Dm} - (1-\text{p})S_{\alpha\beta}(\text{anti})/\text{Dm} \\ &= (2\text{p}-1)S_{\alpha\beta}(\text{anti})/\text{Dm} \end{aligned} \qquad \textbf{(24)}$$

which vanishes for p = ½.

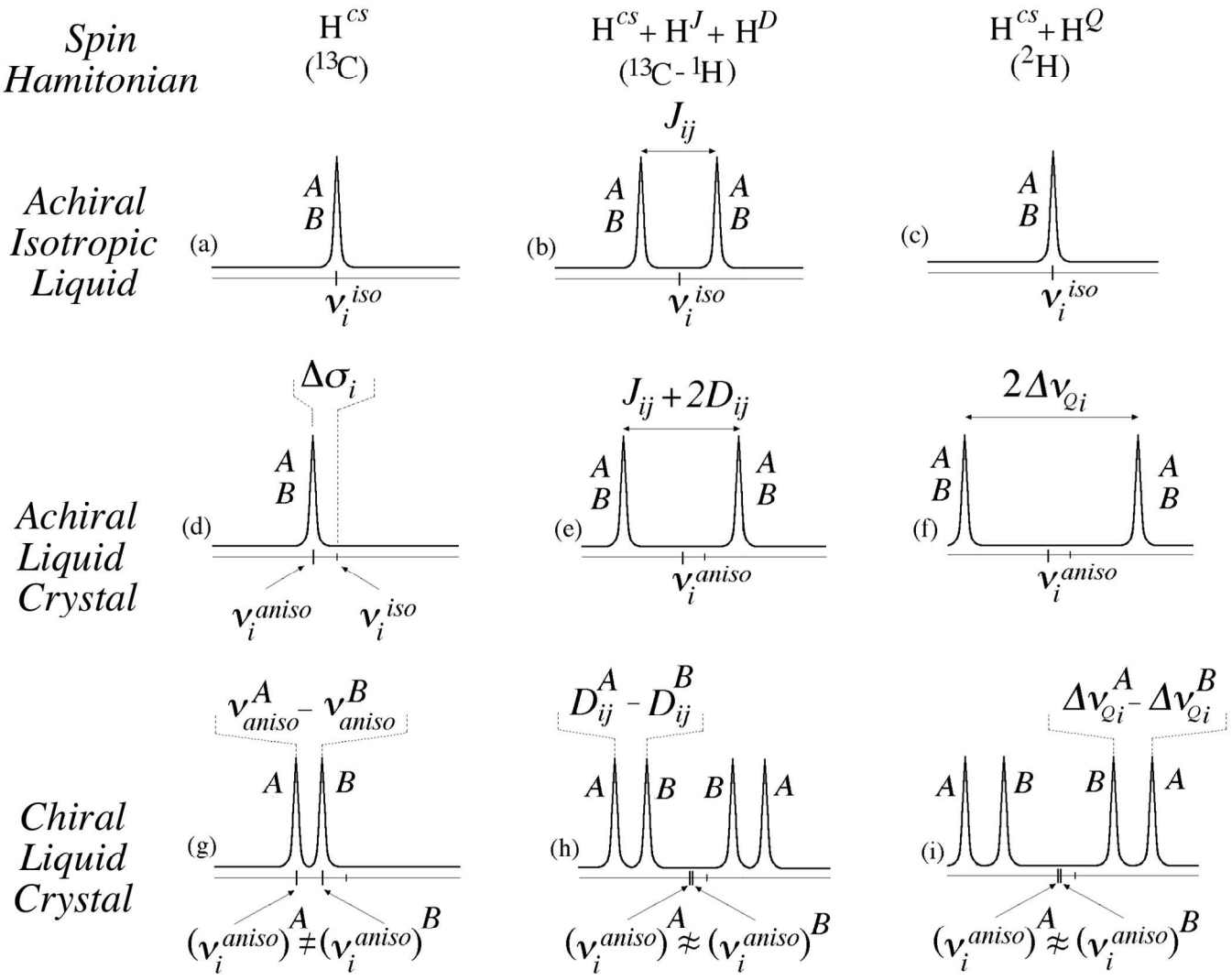

Fig. 3. Principle of the spectral enantiodiscrimination in CLC based on a difference of (a) chemical shifts, $\delta(^{13}C)$, (b) residual dipolar couplings, $D(^{13}C\text{-}^{1}H)$ and (c) residual quadrupolar splittings, $\Delta\nu_Q(^{2}H)$. For each case, either an isolated spin or a spin-spin pair is considered. On all schemes, $\Delta\sigma_i$ was assumed to be negative. In addition the schemes h and i are depicted assuming the CSA difference ($\Delta\sigma_i^A - \Delta\sigma_i^B$) between the enantiomers in chiral anisotropic phase was negligible. D_{ij}^A and D_{ij}^B are chosen to be smaller than J_{ij}, and having a positive and negative sign, respectively. $\Delta\nu_Q^i$ can be positive or negative. The various spectra are not plotted to scale. The notation *A*/*B* corresponds to stereodescriptors *R*/*S* (enantiomeric pairs) or *r*/*s* (enantiotopic pairs). The assignments shown in all spectra are arbitrary. Figure adapted from ref. **28**.

A similar situation applies in enantiomeric discrimination, namely that the ΔT^k observed in an ALC corresponds approximately to the average of the signals positions in CLC, $\frac{1}{2}(\Delta T^{kR} + \Delta T^{kS})$. Here, the argument is somewhat different and relies on the assumption that (at

least for p ~ ½) the ordering of an optically active solute (*R* or *S*) in an enantiomeric mixture of a lyomesophases can be written as the weighted average of the ordering in the neat enantiomers. Then, using the symmetry relations, $S^R_{\alpha\beta}/D_m = S^S_{\alpha\beta}/L_m$ and likewise, $S^S_{\alpha\beta}/D_m = S^R_{\alpha\beta}/L_m$,

$$\begin{aligned} S^R_{\alpha\beta}/[pDm + (1-p)Lm] &\approx p\,S^R_{\alpha\beta}/Dm + (1-p)\,S^R_{\alpha\beta}/L_m \\ &= p\,S^R_{\alpha\beta}/Dm + (1-p)\,S^S_{\alpha\beta}/D_m \\ &= [p\,S^R_{\alpha\beta} + (1-p)\,S^S_{\alpha\beta}]/D_m \end{aligned} \qquad \textbf{(25)}$$

and similarly for $S^S_{\alpha\beta}$. For p = ½, it then follows that $S^R_{\alpha\beta}$/racemate = $S^S_{\alpha\beta}$/racemate = ½($S^R_{\alpha\beta}/D_m + S^S_{\alpha\beta}/D_m$) = ½($S^R_{\alpha\beta}/L_m + S^S_{\alpha\beta}/L_m$).

3.3. The use of ^{2}H NMR

Proton-decoupled deuterium NMR of deuterated compounds or even in natural abundance (NAD), proved to be a most powerful tool for studying chiral discrimination.[28,57,58,59,60,61,62] Deuterium nuclei are present (in natural abundance) in essentially all organic solutes and can often be specifically introduced by isotopic labeling. Its nuclear spin is $I = 1$ and consequently in the NMR spectrum in a liquid-crystalline solvents exhibits a single doublet for each type of hydrogen (see **Table 2**). The moderately small quadrupole moment of the deuteron (Q_D = 0.286 fm^2), results in relatively narrow lines and a convenient range of quadrupolar splittings. Yet due to its low magnetic moments (γ_H = 6.515×$\gamma_{D)}$, its spectrum is not significantly complicated by dipolar interaction with near-by protons ($D_{HD} = 6.515 \times D_{HH}$). Morover, its quadrupole tensor in C-D bonds may safely be assumed axially symmetric, about the CD internuclear direction, rendering the interpretation of the spectrum in terms of the Saupe order tensor fairly straightforward. The full splitting of the doublet for the i'th deuteron then becomes,[26,28,61,62]

$$2\Delta\nu_Q^i = 2q_{zz}^i S_{zz} = \left(\frac{3}{2}\right) K_{C-Di} S_{C-Di} \quad \textbf{(26)}$$

where z is the principal direction (parallel to the C-D bond) of the quadruple tensor, $K_{C\text{-}Di}$ is the quadrupole coupling constant and $S_{C\text{-}Di}$ the ordering parameter along the C-D_i bond. **Eq. 25** can be transformed to the form given in **Table 2**, using **Eq. 8** (provided the geometry of the solute is known). The $K_{C\text{-}Di}$'s in organic molecules depend on the degree of hybridization of the directly bonded carbon atom (and to some extend on neighboring groups) and are about 175 kHz and 185 kHz for sp^3 and sp^2 type carbon atoms, respectively.[26,58,62] For orientational order parameters in the range 10^{-3} to 10^{-4}, this result in experimental splittings in the convenient high-resolution range of several tens to several hundred Hz.

A special point concerns the signs of the $\Delta\nu_Q^i$'s, which are required to solve for the $S_{\alpha\beta}$'s, but are not directly obtainable from the ^{2}H spectrum analysis. They can, however, often be obtained by comparing the magnitudes of the $2\Delta\nu_Q^i$ with those of the ^{13}C-^{1}H dipolar interaction, $^1D_{C\text{-}H}^i$, of the corresponding bond. For sp^3 or sp^2 type of carbon atoms this ratio is, $2\Delta\nu_Q^i/{}^1D\text{-}_{CH}^i \approx$ -10 to -12.[49,63] Thus if the sign of is $^1D_{C\text{-}H}^i$ is known that of $\Delta\nu_Q^i$ can be deduced. The magnitude and sign of $^1D_{CH}^i$ can, in turn, be obtained from the total ^{13}C-^{1}H splitting, $^1T_{C\text{-}H} = {}^1J_{C\text{-}H} + 2{}^1D_{C\text{-}H}$, as measured on the proton coupled ^{13}C NMR spectrum of the corresponding bond in the same solution (for NAD) or in an equivalent, isotopically normal solution, if a deuterated solute was used. In the analysis it is assumed that the sign of the single bond $^1J_{C\text{-}H}$ ($^1J_{C\text{-}H} \approx$ +120-140 Hz, usually known from measurements in isotropic solutions) is always positive and its magnitude larger than that of $^1D_{C\text{-}H}$ in the weakly ordering polypeptide lyomesophases. Under these conditions, if $|{}^1T_{C\text{-}H}| > |{}^1J_{C\text{-}H}|$, $^1D_{C\text{-}H}$ is positive and $\Delta\nu_Q^i$ negative, while if $|{}^1T_{C\text{-}H}| < |{}^1J_{C\text{-}H}|$, $^1D_{C\text{-}H}$ is negative and $\Delta\nu_Q^i$ positive.

The main disadvantage of ^{2}H NMR lies in its low natural abundance (1.55×10^{-4}). This can often be overcome by specific (or full) isotopic labeling. In recent years, high-field modern NMR spectrometers equipped (or not) with specifically deuterium tuned cryogenic probes made it possible to perform advanced NAD nD-NMR (n = 1 to 3) even using low concentration samples.[60,61,62] Several examples of NAD 2D-NMR spectra are presented in this review. The analysis of complex, anisotropic ^{2}H 1D spectra at natural abundance level (or for perdeuterated solutes) can be simplified using QUOSY-type (Quadrupole Ordered SpectroscopY) 2D experiments[64,65] (such as *Q*-COSY/*Q*-COSY Fz or *Q*-resolved/*Q*-resolved Fz 2D sequences) or even 3D schemes.[66,67] Such experiments permit pairwise correlation of the quadrupolar doublet components, followed by their assignment on the basis of their (known ^{1}H) chemical shift. Concommitantly, a specific, tailored cartesian spin-operator formalism to NAD NMR in weakly oriented solvent has been proposed.[68] ^{2}H-^{13}C correlation 2D experiments,[69] such as CDCOM (Carbon and Deuterium Correlation in Oriented Media)[70,71] or NASDAC (Natural Abundance Spectroscopy of Deuterium And Carbon)[72] have also been applied successfully for the assignment of deuterium QDs.

Finally it should be noted that the (*r*/*s*) discriminated enantiotopic signals in natural abundance, actually arise from the corresponding pairs of the mono substituted isotopic enantiomers (*R*/*S*), also named enantio-isotopomers. The discrimination between such pairs can, in principle, be claimed to result from an isotope effect on the ordering of the (isotopic *R*/*S*) enantiomers. Numerous experiments indicate, however, that the deuterium isotope effect on solute ordering is completely negligible compared with the experimentally observed discrimination.[73,74]

4.1 Molecules with D_{2d} symmetry

The D_{2d} group is the simplest of the allowed point groups to interpret. From **Table 3** only a single order parameter, $S(\mathrm{sym}) = S_{aa}$ (a parallel to the principal C_2 axis) is required

to describe the ordering in ALC, and one additional parameter $S(\text{anti}) = S_{bb} - S_{cc}$, is needed to fully determine the ordering in CLC. Consequently, data from a single enantiotopic pair is sufficient to fully characterize the ordering of a D_{2d} solute in CLC.

4.1.1 Spiropentane. The only example with this symmetry that has so far been analyzed in terms of ordering in CLC is spiropentane (see **Figure 4a**).[54] This rigid molecule consists of eight methylene hydrogens, that can be divided into two sets of four homomers (labeled *r* and *s*), related to each other by the three orthogonal C_2 axes. The *r* and *s* hydrogens are pairwise related by the σ_d reflection planes to form four equivalent enantiotopic pairs. In chiral oriented solvents, these reflection planes are quenched rendering the ordering tensor nonaxial and the enantiotopic elements spectrally dissimilar. This is well demonstrated by the NAD spectra (**Figure 4b**) of spiropentane; a single doublet is observed in ALC (top) while two are detected in CLC (bottom). From the relevant entries in **Tables 2** and **3**, the quadrupolar splitttngs for the *r* and *s* deuterons in the CLC solution become,

$$\Delta\nu_Q^r = q_{aa}^e S_{aa} + \tfrac{1}{3}(q_{bb}^e - q_{cc}^e)(S_{bb} - S_{cc}) \quad \textbf{(27)}$$

and

$$\Delta\nu_Q^s = q_{aa}^e S_{aa} - \tfrac{1}{3}(q_{bb}^e - q_{cc}^e)(S_{bb} - S_{cc}) \quad \textbf{(28)}$$

Taking the symmetric (average) and antisymmetric (half the difference) combinations of the two splittings in CLC yields,

$$\Delta\nu_Q^e(\text{sym}) = \frac{1}{2}(\Delta\nu_Q^r + \Delta\nu_Q^s) = q_{aa}^e S_{aa} \quad \textbf{(29)}$$

and

$$|\Delta\nu_Q^e(\text{anti})| = \frac{1}{2}|\Delta\nu_Q^r - \Delta\nu_Q^s| = \frac{1}{3}|(q_{bb}^e - q_{cc}^e)(S_{bb} - S_{cc})| \quad \textbf{(30)}$$

where, as explained following **Eq. 23**, only the absolute value of $\Delta\nu_Q^e(\text{anti})$ can be derived, since it is not possible to identify the sites *r*, *s*, in the structural formula of

spiropentane with the particular QD, $\Delta\nu_Q^r$ and $\Delta\nu_Q^s$, observed in the spectrum. From the entries in the **Fig. 4b** and the calculated $q_{\alpha\beta}$'s the following order parameters were obtain, $S_{aa} = +1.73 \times 10^{-3}$ and $|(S_{bb} - S_{cc})| = 0.08 \times 10^{-3}$. The fact that in **Figure 4b**, $\Delta\nu_Q^{r,s}$ in ALC does not exactly match the average splitting in CLC is most likely due to slight slight experimental differences during sample preparations.

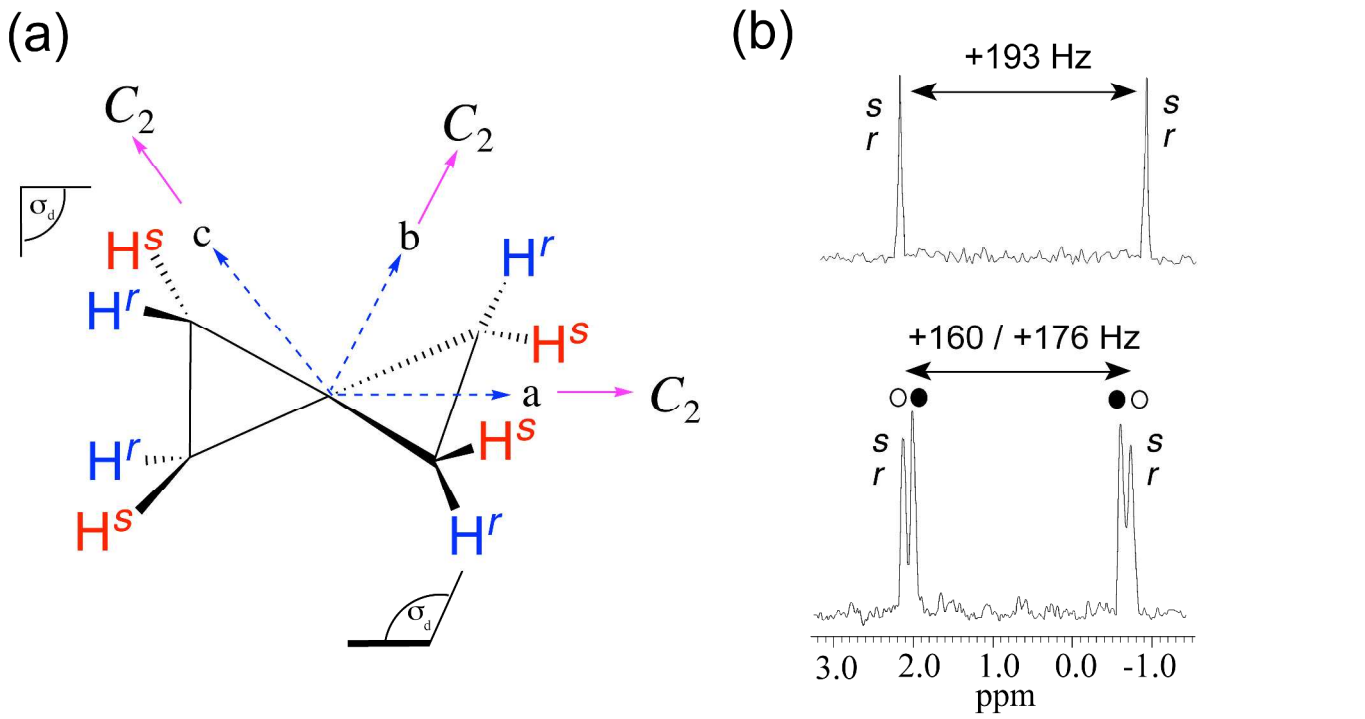

Fig. 4. (a) Structure and axis system used for **spiropentane**. The axes *a, b* and *c* are along the molecular C_2 axes, with *a* along the bisector of the symmetry planes (b) 61.4 MHz NAD NMR signals of spiropentane dissolved in achiral (top) and chiral (bottom) lyotropic mesophases based on poly-γ-benzylglutamate at 295 K. The traces are 1D projections of associated tilted NAD *Q*-COSY 2D spectra. Note the doubling (solid and open circles) of ^{2}H signals in CLC. Figure adapted from ref. **54**.

4.2 Molecules with C_{2v} symmetry

The C_{2v} group is next in complexity. Molecules with such symmetry effectively reduce to C_2 in CLC and, from **Table 3**, instead of two order parameters in ALC (S_{aa} and $S_{bb} - S_{cc}$), one additional parameter (S_{bc}) is needed to describe their orientation in CLC. Consequently at least one enantiotopic pair and one additional site (homotopic pair or

diastereotopic element) suffice to solve for the ordering matrix in the latter. Molecules with such symmetry are abundant in nature. We shall describe several of them in order to demonstrate the kind of information that can be derived.

4.2.1 Acenaphthene. As a first example we consider the deuterium spectrum of perdeuterated acenaphthene (**Figure 5a**).[53,75] The molecule contains three pairs of homotopic (aromatic) hydrogens (labeled *o*, *m* and *p*) and two equivalent pairs of (aliphatic) enantiotopic sites (*r*/*s*) each located on two prostereogenic carbon atoms. Accordingly, the deuterium 1D-NMR spectrum in ALC exhibits three doublets centered in the aromatic region (indicated by asterisks) and a single doublet, of double intensity (*r*/*s*), in the aliphatic range (**Figure 5b**). In CLC the aliphatic signal exhibits enantiotopic discrimination as shown in part c of the figure. The interpretation of the spectra in terms of the ordering matrix is now straightforward. Using **Eqs. 19,20** and the entries in **Table 3** for the C_{2v} group we obtain for the enantiomeric sites,[54]

$$\Delta\nu_{\mathrm{Q}}^{r} = q_{aa}^{\mathrm{e}}S_{aa} + \frac{1}{3}(\mathrm{q}_{\mathrm{bb}}^{\mathrm{e}} - \mathrm{q}_{\mathrm{cc}}^{\mathrm{e}})(S_{bb} - S_{cc}) + \frac{4}{3}\mathrm{q}_{\mathrm{bc}}^{\mathrm{e}}S_{bc} \quad \textbf{(31)}$$

$$\Delta\nu_{\mathrm{Q}}^{s} = q_{aa}^{\mathrm{e}}S_{aa} + \frac{1}{3}(\mathrm{q}_{\mathrm{bb}}^{\mathrm{e}} - \mathrm{q}_{\mathrm{cc}}^{\mathrm{e}})(S_{bb} - S_{cc}) - \frac{4}{3}q_{bc}^{\mathrm{e}}S_{bc} \quad \textbf{(32)}$$

Taking the symmetric and antisymmetric combinations,

$$\Delta\nu_{\mathrm{Q}}^{\mathrm{e}}(\mathrm{sym}) = \mathrm{q}_{\mathrm{aa}}^{\mathrm{e}}S_{aa} + \frac{1}{3}(\mathrm{q}_{\mathrm{bb}}^{\mathrm{e}} - \mathrm{q}_{\mathrm{cc}}^{\mathrm{e}})(S_{bb} - S_{cc}) \quad \textbf{(33)}$$

and

$$\left|\Delta\nu_{\mathrm{Q}}^{\mathrm{e}}(\mathrm{anti})\right| = \frac{4}{3}|\mathrm{q}_{\mathrm{bc}}^{\mathrm{e}}S_{bc}|, \quad \textbf{(34)}$$

while for the homotopic sites (using **Eq. 21**)) we obtain,

$$\Delta\nu_{\mathrm{Q}}^{\mathrm{h}}(\mathrm{sym}) = \mathrm{q}_{\mathrm{aa}}^{\mathrm{h}}S_{aa} + \frac{1}{3}(\mathrm{q}_{\mathrm{bb}}^{\mathrm{h}} - \mathrm{q}_{\mathrm{cc}}^{\mathrm{h}})(S_{bb} - S_{cc}) \quad \textbf{(35)}$$

as for $\Delta\nu_Q^e$(Sym). The antisymmetric order parameter, $|S_{bc}|$, can thus directly be determined from the splitting of the enantiotopic pair (**Eq. 34**) – as explained above, only its absolute value can be derived. The elements of the symmetric part, S_{aa} and $S_{bb} - S_{cc}$, can then be calculated from the average splitting of the enantiotopic pair (**Eq. 33**) and one of the homotopic aromatic pairs (**Eq. 35**). Most convenient is the para deuteron for which the rhombic term may be deleted from the equation (on the basis of axial symmetry of the q – tensor). Actual analysis of the experimental data then yields, $S_{aa} = +1.38 \times 10^{-3}$, $(S_{bb} - S_{cc}) = +3.81 \times 10^{-3}$ and $|S_{bc}| = 0.06 \times 10^{-3}$. These results are consistent with the (partially accidental) bunching of the doublets due to the aromatic deuterons, with $\Delta\nu_Q^m \approx \Delta\nu_Q^o \approx -\Delta\nu_Q^p$. Indeed, assuming hexagonal geometry for the benzene (ac) plane (with polar angles of 60°, 120° and 180° for the *ortho*, *meta* and *para* C-D bonds) one obtains from **Eq. 35** (using **Eqs. 18,19** and **Eqs. 22,23**).

$$\Delta\nu_Q^m = \Delta\nu_Q^o = q_{zz}\left[-\tfrac{1}{8}S_{aa} - \tfrac{3}{8}(S_{bb} - S_{cc})\right] \quad \textbf{(36)}$$

and

$$\Delta\nu_Q^p = q_{zz}S_{aa} \quad \textbf{(37)}$$

where $q_{zz} = (3/4)K_{C\text{-}D}$. From **Eqs. 36** and **37** we thus obtain, $(S_{bb} - S_{cc})/S_{aa} = +2.33$, which is consistent with the result quoted above (+2.76).

Finally, the so obtained *S*-matrix can be analytically diagonalized to yield its principal values and principal directions (primed indices) as drawn in **Figure 5**,

$$S_{a'a'} = S_{aa} \quad \textbf{(38)}$$

and

$$(S_{b'b'} - S_{c'c'}) = 2S_{bc}\sin(2\alpha) + (S_{bb} - S_{cc})\cos(2\alpha) = 2[S_{bc}^2 + \tfrac{1}{4}(S_{bb} - S_{cc})^2]^{1/2}$$

where,

$$\mathrm{tg}(2\alpha) = 2S_{bc}/(S_{bb} - S_{cc}) \quad \textbf{(39)}$$

Substituting the experimental splitting and using calculated $q_{\alpha\beta}$ yields, $|\alpha| = 0.9$ deg, $S_{a'a'} = +1.38\times10^{-3}$, $(S_{b'b'} - S_{c'c'}) = +3.81\times10^{-3}$. Due to the smallness of α, the rhombic term is essentially identical in both axis systems.

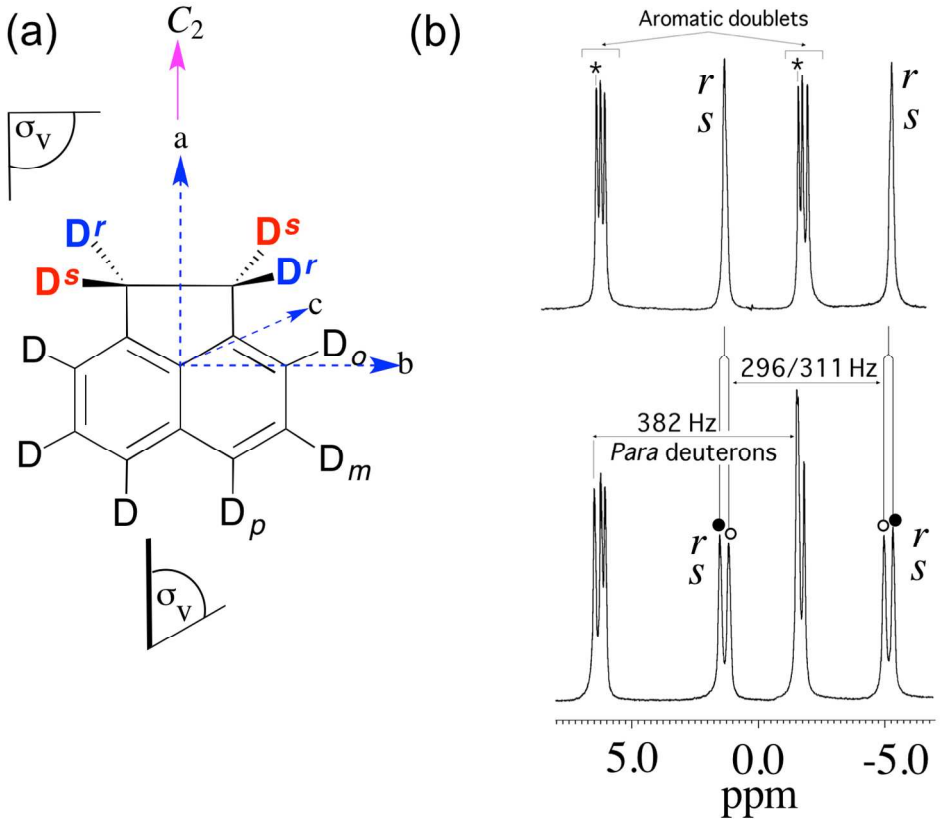

Fig. 5. (a) Structure and axis system used in analyzing the spectra of **acenaphthene-d_{10}**. (b) Associated ^{2}H 1D-NMR spectrum (61.4 MHz) recorded in achiral PBG/$CHCl_3$ (top) and in chiral PBLG/$CHCl_3$ (bottom) solvents. Figure adapted from ref. **53**.

4.2.2 Norbornadiene and quadricyclane. Two illustrative examples of polycyclic rigid molecules with C_{2v} symmetry are the norbornadiene (**NBD**) and quadricyclane (**QC**) (see **Figure 6**).[51,76] Both compounds are structurally similar and chemically related. Indeed **QC** can be synthetized from **NBD** using a photochemically induced [2+2] cycloadditon.[76] Contrarily to **NBD**, the **QC** structure allows to store photochemical energy. Both possess two pairs of homotopic and two pairs of enantiotopic hydrogens. Their enantiotopic sites reside, however, on two prostereogenic carbon atoms related by reflection, rather than on a single one, as in acenaphthene. In the ^{2}H spectrum, they thus exhibit ample signals for a

complete derivation of the ordering matrices as demonstrated above for the acenaphtene molecule. The associated *Q*-COSY NAD 2D spectra in CLC solvents are shown in **Figure 6**, with peak assignment (for experimental splittings, see refs. **51,76**). Using experimental or computed structural data, the Saupe matrices can thus readily be derived.

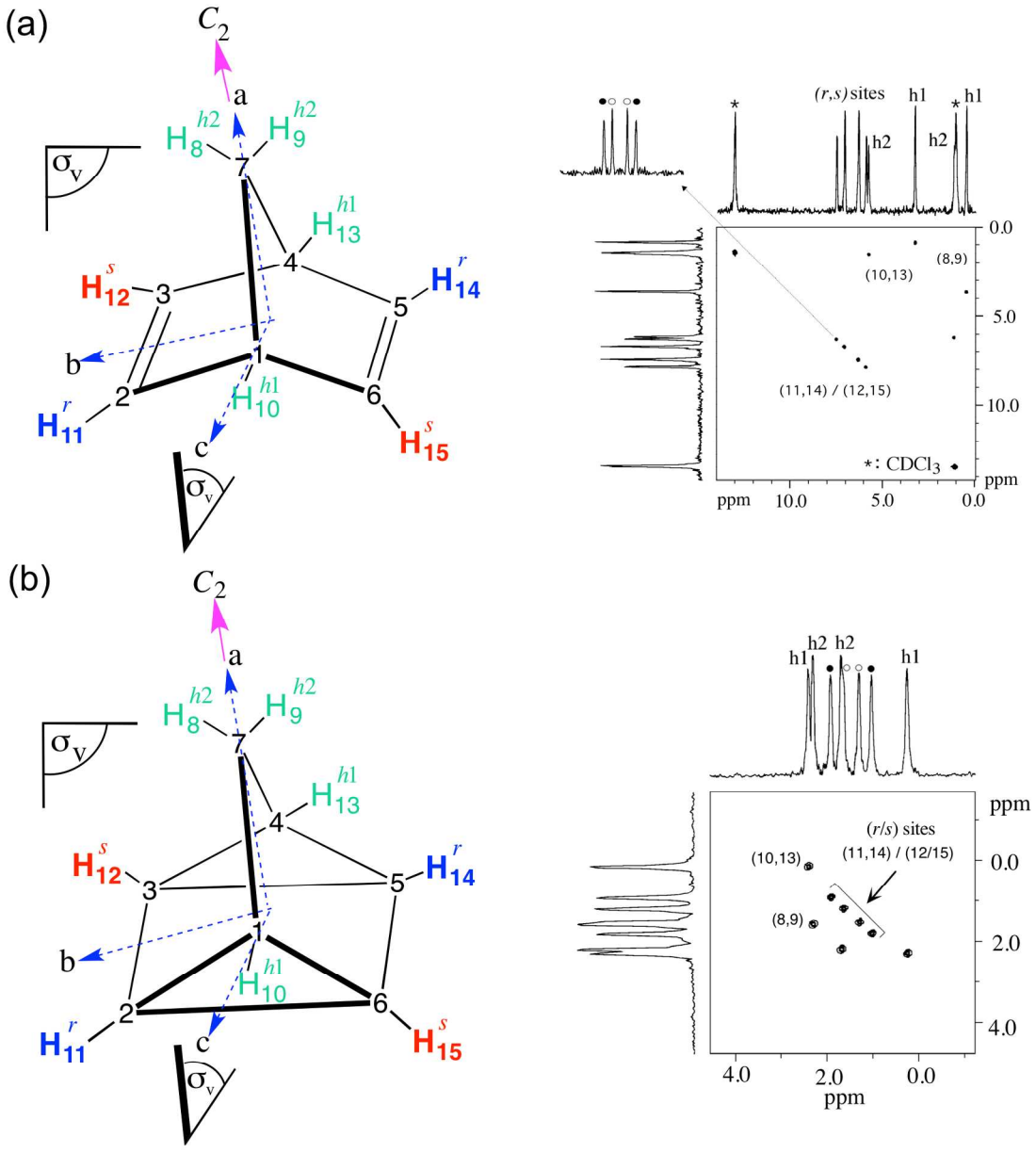

Fig. 6. (a) Molecular structure, atomic numbering and coordinates used in the analysis of the ^{2}H spectra of **norbornadiene** (a) and **quadricylane** (b). The *r*/*s* notation shown is arbitrarily given here. (b) Corresponding tilted NAD *Q*-COSY 2D spectra (61.4 MHz) recorded in the chiral PBLG/$CHCl_3$ mesophase at around room temperature. Figure adapted from refs. **51** and **76**

4.2.3 Malononitrile. **Malononitrile** (**MN**) provides a special example of a C_{2v} molecule in that it allows demonstrating enantiotopicity of structural elements other than sites, as in the previous cases.[51,76] The molecule consists of a central tetrahedral carbon bonded to two homotopic hydrogens and two homotopic nitrile groups, related by the molecular C_2 axis (see **Figure 7a**). No proper enantiotopic sites, related solely by reflection exist in the molecule. On the other hand we note that the edges linking the atoms C_2-H_4 and C_2-H_5, form a proper enantiotopic pair, as they are related by the molecular symmetry plane, σ_{ab}, but not by its C_2 rotation axis.[51] Similar relations exist between the edges linking atoms C_3–H_4 and C_3–H_5. Dipolar interactions between such pairs of ^{13}C and ^{1}H nuclei should be identical in ALC, but discriminated in CLC.

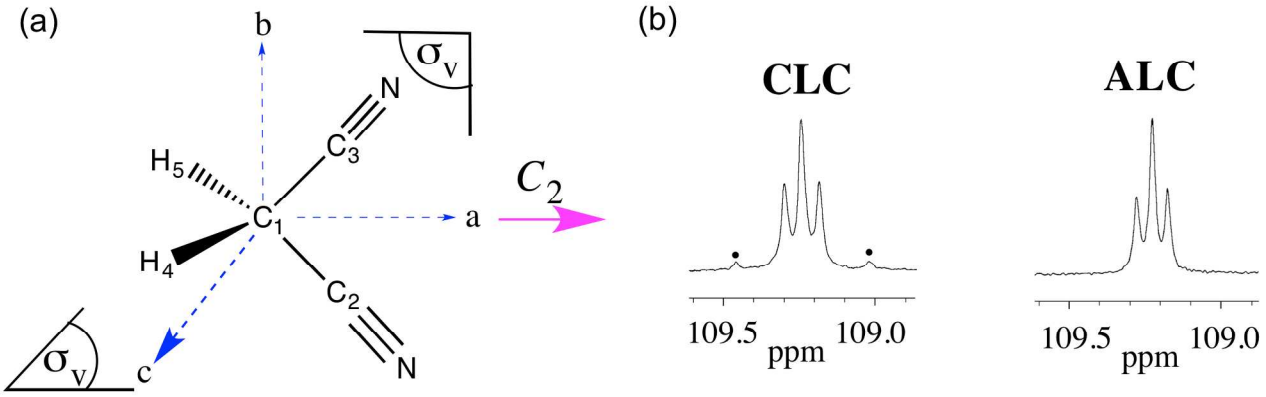

Fig. 7. (a) Structure, atomic numbering and coordinates used in the analysis of the proton-coupled ^{13}C signal of nitrile carbon of **malononitrile**. (b) 100.4 MHz proton coupled ^{13}C NMR spectra (natural abundance) of the nitrile groups in CLC (PBLG/$CHCl_3$) and ALC (PBG/$CHCl_3$) at 295 K. Figure adapted from ref. **51.**

This is well manifested in the proton coupled natural abundance ^{13}C spectra of the carbon of nitrile groups in **MN** dissolved in ALC and CLC, (see **Figure 7b**). The associated spectra in both solvents exhibit splitting due to through space ^{1}H-^{13}C dipolar interaction. In ALC it consists of a symmetric 1:2:1 triplet, characteristic of the A part of a heteronuclei AX_2 spin system ($I_A = I_X = ½$), with A = ^{13}C and X = ^{1}H. The spacings between the triplet components are $2^2D_{C\text{-}H}$, namely twice the dipolar interaction between

the nitrile carbon atoms and the methylene hydrogens (the corresponding scalar spin-psin couplings, $^2J_{C\text{-}H}$, are neglected). Expressions for the dipolar coupling are given in the penultimate line (and footnote b) of **Table 2**. The spectrum in CLC is quite different; it exhibits additional weak outer peaks and a small reduction in the relative intensity of the inner doublet. The spectrum is now of the type AXX', with different coupling between A-X and A-X'.[51] The line positions and intensities now depend on $^1D_{C\text{-}H}$, $^1D_{C\text{-}H'}$, as well as on $^2D_{H\text{-}H'}$ and $^2J_{H\text{-}H'}$. Assuming that $(^1D_{C\text{-}H} - {}^1D_{C\text{-}H'})^2 << (^2J_{H\text{-}H'} - {}^2D_{H\text{-}H'})^2$, the line positions and intensities can be calculated by perturbation theory and are shown in the bottom two lines of **Table 4**.

Table 4 (to insert here)

Analysis of the experimental ^{13}C spectra in CLC in terms of the approximate equations in the above table, and additional ^1H NMR measurements yielded (in Hz), $^1D_{C\text{-}H} = 0.0$, $^1D_{C\text{-}H'} = +5.3$, $^1D_{H\text{-}H'} = +1.1$ and $^2J_{H\text{-}H'} = -20.3$. From the entries in **Tables 2** and **3**, one can write three following three relations from which the ordering matrix in CLC can be computed as following:

$$D_{C-H}(\text{sym}) = -\left(\frac{K_{C-H}}{r_{C-H}^3}\right)^{1/2}\left[S_{aa}(3cos^2\theta_{C-H}^a - 1) + (S_{bb} - S_{cc})(cos^2\theta_{C-H}^b - cos^2\theta_{C-H}^c)\right] \quad \textbf{(40)}$$

$$|D_{C-H}(\text{anti})| = \left| 2\left(\frac{K_{C-H}}{r_{C-H}^3}\right)^{1/2} S_{bc} cos\theta_{C-H}^b \, cos\theta_{C-H}^c \right| \quad \textbf{(41)}$$

$$D_{H-H}(\text{sym}) = -\left(\frac{K_{H-H}}{r_{H-H}^3}\right)[S_{aa} + (S_{bb} - S_{cc})] \quad \textbf{(42)}$$

and inserting the relevant term K_{i-j}'s and geometrical parameters for **MN** finally yields $S_{aa} = -6.4 \times 10^{-3}$, $(S_{bb} - S_{cc}) = +6.6 \times 10^{-3}$, $|S_{bc}| = +1.69 \times 10^{-3}$ and after diagonalisation, $S_{a'a'} = -6.4 \times 10^{-3}$, $(S_{b'b'} - S_{c'c'}) = +7.4 \times 10^{-3}$, $|\alpha| = 14°$.

These results are fully consistent with the generalized, symmetry based, definition of prochirality as compounds consisting of (rigid) molecules possessing improper symmetry with enantiotopically related elements (atoms, groups of atoms, faces or edges). In the above case of **MN** the enantiotopically related elements are the (none directly bonded) C-H directions and their enantiotopic discrimination is manifested by the lifting of their corresponding internuclear dipolar interaction degeneracy. We will encounter similar cases below.

4.3 Molecules with C_s symmetry

The C_s symmetry is the most complex of the four allowed groups, requiring a total of five order parameters to fully determine the *S*-matrix in a CLC [three $S_{\alpha\beta}$(sym) and two. $S_{\alpha\beta}$(anti)]. Nevertheless, just three independent enantiotopic pairs (or two such pairs and a single diastereotopic site) are, in principle, sufficient to provide all elements of the *S*-matrix. Many common molecules belong to this symmetry; however, often they are too simple to provide sufficient experimental data for deriving the ordering matrix. An example of the latter is **1,1-dimethyloxyrane** (**DMO**) which is described in the section below. It is followed by an example with sufficient experimental data to even determine the relative signs of the *S*(anti) part of the ordering matrix.

4.3.1 1,1-dimethyloxyrane. The structure of this compound (**DMO**) and its NAD signals recorded in CLC are depicted in **Figure 8**. There are clearly insufficient hydrogen sites to derive even the symmetric part of the ordering matrix; three such sites are needed, while just two (actually not strictly independent) are available. Of these the methylene hydrogens exhibit a clear enantiotopic discrimination, but the equivalent effect on the

methyl signal is obviously within the (quite narrow) linewidth and not observed. The ^{13}C-^{1}H dipolar interaction, $^{1}D_{\text{C-H}}$, would not be of much use as it is not independent of the $\Delta\nu_{\text{Q}}^{\text{C-D}}$. The dipolar coupling $^{2}D_{\text{H-H}}$ would be useful, but not sufficient for the analysis. The most one can do is to estimate the specific ordering of the C-D and the C-Me bonds from equations of the type.

$$\Delta\nu_{\text{Q}}^{\text{C-D}} = \text{q}_{zz}S_{\text{C-D}} \quad \textbf{(43)}$$

Clearly, a more complex molecule is required to demonstrate the derivation of the ordering matrix in a C_s compound. Two examples are described below.

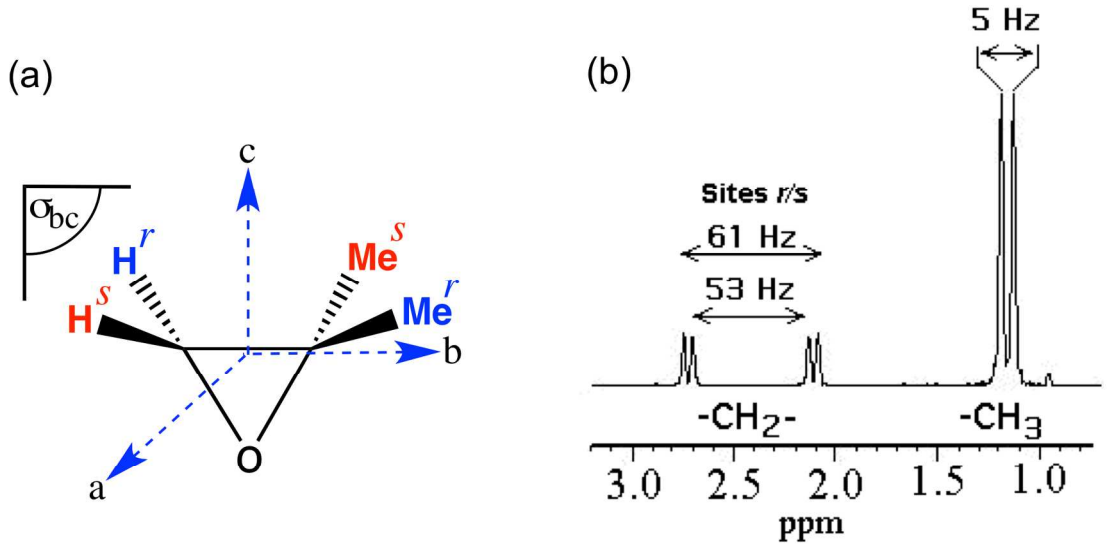

Fig. 8. (a) The structure of **dimethyloxyde**. (b) Associated proton-decoupled NAD 1D trace (92.1 MHz) obtained by F_2 projection from a Q-COSY 2D spectrum recorded in PBLG/$CHCl_3$ at 300 K (unpublished results).

4.3.2 Norbornene. The molecular structure and the 2D NAD spectrum of norbornene (**NBN**) are shown in **Figure 9**.[51,76] The molecules include four pairs of enantiotopic and two diasterotopic bridgehead hydrogens. Their signals in the NAD/CLC spectrum can readily be identified on the basis of their chemical shift, their quadrupole splittings in ALC (not shown, see ref. **76**) and the presence or absence of chiral discrimination in CLC. In particular the signals of the *syn* and *anti* deuterons are conspicuous in the

absence of chiral splitting. The peak assignment so obtained is indicated on the 1D chemical shift projections of the various signals.

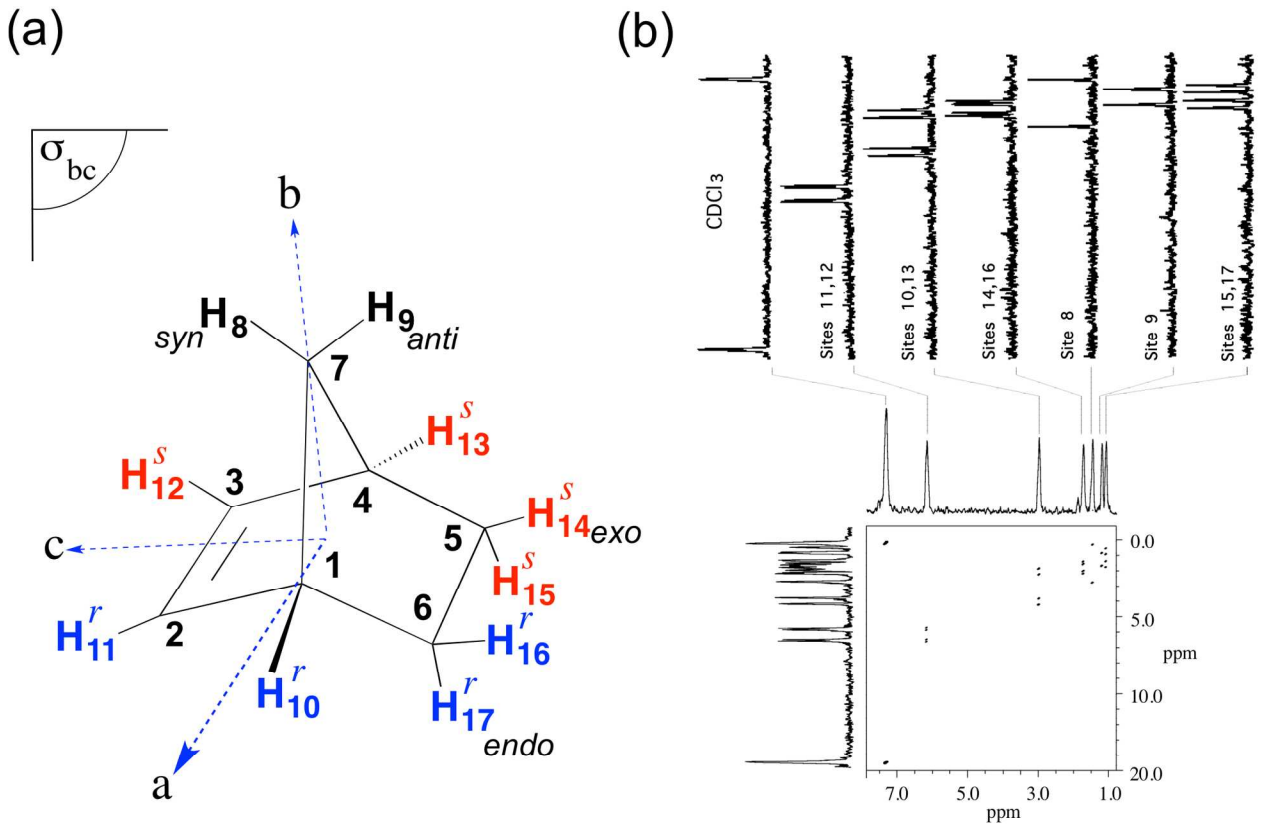

Fig. 9. (a) Molecular structure, atomic numbering and coordinates used in the analysis of the ^{2}H spectrum of **norbornene**. As explained in **Section 3.2**, the terminology *r*/*s* displayed on the structure corresponds to the *Re*/*Si* one. (b) Associated proton-decoupled NAD *Q*-COSY 2D (61.4 MHz) 2D spectrum (symmetrized and tilted) of recorded in PBLG/$CHCl_3$. 1D traces corresponding to the chemical shifts of the various deuterium sites are spread out at the top. Figure adapted from ref. **76.**

From the entries in **Tables 2** and **3** the expressions for the quadrupole coupling of the enantiotopic pairs in CLC become,

$$\Delta\nu_{\mathrm{Q}}^{r} = \mathrm{q}_{\mathrm{aa}}^{\mathrm{e}} S_{\mathrm{aa}} + \frac{1}{3}(\mathrm{q}_{\mathrm{bb}}^{\mathrm{e}} - \mathrm{q}_{\mathrm{cc}}^{\mathrm{e}})(S_{bb} - S_{cc}) + \frac{4}{3}\mathrm{q}_{\mathrm{bc}}^{\mathrm{e}} S_{\mathrm{bc}} + \frac{4}{3}\mathrm{q}_{\mathrm{ab}}^{\mathrm{e}} S_{\mathrm{ab}} + \frac{4}{3}\mathrm{q}_{\mathrm{ac}}^{\mathrm{e}} S_{\mathrm{ac}} \qquad \textbf{(44)}$$

and

$$\Delta\nu_{\mathrm{Q}}^{s} = \mathrm{q}_{\mathrm{aa}}^{\mathrm{e}} S_{\mathrm{aa}} + \frac{1}{3}(\mathrm{q}_{\mathrm{bb}}^{\mathrm{e}} - \mathrm{q}_{\mathrm{cc}}^{\mathrm{e}})(S_{\mathrm{bb}} - S_{\mathrm{cc}}) + \frac{4}{3}\mathrm{q}_{\mathrm{bc}}^{\mathrm{e}} S_{\mathrm{bc}} - \frac{4}{3}\mathrm{q}_{\mathrm{ab}}^{\mathrm{e}} S_{\mathrm{ab}} - \frac{4}{3}\mathrm{q}_{\mathrm{ac}}^{\mathrm{e}} S_{\mathrm{ac}} \qquad \textbf{(45)}$$

Consequently,

$$\Delta\nu_{\mathrm{Q}}^{e}(sym) = \mathrm{q}_{\mathrm{aa}}^{\mathrm{e}}S_{\mathrm{aa}} + \frac{1}{3}(\mathrm{q}_{\mathrm{bb}}^{\mathrm{e}} - \mathrm{q}_{\mathrm{cc}}^{\mathrm{e}})(S_{\mathrm{bb}} - S_{\mathrm{cc}}) + \frac{4}{3}\mathrm{q}_{\mathrm{bc}}^{\mathrm{e}}S_{\mathrm{bc}} \quad \textbf{(46)}$$

$$\left|\Delta\nu_{\mathrm{Q}}^{s}(\mathrm{anti})\right| = \frac{4}{3}\left|\mathrm{q}_{\mathrm{ac}}^{\mathrm{e}}S_{\mathrm{ac}} + \mathrm{q}_{\mathrm{bc}}^{\mathrm{e}}S_{\mathrm{bc}}\right| \quad \textbf{(47)}$$

while for the diastereotopic sites, which necessarily lie on the molecular symmetry plane,

$$\Delta\nu_{\mathrm{Q}}^{\mathrm{d}} = \mathrm{q}_{\mathrm{aa}}^{\mathrm{d}}S_{\mathrm{aa}} + \frac{1}{3}(\mathrm{q}_{\mathrm{bb}}^{\mathrm{d}} - \mathrm{q}_{\mathrm{cc}}^{\mathrm{d}})(S_{\mathrm{bb}} - S_{cc}) + \frac{4}{3}\mathrm{q}_{\mathrm{bc}}^{\mathrm{d}}S_{\mathrm{bc}} \quad \textbf{(48)}$$

as for $\Delta\nu_{\mathrm{Q}}^{\mathrm{e}}$(sym).[54] The three components of S(sym), S_{aa}, (S_{bb} - S_{bb}) and S_{bc}, can thus readily be obtained from any set of three or more $\Delta\nu_{\mathrm{Q}}^{\mathrm{e}}$(sym)'s and $\Delta\nu_{\mathrm{Q}}^{\mathrm{d}}$'s. Since for **NBN** there are a total of six such results the problem is highly over-determined and accurate values for the S(sym) elements can be derived from the experimental spectra and suitably calculated $\mathrm{q}_{\alpha\beta}$'s. The results so obtained are $S_{\mathrm{aa}} = -5.36 \times 10^{-3}$, $(S_{\mathrm{bb}} - S_{\mathrm{cc}}) = -8.07 \times 10^{-3}$ and $S_{\mathrm{bc}} = +2.68 \times 10^{-3}$.

The situation is more subtle for the S(anti) part of the ordering matrix. Although S(anti) consists of only two elements, S_{ab} and S_{ac}, and four $\Delta\nu_{\mathrm{Q}}^{\mathrm{e}}$(anti)'s are available, only the absolute values of the latter are known. As explained above, this is so because we are unable to identify signals in the spectrum with one or another member of an enantiotopic pair. For instance which of the doublets labeled 10, 13 in the spectrum (see the 1D traces in **Figure 9b**) corresponds to the front face of the norbornene molecule (labeled 10) and which to the back one (labeled 13). It is possible, nevertheless, to go one step further and at least determine the relative signs of the S_{ab} and S_{ac} by a least square procedure, provided data for more than two enantiotopic pairs are available. To do so, the available $\Delta\nu_{\mathrm{Q}}^{\mathrm{e}}$(anti)'s with all possible relative signs are subjected to a best fit analysis. There are 2^{n} such combinations, where n is the number of $\Delta\nu_{\mathrm{Q}}^{\mathrm{e}}$(anti)'s available (n must be larger

than 2). The 2^n combinations comprise two sets of equations related to each other by inversion of all signs of the $\Delta\nu_Q^e$(anti)'s. The two sets will give identical, best fit $S_{\alpha\beta}$(anti)'s with the same uncertainty, but of opposite signs. It is therefore sufficient to perform only 2^{n-1} such analyses, with the understanding that for the best-fit result, so obtained, there is an equally likely result with the same absolute values for the $S_{\alpha\beta}$(anti)'s, but with opposite signs. The procedure thus provides the magnitudes and relative signs of the elements of S(anti), but not their absolute signs.[54] Actual analysis of the **NBN** spectra using all four available enantiotopic pairs (10/13, 16/14, 17/15, 11/12) yielded, $S_{ab} = \pm 1.29 \times 10^{-4}$ and $S_{ac} = \pm 1.33 \times 10^{-4}$, where the signs are correlated, namely either both are positive or both are negative.

This result amount to identifying the sets of nuclei belonging to the same stereogenic faces of the molecule, even though the ambiguity about which of the faces remains unsolved. For the particular case of **NBN** the analysis showed that the signals identified in the spectrum as 10, 16, 15, 11 belong to one stereogenic face, while those labeled, 13, 17, 14, 12, to the other.

An important advantage of the factorization method concerns the accuracy of the resulting $S_{\alpha\beta}$'s. The factorization separates the equations for $\Delta\nu_Q^e$(sym) from those for $\Delta\nu_Q^e$(anti). The former consists of averages of usually large numbers, which are therefore known relatively accurately, yielding S(sym) values of high accuracy. On the other hand the results for $\Delta\nu_Q^e$(anti) are usually small differences between large numbers and carry, therefore, larger intrinsic uncertainty. This distinction is not manifested when the $S_{\alpha\beta}$'s are calculated from the unfactorized **equations of the type 44, 45**. The uncertainty in the final results is then a blend due to both type of $S_{\alpha\beta}$'s, lending uncertainty from one type to the other.

Before the introduction of the factorization method a scheme was developed for best fitting the NMR results in CLC (and ALC) using an iteration procedure. In so doing the

degeneracy of the results with respect to the $S_{\alpha\beta}$(anti)'s disappeared (apparently due to rounding off of numbers) and single sets of "best fit" order parameters, including absolute signs even for the antisymmetric elements, were obtained. As discussed above, this is equivalent to absolutely identifying signals of enantiotops with specific sites in the molecule, contrary to the principles of chirality.

4.4 Molecules with S_4 symmetry

The last of the allowed symmetry groups is S_4. It is, however rare amongst rigid molecules, although it often appears as intermediate conformation in flexible molecules. A rare exception is the 1,3,5,7-tetramethylcyclooctatetrene (**TMCOT**) that will be referred to in **Section 6**, in connection with dynamic effects. The only example of a rigid S_4 molecule for which deuterium NMR measurements in CLC were performed and its chiral discrimination completely analyzed is 1,3,5,7-tetraazapentacyclo-[3.3.2.4^{9,10}.4^{11,12}]-icosane denoted hereafter **icosane** (**Figure 10b**).[77] ^{2}H measurements were done on both isotopically normal and octa-deuterated (in the C_4 methylenes, **icosane-d$_8$**) compounds.

4.4.1 Icosane. In ALC, this particular molecule is effectively axial along its S_4 axis and consequently only a single independent parameter, S_{aa}, is needed to describe its orientation in such solvents. In CLC this (improper) symmetry element is quenched and the molecule acquires an effective C_2 symmetry (see **Table 2**). Three order parameters are required to describe its ordering in such solvents, S_{aa}, ($S_{bb} - S_{cc}$) and S_{bc}, with the latter two belonging to S(anti). The deuterium quadruple splitting of a pair of enantiotopically related sites in CLC thus becomes,[77]

$$\Delta\nu_{\mathrm{Q}}^{r} = \mathrm{q}_{\mathrm{aa}}^{\mathrm{e}} S_{\mathrm{aa}} + \left[\frac{1}{3}(\mathrm{q}_{\mathrm{bb}}^{\mathrm{e}} - \mathrm{q}_{\mathrm{cc}}^{\mathrm{e}})(S_{\mathrm{bb}} - S_{\mathrm{cc}}) + \frac{4}{3}\mathrm{q}_{\mathrm{bc}}^{\mathrm{e}} S_{\mathrm{bc}}\right] \qquad \textbf{(49)}$$

$$\Delta\nu_{\mathrm{Q}}^{s} = \mathrm{q}_{\mathrm{aa}}^{\mathrm{e}} S_{\mathrm{aa}} - \left[\tfrac{1}{3}(\mathrm{q}_{\mathrm{bb}}^{\mathrm{e}} - \mathrm{q}_{\mathrm{cc}}^{\mathrm{e}})(S_{\mathrm{bb}} - S_{\mathrm{cc}}) + \tfrac{4}{3}\mathrm{q}_{\mathrm{bc}}^{\mathrm{e}} S_{\mathrm{bc}}\right] \quad \textbf{(50)}$$

and taking the symmetric and antisymmetric combinations yields,

$$\Delta\nu_{\mathrm{Q}}^{e}(\mathrm{sym}) = \mathrm{q}_{\mathrm{aa}}^{\mathrm{e}} S_{\mathrm{aa}} \quad \textbf{(51)}$$

$$\left|\Delta\nu_{\mathrm{Q}}^{e}(\mathrm{anti})\right| = \left|\tfrac{1}{3}(\mathrm{q}_{\mathrm{bb}}^{\mathrm{e}} - \mathrm{q}_{\mathrm{cc}}^{\mathrm{e}})(S_{\mathrm{bb}} - S_{\mathrm{cc}}) + \tfrac{4}{3}\mathrm{q}_{\mathrm{bc}}^{\mathrm{e}} S_{\mathrm{bc}}\right| \quad \textbf{(52)}$$

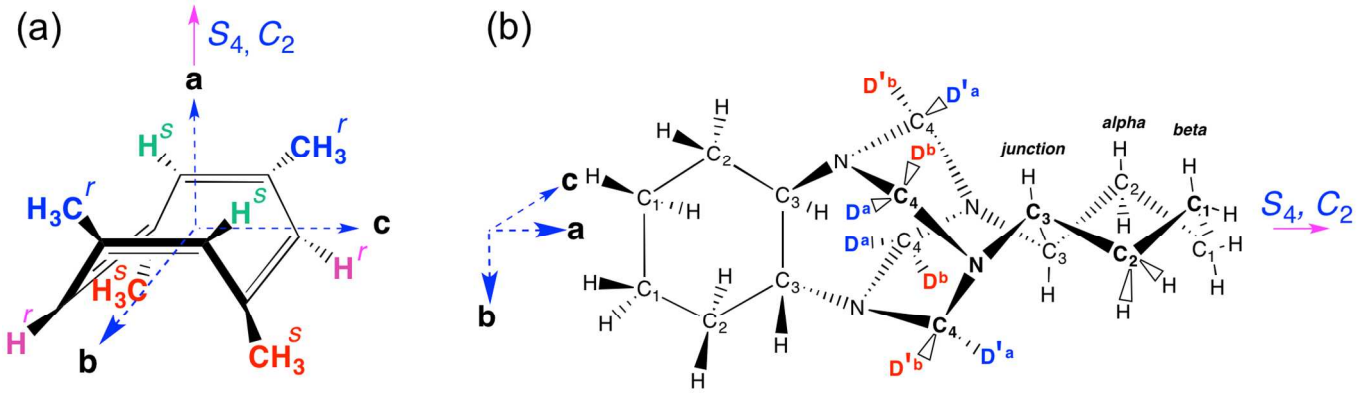

Fig. 10. (a) Structure of **TMCOT**. (b) Molecular structure, atomic numbering and coordinate systems of **icosane-d$_8$**. The *r*/*s* notation shown is arbitrarily given here. Figure adapted from ref. **77**.

Hence, measurement on a single diastereotopic site or a single pair of homotopic or enantiotopic sites with known $\mathrm{q}_{\alpha\beta}$ is sufficient to determine S_{aa}, while at least three pairs of enantiotopic sites are required for determining the *S*(anti)'s, including their relative signs, by the best-fit method. Since no atoms are located along the C_2 axis of the icosane molecule (no diastereotopic sites) the molecule consists entirely of enantiotopic (and homotopic) pairs, rendering the best fit analysis highly over determined. This approach was in fact successfully applied, in the original work, using the NAD spectrum of icosane solutions in CLC.

For the present example, however, we choose to demonstrate an alternative approach for correlating enantiotopic sites using a special 2D-NMR correlation experiment on a specifically deuterated icosane in the core methylene group (**icosane-d$_8$**).

One-dimensional proton decoupled deuterium NMR spectra of this compound in ALC and CLC are shown in the top and bottom traces of **Figure 11a**. In ALC two quadrupole doublets are observed due to the two inequivalent deuterons, labeled a and b, in the structural formula of **Figure 11**. Their signals were unequivocally identified on the basis of their known chemical shifts, the ratio of their quadrupole splitting and computed geometry of the icosane molecule. From the quadrupolar splittings in ALC and the computed q_{aa}'s for the 4a and 4b deuterons (-18.84 kHz and +70.66 kHz) an average value of $S_{aa} = 6.59 \times 10^{-3}$ is obtained for the order parameter in the ALC solution.[77]

When dissolved in CLC, each of the doublets splits into two since the primed a', b', and unprimed, a, b, enantiotopic positions become non-equivalent. At this stage of the analysis, not only can the signal a, a' (b, b') be identified with the similarly labeled sites in the structural formula, but even which signals belong to the same methylene group is not known. Such an identification allows the determination of the relative signs of the $\Delta\nu_Q^e$(anti) for the a and b pairs. The high enrichment of the methylene groups in icosane-d_8 made it possible to perform a ^{2}H-^{2}H COSY-90 2D experiment. The experiment correlates between neighboring deuterons via their scalar and dipolar interactions. An example of such a spectrum for **icosane-d_8** dissolved in CLC is shown in **Figure 11b**. In this system only dipolar interactions between deuterons belonging to the same methylene group are sufficiently strong to produce observable correlation peaks. They are connected in the figure with dashed lines, forming two octagons, each associated with a particular (primed or unprimed) methylene group. This labeling does not necessarily correspond to the primed or unprimed labels in the structural formula, but it does identify signals of deuterons belonging to the same methylene and thus provides the relative signs of $\Delta\nu_Q^{4a}$ (anti) and $\Delta\nu_Q^{4b}$(anti). From the data in the spectra they are ±175 Hz and ∓61.5 Hz, respectively and using **Eq. 52** with the appropriate $q_{\alpha\beta}$ finally yields, $(S_{bb} - S_{cc}) = \pm 1.87 \times 10^{-3}$ and $S_{bc} = \mp 1.52 \times 10^{-3}$, i.e. if one is positive, the other is negative and *vice*

versa, and after diagonalization, $S_{aa} = S_{a'a'} = +6.59 \times 10^{-3}$, $(S_{b'b'} - S_{c'c'}) = \pm 3.58 \times 10^{-3}$ and $\alpha = -29.2°$. Note that the sign of the rhombicity is undetermined but the angle is negative. This is a consequence of the sign correlation of the *S*(anti) leading to only one sign uncertainty.[77]

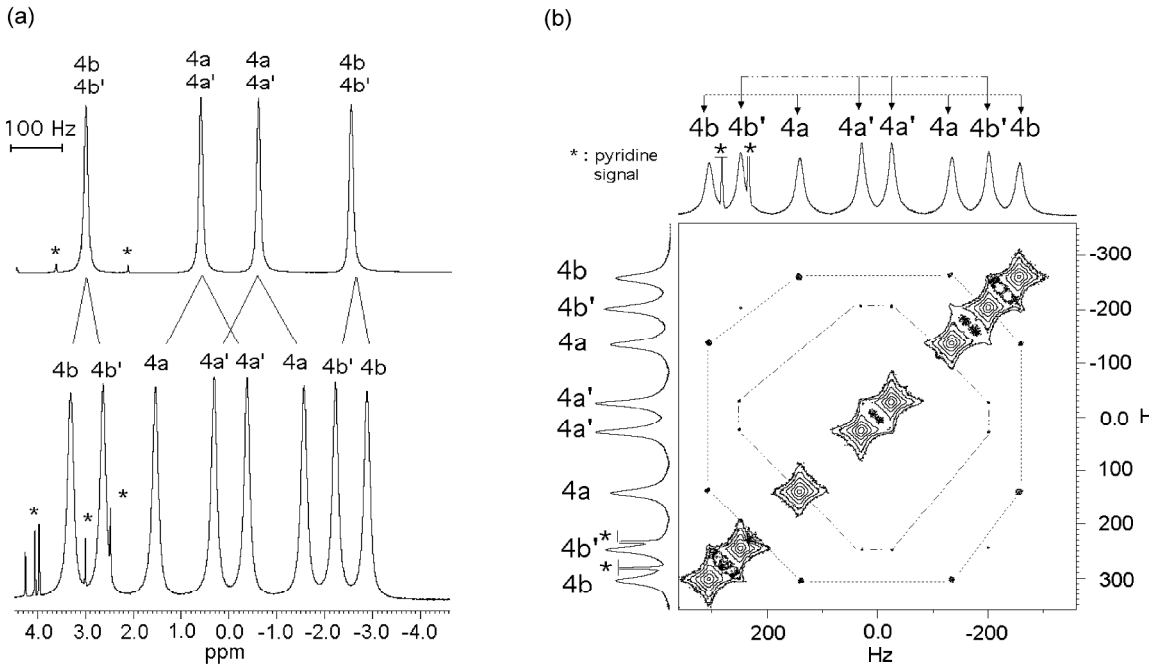

Fig. 11. (a) ^{2}H-{^{1}H} 1D-NMR spectra (92 MHz) of **icosane-d$_8$** in ALC (PBG/pyridine) (top) and in CLC (PBLG/pyridine) (bottom) both recorded at 310 K (asterisk indicate pyridine NAD signals). (b) Associated ^{2}H-^{2}H COSY-90 2D spectrum in CLC at the same temperature. The dashed lines connect signals of deuterons that are correlated by dipolar interactions (belonging to the same methylene groups). Figure adapted from ref. **77**.

This example completes the list of symmetries of rigid molecules that can display enantiotopic discrimination by ordering in CLC. It is remarkable that amongst the essentially infinite improper groups only the four described above (D_{2d}, C_{2v}, C_s and S_4) can exhibit such discrimination. Among these the groups C_{2v} and C_s are very common in nature and include many rigid organic molecules. The procedures described above for analyzing their discrimination in NMR spectroscopy may therefore be of general use in investigating such compounds.

5. Enantiotopic discrimination in flexible solutes

So far we have discussed enantiotopic discrimination in rigid prochiral solutes, with well-defined structure and symmetry. A special category of solutes which exhibit discrimination similar in nature to that of rigid prochiral solutes, but of quite different origin, consist of (racemic) mixtures of flexible chiral compounds whose enantiomers rapidly interconvert on the NMR timescale. Solutions of such compounds exhibit NMR spectra corresponding to the average Hamiltonian of the interconverting enantiomers. If the enantiomers possess nonequivalent sites that interchanged by the racemization process they become on the average enantiotopic and will exhibit enantio discrimination when dissolved in CLC. We refer to this phenomenon as dynamic enantio-discrimination. In the present section we discuss the origin of this effect and present a few examples. We begin by defining what is meant by the symmetry of this average Hamltonian, or rather, the symmetry of the average structure of the interconverting species. It is convenient to do so using Altmann's formalism for average symmetry.[78]

In this formalism, different conformers possessing identical number of A–B bonds (A, B are atoms) with identical lengths are considered equivalent and referred to as isodynamic. The symmetry group of these isodynamic conformers is called the Schrödinger group, G. For our purpose, since we are dealing with optical isomers G is a proper point group. In achiral solvents, the various chiral conformers have identical energies. The operations that transform one isodynamic conformer (enantiomer) to another are not symmetry operations, but are isomorphic to such operations. These operations form a group, referred to as the isodynamic group, I. In the present case these transformations correspond to racemization, hence I is isomorphic with an improper group. It has no common elements with G (except the identity, *E*), but it is invariant with respect to the elements of G. When these transformations are fast (on the NMR timescale, or feasible in Altmann's terminology) the symmetry of the resulting average species corresponds to the group product of I and G,

$$S = I \times G \quad \textbf{(53)}$$

where S is referred to as the Schrödinger super group. As I is improper so is S and thus the symmetry of the average structure corresponds to that of an improper group, rendering it prochiral. In general, no real molecule with such an average structure actually exists, but it is nevertheless possible to associate with it a spin Hamiltonian, that gives rise to the observed spectrum. Enantiotopic sites in this average structure, resulting from interchange of nonequivalent sites in the enantiomers will exhibit enantiodiscrimination in CLC.[79,80,81] Although the effect is formally similar to enantiotopic discrimination in rigid solutes, its origin is entirely different and it follows different selectivity rules.

As a model example consider the rapidly interconverting chiral conformers (*R* and *L*) of a phenyl dioxyethylene moiety (**Figure 12**). The (Schrödinger) symmetry group of these conformers is, G = C_2 = (*E*, C_2), while the isodynamic operation that interconverts the two isodynamic conformations is isomorphic with σ_v, i.e. a reflection about a plane that includes the C_2 axis. Hence I = C_s = (*E*, σ_v), and the Schrödinger super group becomes,

$$S = I \times G = C_s \times C_2 = C_{2v} \quad \textbf{(54)}$$

We note in **Figure 12** that the pairs of atoms A, A' and B, B' are homotopic (related by the C_2 operation), while the pairs A, B and A', B' are nonequivalent and interchange by the racemization. Hence the A and B atoms become enantiotopic in the average (Schrödinger super group) structure and should exhibit discrimination in CLC. Assuming that A and B are deuterons, their NMR spectrum in a liquid crystalline solution will consists of quadrupole doublets with splittings corresponding to the weighted average splittings in the two enantiomers,

$$\langle \Delta\nu_Q^A \rangle = p^R q_{C-D} S_{C-A}^R + p^L q_{C-D} S_{C-A}^L \quad \textbf{(55)}$$

$$\langle \Delta\nu_{\mathrm{Q}}^{\mathrm{B}} \rangle = \mathrm{p}^{R} q_{\mathrm{C-D}} S_{\mathrm{C-B}}^{R} + \mathrm{p}^{L} q_{\mathrm{C-D}} S_{\mathrm{C-B}}^{L} \qquad (56)$$

where p^{J} (J = *R*, *L*) is the equilibrium fractional population of enantiomer J, $S_{\mathrm{C-K}}^{\mathrm{J}}$ (K = A, B or A', B') is the orientation order of the C-K bond in the J enantiomer and $q_{\mathrm{C-D}}$ is q_{zz} along the C-D bond (see **Table 2**). In an ALC, the population of the two enantiomers is the same, hence, $\mathrm{P}^{R} = \mathrm{P}^{L} = ½$. Since the C-$\mathrm{A}^{R}$ and C-B^{L} bonds are enantiomeric images their ordering in ALC is identical, $S_{\mathrm{C-A}}^{R} = S_{\mathrm{C-B}}^{L}$ and likewise $S_{\mathrm{C-B'}}^{R} = S_{\mathrm{C-A'}}^{L}$. Substituting these equalities in **Eqs. 55,56**, gives $<\Delta\nu_{\mathrm{Q}}^{\mathrm{A}}> = <\Delta\nu_{\mathrm{Q}}^{\mathrm{B}}>$, namely in the fast exchange limit in ALC deuterons A and B (A', B') exhibit identical splitting.

The situation is different in CLC; the two enantiomers may have different populations, $\mathrm{P}^{R} \neq \mathrm{P}^{L}$, and more importantly their ordering will in general be different, $S_{\mathrm{C-A}}^{R} \neq S_{\mathrm{C-B}}^{L}$. Hence, instead of a single quadrupolar doublet as in ALC, two doublets are expected in CLC with $<\Delta\nu_{\mathrm{Q}}^{\mathrm{A}}> \neq <\Delta\nu_{\mathrm{Q}}^{\mathrm{B}}>$. The extend of the discrimination can be obtained from the difference of the two splittings,

$$\langle \Delta\nu_{\mathrm{Q}}^{\mathrm{B}} \rangle - \langle \Delta\nu_{\mathrm{Q}}^{\mathrm{B}} \rangle = q_{\mathrm{C-D}}[\mathrm{p}^{R}(S_{\mathrm{C-A}}^{R} - S_{\mathrm{C-B}}^{R}) - \mathrm{p}^{L}(S_{\mathrm{C-A}}^{L} - S_{\mathrm{C-B}}^{L})] \qquad (57)$$

Thus the dynamic enantio-discrimination of flexible (on the average prochiral) solutes in CLC, originates in the discrimination (different ordering/population) of the rapidly interconverting enantiomers and is not directly related to the (average) symmetry of the molecule. In fact this type of enantio-discrimination can occur in any flexible solute with an average improper symmetry possessing (on the average) enantiotopic sites. In particular it is not limited to the allowed, forbidden or any other category of improper symmetries. In practice, the main effect responsible for the dynamic discrimination is the difference in ordering of the interconverting enantiomers, rather than in their populations.

The strength of solute-solvent interactions in such solutions are neither sufficient to affect the relative populations of the enantiomers nor to modify significantly their structure or magnetic parameters. These interactions, which are shape dependent, are exactly those that determine the ordering of solutes in liquid crystals and will therefore be different for different enantiomers dissolved in a CLC, as indeed observed experimentally. In contrast, no effects on the relative population of equilibrating enantiomers in such systems are observed. In the following discussion it is therefore assumed that $p^R = p^S = 0.5$ and also $S^R_{C-K} \neq S^L_{C-K}$. Also we shall use molecular, rather than bond, ordering and express it in terms of the elements of the Saupe ordering matrices. It should finally be noticed that since the averaging process (racemization) must be fast on the NMR timescale it is less likely to occur in compounds with stereogenic centers. More likely candidates are structurally chiral compound where racemization involves bond rotation or bond twisting. The examples presented below belong to this category.

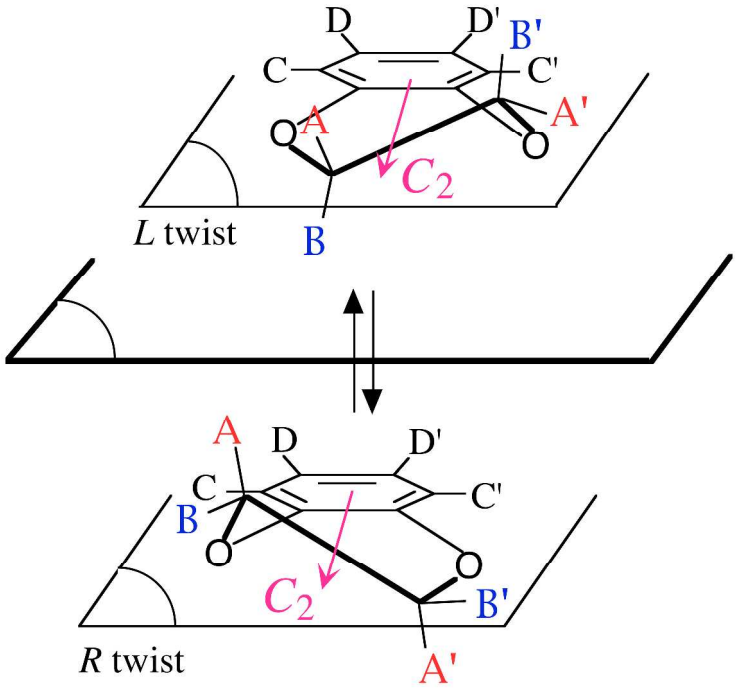

Fig. 12. Schematic representation of the two enantiomers of a phenyl dioxyethylene moiety. The C_2 axes of the Schrödinger group and the σ_v plane of the isodynamic group are indicated. Figure adapted from ref. **79**.

5.1 Molecules with average planar symmetry

An often occurring situation in flexible molecules is one in which the fast interconversion between equivalent (or sometimes also none-equivalent) conformers leads to and average planar symmetry, such as C_s, C_{2h} or C_{2v}. Amongst the numerous examples we present below just three, ethanol, benzylalcohol and diidoferrocene.

5.1.1 Ethanol. A typical example of a flexble molecule with such average symmetry is ethanol. The fast rotation of the methyl groups results in interconversion between many rotamers differing from each other by the dihedral angles of the hydroxyl and methyl groups relative to the methylene frame. Most of these rotamers are of C_1 symmetry. They appear, however, in pairs of isodynamic enantiomers related to each other by reflection about a plane bisecting the methylene group. The methylene hydrogens are nonequivalent in these rotamers, but become so during the inter-exchange of the rotamers. Hence, on the average, the molecule acquires a C_s symmetry and the methylene hydrogens become enantiotopically related. In CLC they should therefore exhibit dynamic discrimination. This is well confirmed in the three spectra of ethanol dissolved in CLC depicted in **Figure 13**.[50] In part a of the figure is shown the ^{2}H spectrum of a perdeuterated ethanol dissolved in PBLG/$CDCl_3$. The spectrum clearly exhibits two doublets for the methylene deuterons (indicated by solid and open circles) and just one for the methyl (labeled A) and hydroxyl (OD) groups (just one component is shownfor the latter).

In **Figure 13b** is shown the ^{13}C spectrum of the methylene group in a solution containing a mixture of isotopically normal and perdeuterated ethanol in PBLG/$CDCl_3$. The perdeuterated solute shows a clear (1:1:1) triplet of triplets (indicated by solid circles) due to splittings with two none-equivalent deuterons (I = 1), while the isotopically normal solute (indicated by asterisks) shows a typical (X) pattern due to an AA'X spin system (note the weak satellites of the center peak) with unresolved splittings with the

methyl hydrogens. Note also the difference of chemical shift of C-1 signal in the CH_2 and CD_2 group due to ^2H isotope effect on the $\delta(^{13}C)$.[73] The case of isotopically normal ethanol dissolved in PBCLL/$CDCl_3$ will be examined in **Section 11**.

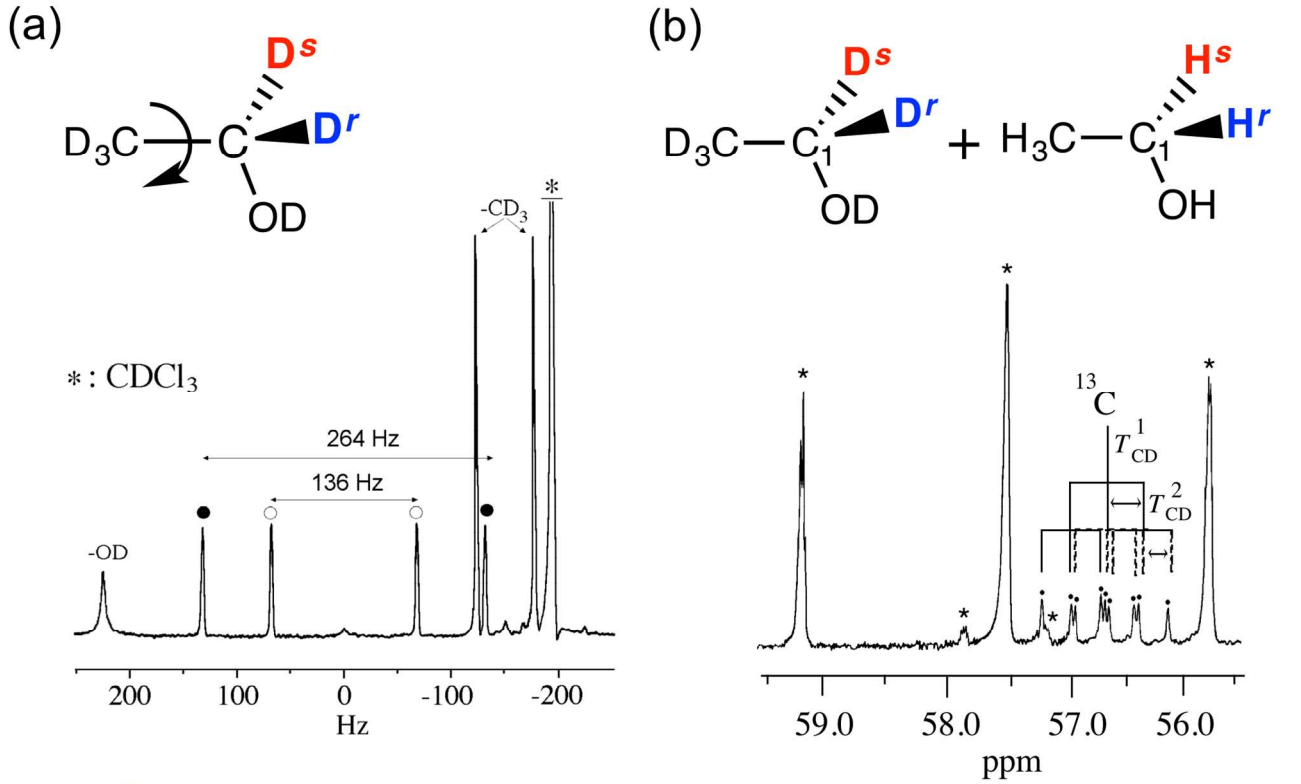

Fig. 13. (a) ^2H-{^1H} (partial) 1D spectrum (61.4 MHz) of **ethanol-d_6** dissolved in PBLG/$CDCl_3$. QDs of methylene group are labeled with solid and open circles. (b) Proton and deuterium coupled ^{13}C 1D signals (100.1 MHz) of the C-1 carbon in a mixture of isotopically normal and perdeuterated ethanol dissolved in PBLG/$CHCl_3$. Figure adapted from **ref. 50**.

5.1.2 Benzylalcohol. A similar situation applies to benzylalcohol (**BZA**). The fast combined rotation/flipping of the benzene ring on one hand and that of the hydroxyl group on the other, results in and average, $C_s \times C_2 \times C_1 = C_{2v}$ symmetry, rendering the methylene (but not the *ortho*- and *meta*-aromatic) hydrogens, enantiotopically related. This has been successively demonstrated on the ^2H-{^1H} 1D spectrum of the dideuterated benzylalcohol (**BZA-d_2**), the enantioselectively enriched monodeuterated **BZA** (**BZA-d_1**),[83] and observed as well at natural abundance deuterium level,[58] and on NASDAC correlation 2D-NMR spectra,[72] as depicted in **Figure 14b**. On this heteronuclear map,

two ^{2}H QDs correlate to the ^{13}C peak of the methylene carbon, but only single QDs to the aromatic *ortho*- and *meta*-carbons. Note that the NASDAC 2D spectrum was recorded at the natural abundance of the doubly labeled ^{13}C-^{2}H molecules (1.7×10^{-6} relative to ^{1}H). This heteronuclear correlation 2D sequence based on a classical HETCOR-type transfer scheme was specifically designed to select only the signal of ^{13}C-^{2}H isotopomers while those of ^{13}C-^{1}H and ^{12}C-^{2}H isotopomers are eliminated.[69,72]

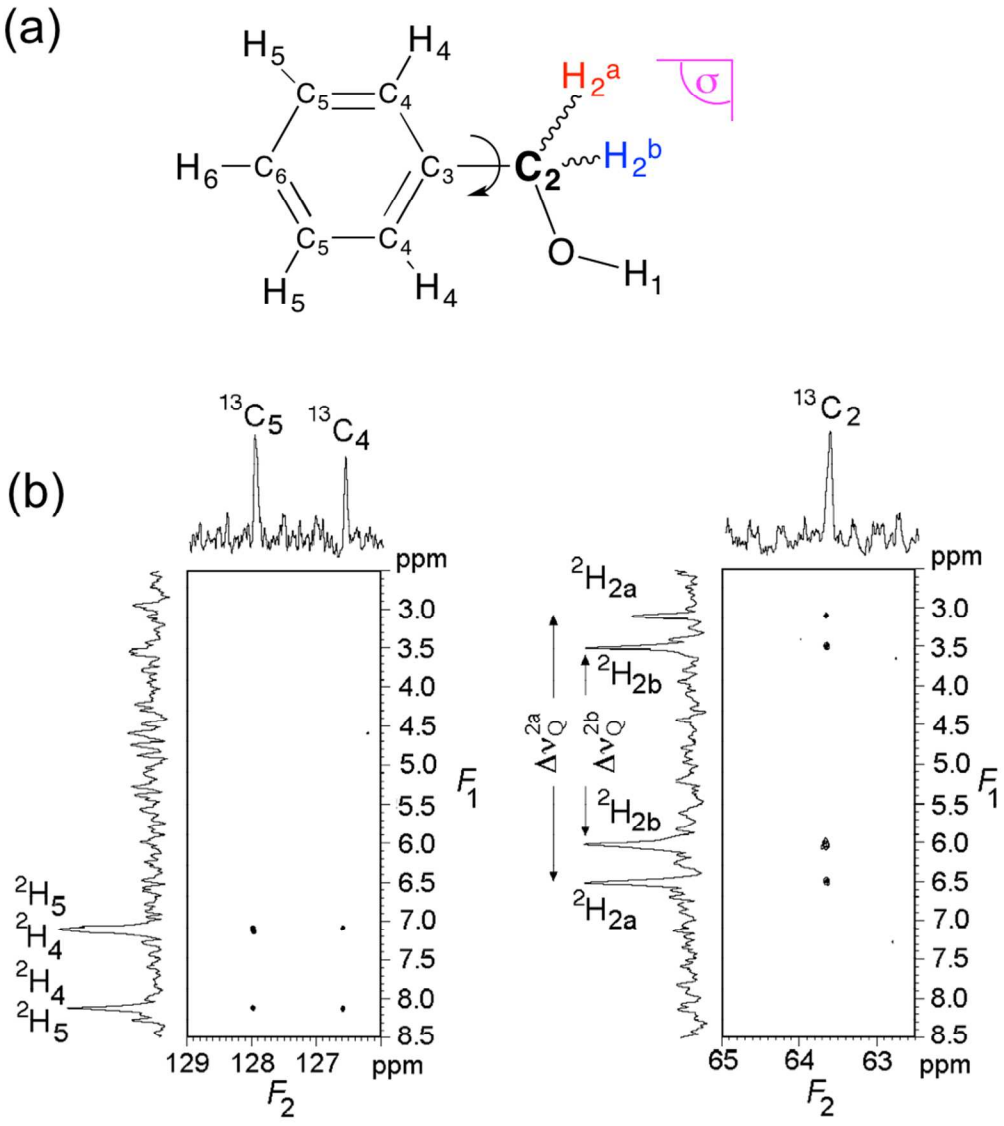

Fig. 14. (a) Structure and atomic numbering of **benzyl alcohol**. (b) Expansions (aromatic and aliphatic parts) of the associated NASDAC 2D map dissolved in PBLG/$CHCl_3$ at 300 K and recorded at 21.1 T on a TCI cryogenic probe. Figure adapted from ref. **72**.

5.1.3 1,2-diiodoferrocene. The last example in this category is diiodoferrocene, (**DIF**) consisting of rapidly reorienting pentagonal rings with average C_s symmetry (see **Figure 15a**).[84] This motion renders hydrogens b and b' enantiotopic and as expected they exhibit doubling in the NAD *Q*-COSY spectrum when dissolved in a CLC solution (see **Figure 15b**). There is little that one can do with results of the type described above by way of quantitative analysis, because of the large number of rotamers that needs to be considered, exceeding by far the amount of experimental data that can be recorded. Although it is nevertheless possible to derive ordering parameters from the average spectra in ALC or from the discriminated results in CLC, they are of little use since they do not correspond to genuine geometries.

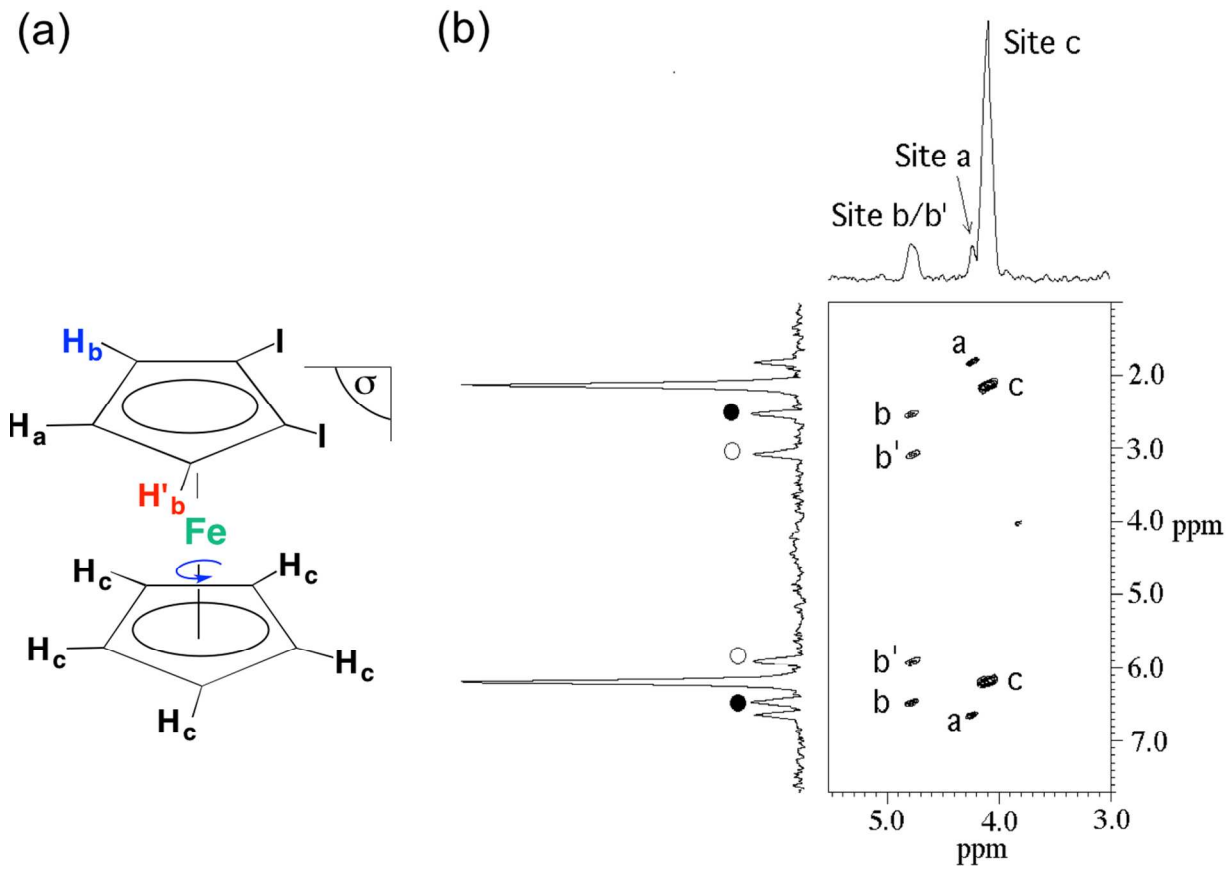

Fig. 15. (a) Structure of **1,2-di-iodoferrocene**. (b) Associated tilted NAD *Q*-COSY Fz 2D spectrum (92.1 MHz) recorded in the CLC (PBLG/$CHCl_3$) at 300 K. Figure adapted from ref. **84**.

5.2 Molecules with average *axial* symmetry

In this second category are included molecules that on the average possess a C_n axis (n $\geq$ 3) consisting of flexible side chains and/or flexible cores. Three examples will be presented with average symmetries, D_{3h}, C_{3v} and C_{3h}.

5.2.1 Tridioxyethylenetriphenylene. A typical example is that of tridioxyethylenetriphenylene **(TDT)**, consisting of a rigid triphenylene core and flexible dioxyethylene side chains (see **Figure 16a**),[80] which rapidly interconvert between a right- and a left-twist (*R*/*L*) as shown in **Figure 12**. For this compound there are two types of isodynamic conformers, depending on the relative twists of the three dioxyethylene groups. One consisting of the two enantiomers with D_3 symmetry in which the twist is cyclic *RRR* or *LLL* (see **Figure 16b**). Interchange between these enantiomers is isomorphic with reflection in a plane perpendicular to the C_3 axis. Hence, the isodynamic group is I = C_s and the average symmetry becomes, $C_s \times D_3 = D_{3h}$. The other type of conformers with C_2 symmetry consists of the homomers *RLL*, *LRL*, *LLR* and their corresponding enantiomers. Switching between these homomers is isomorphic with proper group C_3, while interchange between enantiomers corresponds again to C_s. Hence $S = C_3 \times C_s \times C_2 = D_{3h}$, as for the other type of conformers. Clearly interchange between the two types of conformers leaves the average D_{3h} symmetry unchanged. During the interconversion processes the non-equivalent methylene hydrogens interchange and become enantiotopic on the average. Hence they yield a single doublet in the deuterium spectrum recorded in ALC, but two doublets in CLC, as shown in **Figure 16c**.

To analyze the extent of this dynamic discrimination quantitatively it was assumed that the dominant ordering direction for all the conformers is the C_3 axis of the triphenylene core and neglects any biaxial ordering. This is exact for the D_3 conformers and a plausible assumption for the C_2 conformers. It is further assume that the geometry

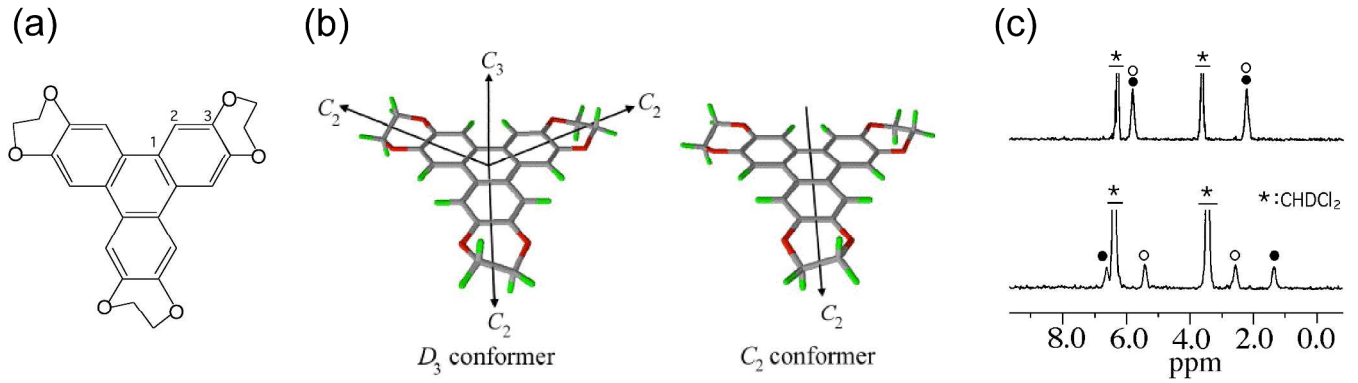

Fig. 16. (a) Structural formula of **TDT**. (b) The two conformers of **TDT**: (left) the *LLL* conformer with D_3 symmetry, (right) one of the *RLL* conformers with C_2 symmetry. (c) F_2 projection of the 92.1 MHz ^{2}H Q-COSY Fz 2D spectra of partially deuterated **TDT** (in the dioxyethylene groups) dissolved in ALC (PBG/CH_2Cl_2) (top) and in CLC (PBLG/CH_2Cl_2) (bottom) at 302 K. The open and closed circles mark the ethylene deuterons, the asterisks the NAD signal of the dichloromethylene. Figure adapted from ref. **80**.

of the enantiomers is not affected by the solvent chirality and they remain mirror images also in CLC. Using the notation of **Figure 12**, one can identify the C-A bonds in the *R* and *L* enantiomers as axial (ax) and equatorial (eq), respectively, and *vice versa* for the C-B bonds. The average quadrupole splitting of the two deuterons then become (see **Eqs. 55,56**):

$$\langle \Delta\nu_{\mathrm{Q}}^{\mathrm{A}} \rangle = \mathrm{p}^{R} \Delta\nu_{\mathrm{Q}}^{\mathrm{ax}} S_{\mathrm{aa}}^{R} + \mathrm{p}^{L} \Delta\nu_{\mathrm{Q}}^{\mathrm{eq}} S_{\mathrm{aa}}^{L} \qquad \textbf{(58)}$$

and

$$\langle \Delta\nu_{\mathrm{Q}}^{\mathrm{B}} \rangle = \mathrm{p}^{R} \Delta\nu_{\mathrm{Q}}^{\mathrm{eq}} S_{\mathrm{aa}}^{R} + \mathrm{p}^{L} \Delta\nu_{\mathrm{Q}}^{\mathrm{ax}} S_{\mathrm{aa}}^{L} \qquad \textbf{(59)}$$

where

$$\Delta\nu_{\mathrm{Q}}^{\mathrm{eq/ax}} = \frac{1}{2} \mathrm{q}_{zz} \left(3\cos^2 \beta^{\mathrm{eq/ax}} - 1 \right) \qquad \textbf{(60)}$$

and $\beta^{\mathrm{eq/ax}}$ is the angle between the C-(eq/ax) bond and the C_3 axis of the triphenylene core. Thus in ALC $<\Delta\nu_{\mathrm{Q}}^{\mathrm{A}}> = <\Delta\nu_{\mathrm{Q}}^{\mathrm{B}}>$ and a single doublet is expected for the methylene deuterons, while in CLC, $<\Delta\nu_{\mathrm{Q}}^{\mathrm{A}}> \neq <\Delta\nu_{\mathrm{Q}}^{\mathrm{B}}>$ and two doublets are expected, as observed experimentally (**Figure 17c**). The extent of this discrimination (taking $\mathrm{p}^{R} = \mathrm{p}^{L} = ½$) then becomes,

$$\langle \Delta\nu_{\mathrm{Q}}^{\mathrm{B}} \rangle - \langle \Delta\nu_{\mathrm{Q}}^{\mathrm{B}} \rangle = \frac{1}{2}\left(\Delta\nu_{\mathrm{Q}}^{\mathrm{ax}} - \Delta\nu_{\mathrm{Q}}^{\mathrm{eq}}\right)\left(S_{\mathrm{aa}}^{L} - S_{\mathrm{aa}}^{L}\right) \quad \textbf{(61)}$$

and thus basically depends on two factors; a geometrical factor, related to the orientation of the C-D bonds relative to the molecular C_3 axis and on the different ordering of the two enantiomers. The first can be calculated from the geometry of the phenylene-dioxyethylene moiety. It is particularly large in the present case because the axial bonds are nearly parallel to C_3, while the equatorial ones are nearly perpendicular to it. From the known geometry of this group, it was possible to determine the discrimination factor, for the spectra shown in **Figure 16c**, yielding $|(S_{\mathrm{aa}}^{R} - S_{\mathrm{aa}}^{L})/½(S_{\mathrm{aa}}^{R} + S_{\mathrm{aa}}^{L})| = 0.25$. This is a particularly large value for chiral solutes and most likely reflects the screw like structure of **TDT** which fits well the CLC environment for one enantiomer and inversely so for the other.

5.2.2 Tridioxyethylenecyclotriveratrylene. A similar situation applies to the crown form of tridioxyethylene derivative of tribenzocycloctatriene (commonly called cyclotriveratrylene, CTV) (and denoted here **c-TDCTV**) (**Figure 17**).[79] The core of this molecule is rigid with C_3 symmetry, while the side chains are flexible and interconvert between two twisted forms, yielding on the average C_{3v} symmetry. The situation is similar to that for the **TDT** compound, except that here in the frozen form the four hydrogens are nonequivalent and the dynamic process averages pairwise the outer (A, B') and inner (B,A') atoms. Consequently in ALC two doublets are observed due to the averaged pairs, while in CLC four, reflecting the effect of the dynamic enantio-discrimination (**Figure 17**). The extent of the discrimination is, however, lower than that in **TDT**, first because of a smaller geometrical factor and also because of a smaller ordering discrimination (0.086 compared with 0.25).

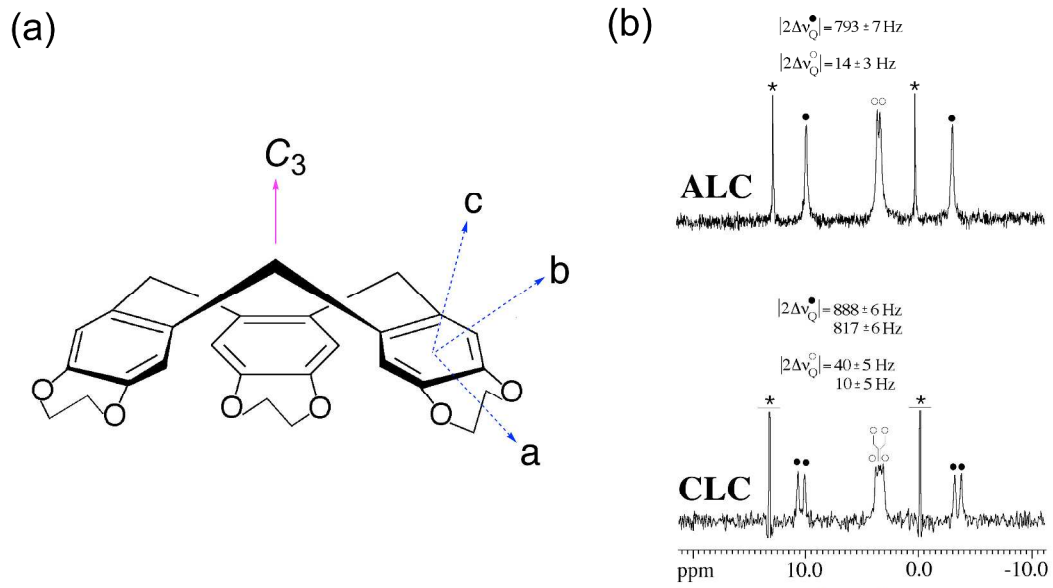

Fig. 17. (a) Structural formula of the crown form of **c-TDCTV**. (b) ^{2}H-{^{1}H} spectra (61.4 MHz) of **TDCTV**, statistically (~10 %) deuterated in the dioxyethylene side chains and recorded at 300 K in PBG/$CHCl_3$ (top) and in PBLG/$CHCl_3$ (bottom). T he solid and open circles label the inward and outward pointing deuterons of the ethylene groups. The asterisks label the signals of the natural abundance deuterium in the chloroform co-solvent. Figure adapted from ref. **79**.

5.2.3 The saddle form of nonamethoxy CTV. A dynamic discrimination of quite a different nature, but still with average axial symmetry is exhibited by the saddle form of substituted CTV.[80] Specifically we shall discuss the cyclicly substituted nonamethoxy CTV, (**s-NMCTV**, see **Figure 18**). It interconverts very slowly (on the timescale of days at room temperature) into its crown form and thus can be readily separated from the latter and studied separately. On the other hand it is highly flexible and rapidly interconverts between six different conformers as depicted in **Figure 18c**. In fact this process remains fast on the NMR timescale even down to below 100 K.

The pseudorotation cycle consists of six interconverting equivalent conformers of C_1 (improper) symmetry; three homotopic pairs of enantiomeric isomers (structures I, III, V and II, IV, VI, respectively). The interconversion between neighboring homomers in the cycle is isomorphic with a S_3 operation, and hence the isodynamic group, as well as the symmetry of the average molecule, is C_{3h}.

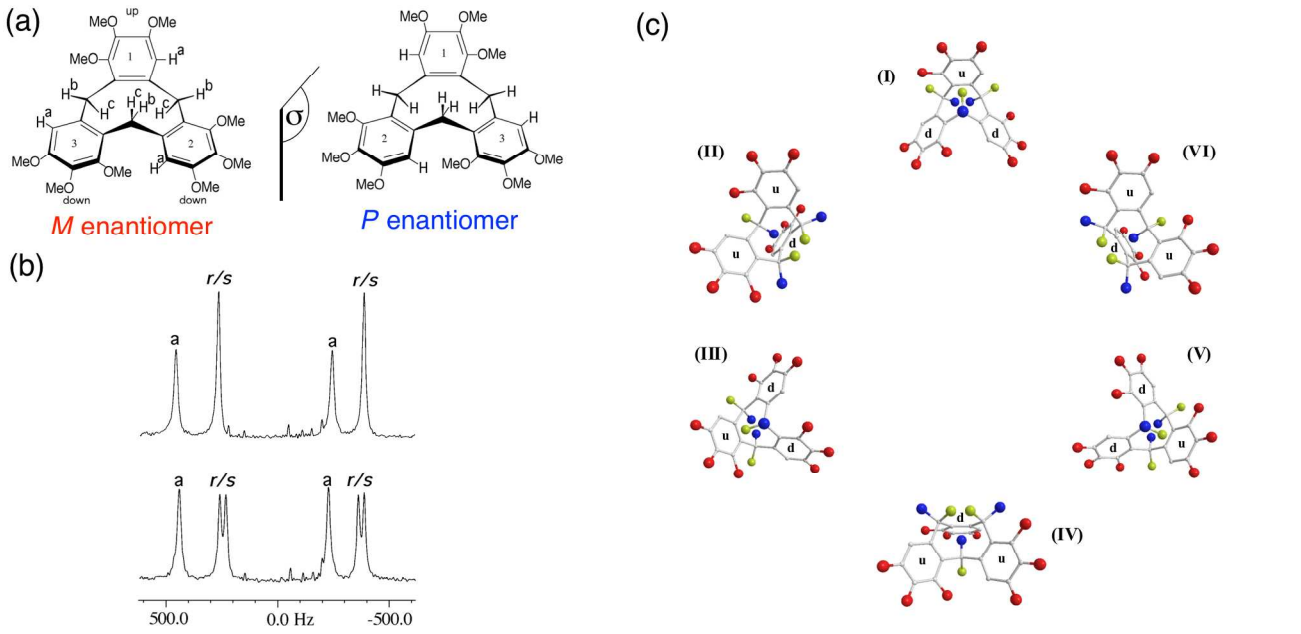

Fig. 18. (a) Structures and numbering of the enantiomers of the "frozen" saddle form **of s-NMCTV**, (b) ^{2}H-{^{1}H} 1D-NMR spectra (61.4 MHz) of an equimolar mixture of **s-NMCTV** deuterated in respectively the aromatic and methylene sites (T = 320 K). Top: dissolved in PBG/DMF; Bottom: dissolved in PBLG/DMF. (c) Schematic representation of the pseudorotation cycle of **s-NMCTV**. Conformers I, III, V and II, IV, VI, correspond, respectively, to the left and right structures in (a). Figure adapted from ref. **80**.

In this group the proper operations (C_3^1 and C_3^2) correspond to transformation between homomers, while the improper ones (S_3^1, S_3^5 and σ_h) to transformation between enantiomers. The analysis of the process is similar to that for the previous axial molecules, but requires a bit more book keeping, as detailed in ref. **80**. The main effect of interest here, namely dynamic enantio-discrimnation, concerns the nonequivalent methylene hydrogens (labeled, respectively, yellow and blue in **Figure 18c**). Under the effect of the improper operations in the psedorotation cycle they interchange and become enantiotopic on the average. Consequently they exhibit spectral discrimination in CLC, as can readily be seen in the deuterium NMR spectra in **Figure 18b**. The extent of the discrimination depends, as before, on a geometrical factor (the bond angles of the yellow and blue methylene hydrongens) and on the difference in ordering of the two enantiomers. Note that the same process also interchanges between groups that are enantiomeric images, such as the aromatic hydrogens and corresponding methoxy groups.

These remain, however, diastereotopic under the pseudorotation process and do not exhibit discrimination in CLC (see the signals of the aromatic hydrogen, a, in **Figure 18b**).

6. Dynamic NMR of chiral systems dissolved in CLC

By dynamic NMR, one usually refers to conditions where dynamic processes affect the lineshape of the spectrum. This occurs when the rate of the process is of the order of the magnitude of the interactions (expressed in the same unit) which give rise to the spectral splitting. Depending on the nuclei involved (most commonly, ^{1}H, ^{2}H, ^{13}C or ^{31}P) and the nature of the NMR interaction (chemical shift, scalar or dipolar coupling, quadrupole interaction), the time scale of such processes may range from seconds down to milli- or microseconds. Here we shall be interested in cases where the dynamic process involves chiral or prochiral solutes. In particular we shall be interested in systems where studying the dynamic effect requires the use of chiral solvents, or more specifically CLC.

6.1 Racemization processes

One class of such processes involves racemization. Enantiomers possessing a single stereogenic center exhibit identical spectra in ALC. Their interconversion corresponds to the exchange between image related atoms, groups and bonds and does not involve modulation of NMR frequencies. Their spectrum in ALC is therefore not affected by the racemization process. To detect and measure such racemization one could dissolve the solute in CLC, the spectra of the enantiomers will then be discriminated and racemization on the NMR timescale will result in dynamic spectra that could be used to derive kinetic parameters of the process. In practice racemization of enantiomers possessing isolated stereogenic centers is usually much too slow to exhibit dynamic effects in the NMR spectra and to our knowledge no cases involving such racemization have been published.

Structurally chiral compounds where the racemization involves bond rotation or bond twisting are much faster and often fall in the range of dynamic NMR. In fact the examples discussed in the previous section on dynamic enantio-discrimination fall in this category. The rates of the processes in these particular examples exceed, however, by far the range of dynamic NMR and remain so even on cooling to very low temperatures. There are nevertheless ample cases of systems belonging to this category of compounds which do exhibit dynamic NMR spectra due to racemization. In such cases, however, the racemization involves exchange of nonequivalent sites and modulation of interactions that exhibit dynamic effect also in achiral solvents. Their study in CLC only complicates the analysis, but does not provide additional information. To the best of our knowledge, no example in which measurements in CLC provided any advantage over that of ALC or even in achiral isotropic solvent has been reported. We shall nevertheless describe below one case of the latter category, namely that of the *cis*-isomer of decahydronaphtahlene (**DHN**).

6.1.1 Decahydronaphthalene. DHN, commonly named *cis*-decalin, consists of two condensed cyclohexane rings, sharing a common C-C bond.[85,86] It exhibits two structural isomers; *trans*- and *cis*-decalin (see **Figure 19a**). The former is rigid and possesses C_{2h} symmetry, with the two cyclohexyl rings related by a reflection plane. The molecule is thus prochiral, with two equivalent sets of four enantiotopic (and one homotopic) pairs of hydrogens. However, as C_{2h} is a forbidden group, no enantiotopic discrimination by ordering is expected nor was it observed experimentally.[87]

The ground state structure of the second isomer, *cis*-decalin, has C_2 symmetry with the two cyclohexanic rings related by two-fold rotation (**Figure 19b**). This isomer is thus optically active, exhibiting enantiomeric isomerism. The molecule is, however, flexible and, depending on the temperature, undergoes a more or less rapid interconversion between the two enantiomers. Spectral consequences can be easily monitored on

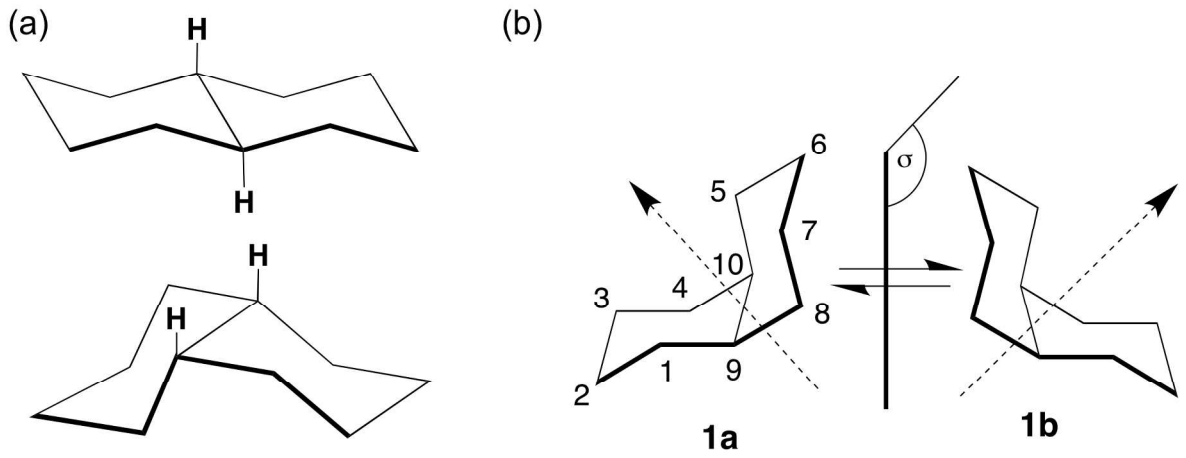

Fig. 19. (a) Structure of (top) *trans*- and (bottom) of ***cis*-decalin**. (b) The two enantiomers, **1a** and **1b**, of the *cis*-decalin, along with its atomic numbering. The position of axial/equatorial hydrogens are not specified here. Enantiomeric conformers **1a** and **1b** of C_2 symmetry that can be differentiated using NMR in CLC. Figures adapted from ref. 85.

anisotropic ^{2}H spectra (**Figure 20**). This process was first studied in the isotropic melt using dynamic ^{13}C NMR[88,89] and in nematic solvents by ^{2}H NMR.[90] Here we discuss the effect of this racemization process on the ^{2}H spectrum of deuterated *cis*-decalin in CLC. The deuterons on the two cyclohexanic rings in the molecule are enantiotopically related and consequently exhibit identical spectra. It is therefore sufficient to consider just the nine deuterons bonded to, say carbon atoms 1 to 4 and one of the methyne carbon atom, say 9. At low temperatures, where racemization is slow, but enantiomeric discrimination effective, a spectrum consisting of eighteen doublets, nine for each enantiomer is expected. Considering some degree of overlap, this is in fact observed experimentally (see bottom trace of **Figure 20**). The various doublets can in principle be assigned to the corresponding deuterons by a three-index symbol, n^{A}_{site}, where n refers to the carbon number to which the deuterium is bonded, subscript stands for axial or equatorial deuteron and supercript for the *R* or *S* enantiomer. The racemization process can then be identified as a reflection through a plane containing the C_2 axis and bisecting the bonds 2,3, 6,7 and 9,10. This results in an average symmetry of $C_2 \times C_s = C_{2v}$ and can be viewed as interchanges between nine pairs of doublets, ($1^{R/S}_{eq/ax} \leftrightarrow 4^{S/R}_{ax/eq}$, $2^{R/S}_{eq/ax} \leftrightarrow 3^{S/R}_{ax/eq}$ and $9^{S/R} \leftrightarrow 10^{R/S}$),

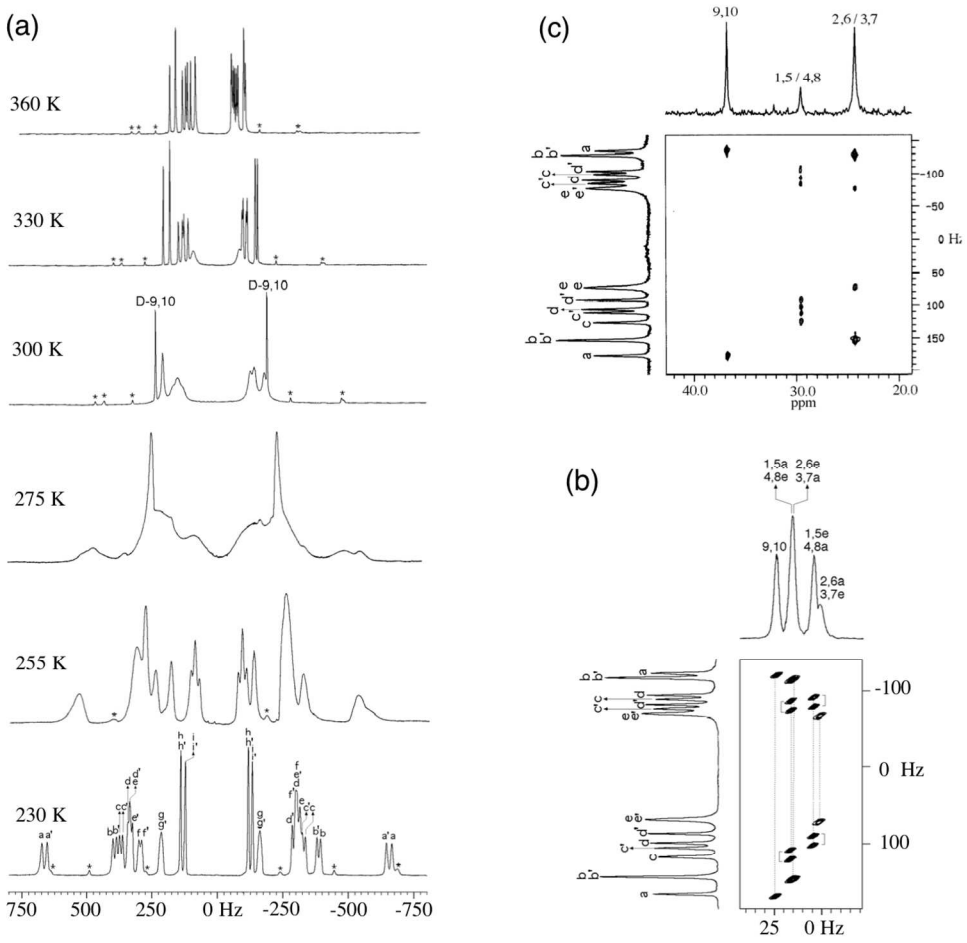

Fig. 20. (a) Series of ^{2}H 1D spectra (61.4 MHz) for ***cis*-decalin-d$_{18}$** in the PBLG/$CHCl_3$ mesophase *versus* T. Note the drastic variations of ^{2}H spectra. (b) Associated *Q*-COSY 2D spectrum (61.4 MHz) and (c) CDCOM 2D-NMR spectrum (9.4 T) recorded at high temperatures (356 K and 360 K, respectively). Figures adapted from **85** and **86**.

Upon heating, as the racemization rate enters the dynamic NMR range, line broadening followed by merging of mutually exchanging pairs of doublets takes place (see spectra in the range 250 to 330 K of **Figure 20a**), leading at high temperatures to a nine doublets spectrum as indeed observed in the 350 K spectrum of the figure. In terms of the dynamic discrimination model discussed in the introduction to **Section 5**, the fast motion spectrum can be understood as due to a flexible molecule with an average C_{2v} symmetry possessing four pairs of enantiotopically related deuterons and a single diastereomeric deuteron. In ALC it is expected to exhibit just five doublets.

In this example, the use of ^{2}H homo- and ^{13}C-^{2}H heteronuclear correlation 2D experiments were of great interest to reveal the spectral discriminations of enantiomeric pairs and enantiotopic pairs of **DHN**, both at low and high temperatures, respectively. This is nicely illustrated in **Figures 20b** and **20c** where tilted *Q*-COSY and CDCOM 2D-NMR experiments of **DHN** in the CLC recorded over 350 K (see above) greatly facilitated the analysis of ^{2}H signals and the assignment of QD. Note that on the CDCOM map, only three ^{13}C resonances are detected as theoretically expected, in agreement with a C_s symmetry molecule in average.[86]

6.2 Exchange processes involving enantiotopic sites

The second class of compounds for which measurements in CLC may provide information not available in ALC involves dynamic effects in prochiral molecules. Interchange of enantiotopic sites that do not modulate any internuclei interactions will not exhibit dynamic effect in the NMR spectrum in achiral solvents, but may do so in CLC. There are very few studied cases in this category. As for enantiomeric conversion, interchange of enantiotopic sites bound to a stereogenic center is usually too slow to fall into the dynamic NMR regime. More likely candidates are compounds in which the enantiotopic sites interchange by bond switching or rotation. We shall discuss three examples.

6.2.1 1-(methylphenyl)naphthalene. The 1-(2′,6′-dideutero-4′-methylphenyl)-naphthalene (**DMPN**, **Figure 21a**) is an interesting case of atropoisomerisms.[91,92] The deuterium NMR spectrum of this molecule deuterated in the α-phenyl sites exhibits, at -60°C, a single doublet in ALC, and two ones in CLC (**Figure 21b**). This is consistent with the molecule possessing C_s symmetry with the plane of the phenyl ring perpendicular to that of the naphthalene moiety.

The structure is probably an average one, with the phenyl ring wobbling rapidly (but not reorienting) about the inter-ring bond. Hence the molecule is (on the average)

prochiral with the two α-deuterons forming an enantiotopic pair. As the temperature of the CLC solution is raised the spectrum exhibits gradual merging of the two doublets into a single one. The behavior is typical of a dynamic effect in which the two nuclei interchange sites and can readily be explained and quantitatively analyzed in terms of reorientation of the phenyl ring about the inter-ring bond (**Figure 21b**). This is a special example since the process can only be detected by NMR in a chiral environment. The two sides of the phenyl ring are enantiotopically related (equivalent in ALC) and no internuclear interaction is modulated by their interchange.

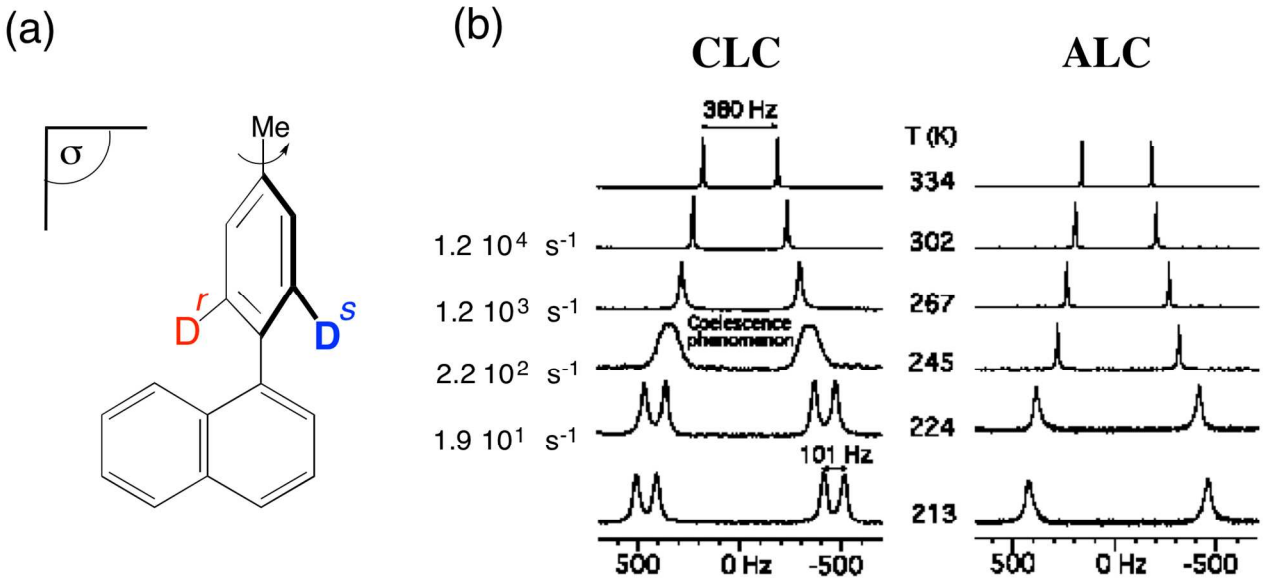

Fig. 21. Structural formula of **DMPN-d_2**. (b) Temperature dependence of the associated ^{2}H-{^{1}H} spectra (61.4 MHz) dissolved in CLC (PBLG/$CHCl_3$) (left) and ALC (PBG/$CHCl_3$) (right). The derived rate constants are indicated on the spectra recorded in CLC. Figure adapted from ref. **91**.

6.2.2 Dodecamethoxyhexathiametacyclophane. The Dodecamethoxyhexathia-metacyclophane **(HTMC)** is a highly flexible 18-membered ring molecule (**Figure 22a**). It has been shown that as a function of the temperature it undergoes a succession of two dynamic processes,[81] identified by NMR measurements to be, respectively, of the type, $C_2 \rightarrow C_{2v}$ (at 170 – 210 K) and $C_{2v} \rightarrow D_{2h}$ (at 290 – 320 K). The latter could only be characterized and measured using CLC as solvent.

Molecular force field calculations suggest a boat conformation with C_2 symmetry as a possible ground state conformer for **HMTC**. This structure is consistent with its ^{1}H NMR spectrum in isotropic solvents at low temperatures and with the dynamic observations described below (see **Figure 23a**). At 169K the spectrum consists of poorly resolved methoxy signals and a pair of aromatic peaks. As the temperature is raised, the latter merge into a single peak indicating the onset of racemization. This alone does not disclose the mechanism of the process; it could involve pair wise switching of the two pairs of benzene ring, as shown schematically in the upper diagram of **Figure 22b**. This process will result in an average C_{2v} symmetry, with the aromatic hydrogens transforming into pairs of enantiotopic elements. Alternatively, the process may involve an umbrella liked inversion of the molecule resulting in an average D_{2h} symmetry, with the aromatic hydrogens homotopically related (bottom diagram in **Figure 22b**). A choice between the alternatives could readily be made on the basis of deuterium NMR in CLC (**Figure 23b**).

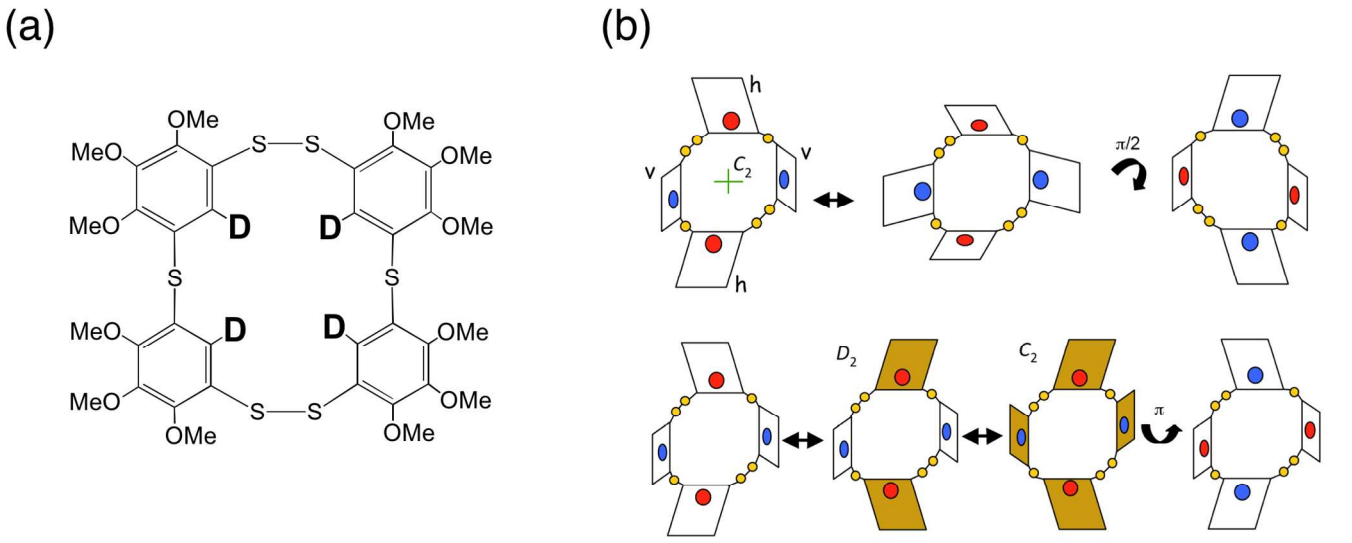

Fig. 22. Molecular formula (a) and proposed boat conformation (b) of **HTMC-d4**. In the latter the methoxy groups and the aromatic hydrogens are drawn as red and grey spheres. (c) The low temperature $C_2 \rightarrow C_{2v}$ (top) and the high temperature $C_{2v} \rightarrow D_{2h}$ (bottom) processes of **HTMC**. In these diagrams the red and blue circles represent the two pairs of aromatic hydrogens. Figure adapted from **81**.

The spectrum of **HTMC** deuterated in the aromatic sites, exhibits a single doublet in ALC, while (below room temperature) two are observed in CLC, reflecting enantiotopic discrimination. This indicates that the low temperature process involves the $C_2 \rightarrow C_{2v}$ mechanism. Moreover, as the temperature is raised to above 300 K the two doublets (in CLC, **Figure 23b**) gradually merge into a single one, indicating the onset of a second dynamic process that renders the aromatic hydrogens homotopic. A process consistent with this observation is the umbrella flipping mechanism described in the lower line of **Figure 23b**. As indicated in this diagram it probably involves two flipping steps with an intermediate saddle conformation. It leads to an average D_{2h} symmetry with all aromatic hydrogen homotopically related. As for the phenyl-naphthalene case, as no internuclear interaction is modulated by the process it can only be detected in a chiral environment. The derivation of the kinetic parameters for both these processes is described in the original papers.

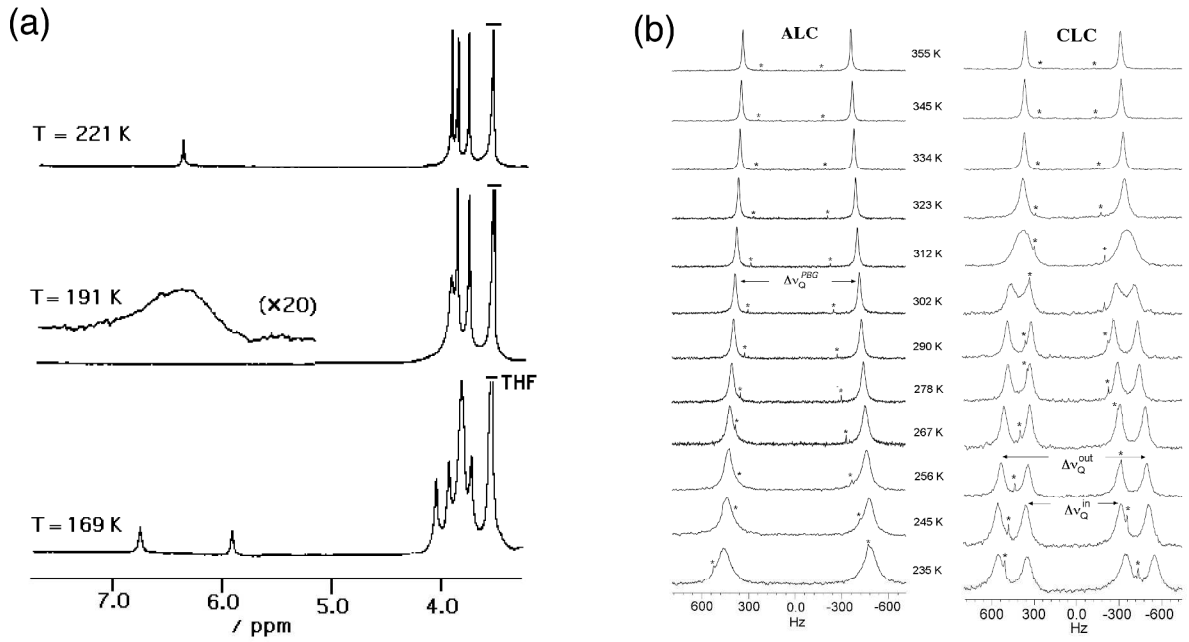

Fig. 23. (a) ^{1}H NMR spectrum of **HTMC** dissolved in THF. (b) ^{2}H-{^{1}H} NMR spectra (61.4 MHz) of **HTMC-d$_4$** (deuterated in the aromatic sites) dissolved in ALC (left) and CLC (right). Figure adapted from refs. **81** and **82** (with permission).

6.2.3 *Cyclooctatetraene and its tetramethylated derivative.* Another special case is that of the prochiral molecule cyclooctatetraene (**COT**) with D_{2d} symmetry. It is highly flexible, undergoing fast bond shift rearrangement that interchanges between enantiotopic sites.[93] The dynamic process is, however, not manifested in the ^{1}H NMR spectrum in (achiral) isotropic solvents since all its eight hydrogens are magnetically equivalent and exhibit a single unsplit signal. An exception is the signal of its ^{13}C satellite, which does exhibit dynamic effects, but allows only rough estimates of the dynamic parameters.[94] To overcome this limitation the ^{1}H NMR spectrum of this compound was studied in ALC solutions. The spectrum then exhibits dipolar interaction that is modulated by the bond shift process, resulting in (quite complicated) dynamic spectra from which kinetic parameters could be derived.[93,95] There is no advantage in using CLC (instead of ALC) in this case; its analysis will be even more complicated and no extra information will be gained. The situation is different if deuterium NMR of deuterated **COT** (or if NAD NMR is used). Here the dipolar interactions are too small to affect the spectrum, while discrimination (by ordering) between enantiotopic sites in CLC, is expected to result, at low temperatures, in two quadrupolar doublets, merging upon heating into a single one, due to the bond shift process. The effect was observed but the study not yet completed.

A related example is that of tetramethylcyclooctatriene (**TMCOT**) with S_4 symmetry.[96] The compound is rigid at room temperature, but exhibits dynamic effect in the ^{1}H NMR spectrum at high temperatures, due to modulation of the scalar coupling between the vinilic and methyl hydrogen, by the bond shift rearrangement.[93,96,97] The process interchanges between enantiotopic pairs and could in principle be studing by NAD NMR in CLC at high temperatures. Enantiotopic discrimination was indeed observed in such a spectrum (see **Figure 24**) at room temperature, but there is no advantage in using it over that of isotropic solvents to study the dynamic process.

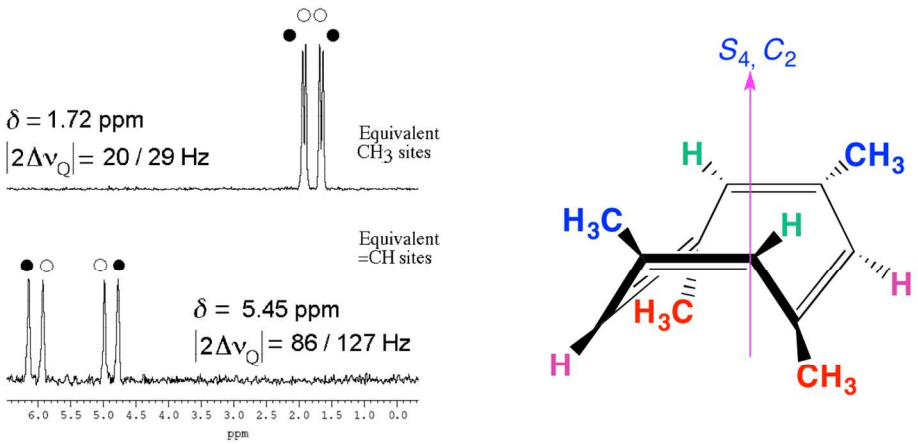

Fig. 24. NAD 1D-NMR signals (92 MHz) of **TMCOT** in CLC. The traces correspond to F_2 projections of a tilted *Q*-COSY Fz 2D map at the chemical shifts of the methyl (top) and ethylenic (bottom) deuterons, respectively (unpublished results).

7. Enantiotopic discriminations using RDCs

7.1 Use of RDCs in spatial structure determination

From the work of Bax in 1997,[100] the use of RDCs for spatial structure analysis of small molecules and biointerest macromolecules as well, in combination with molecular modelling methods has become an essential and worldwide spread analytical tool.[101,102] This approach is a powerful alternative to the conventional NMR techniques involving nOe effects that provided, so far, estimates for internuclear distances, which were used to determine conformational constraints and in turn molecular 3D structures.[103,104,105,106] Various nOe-effects based multidimensional NMR sequences have been designed for this purpose.[101]

Interestingly, anisotropic NMR overcomes some limitations related to nOe-based techniques, that can be summarized as follow: (i) for internuclear distances around 4-5 Å, signals arising from nOe effects are sometime very weak or do not appear on NMR spectra, leading to misinterpreted results; (ii) observation of nOe evidences is strongly dependent from chosen values of mixing time involved in NOESY 2D experiments. Consequently to properly establish the nOe-effects based correlations it is often necessary to repeat the experiment with different mixing time values;[101] (iii) finally, the detection

and evaluation of accurate nOe effects (do) require mandatorily degassed samples as molecular oxygen because of its paramagnetism speed up the nuclear relaxation.

The RDC values, ${}^{n}D_{ij}$, (in Hz unit) between nuclei *i* and *j* can be expressed, in a tensorial form as: [26, 106]

$$D_{ij} = -\frac{1}{4}\frac{h\gamma_i\gamma_j}{\pi^2 r_{ij}^3}\vec{r}_{ij}^{\,T}\hat{A}\,\vec{r}_{ij} \qquad \textbf{(62)}$$

In this equation, μ_0 and *h* denote the vacuum permittivity and the Planck's constant, respectively, γ_i and γ_j the corresponding magnetogyric ratios, $\vec{r}_{ij}$ is a unit vector connecting both nuclei ($\vec{r}_{ij}^{\,T}$ is the transposed vector of $\vec{r}_{ij}$) whereas r_{ij} is the distance between them. Elements of the alignment tensor, $A_{\alpha\beta}$, a traceless 3 × 3 symmetric matrix are equal to two-third of Saupe matrix elements, $S_{\alpha\beta}$.[106] It contains the information about the distribution of the vector $\vec{r}_{ij}$, and hence describes the probability of the internuclear vector ij pointing in a particular direction of space.

The robustness of the "RDCs method" in the structure determination lies in the univocal relationship linking the RDCs, the orientational ordering parameters and the solute geometrical structure. To increase the accurary on the interatomic distances determination, vibrational corrections must be modelled and calculated before to be possibly applied in the RDC calculation methods.[107,108] If for rigid compound, the 3D determination is straightforward as soon as the minimum number of RDs is reached, according to the molecular symmetry, the situation is more complicated when dealing with flexible molecules for which conformational distribution should be properly taken into account. Models initially developed to treat the correlation between conformational and orientational distributions for solutes dissolved in thermotropics were lately successfully extended into weakly ordering LCs solvents.[109,110,111,112,113] The RDC-based strategy was, subsequently, successfully extended to investigate the stereochemistry

(constitutional, configurational and conformational analysis) of chiral natural compounds[102,114,115,116,117,118,119,120,121,122,123,124] or synthesized chiral molecules.[125] Thus, the determination of the relative configuration of possible bioactive molecules from RDCs was described from end of 90's.[116] Thus, combined with chiroptical methods (VCD), the determination the absolute configuration of active molecules such as **Dibromopalau'amine** or **Mefloquine** (drugs) having numerous stereogenic centers was demonstrated.[126,127] Concommittantly to this development, numerous efficient 2D-NMR sequences were obviously designed to facilitate the extraction of one bond and/or long range ^{13}C-^{1}H RDCs in anisotropic spectra recorded in CLC.[128,129,130,131,132,133,134,135]

7.2 Revealing symmetry breakings from RDCs

Similarly to enantiomeric pairs (*R*/*S*), enantiotopic elements (*r*/*s*) in prochiral molecules dissolved in CLC can be discriminated on the basis of RDC's. In this case, each enantiotopic pair of interacting nuclei *i* and *j* produces different RDCs values (RDC(*r*) and RDC(*s*)) defined in Hz as (see also **Tables 1** and **2**):[28]

$$D_{ij}^{s\ or\ r} = -K_{ij}\left\langle \frac{S_{ij}^{s\ or\ r}}{r_{ij}^{3}} \right\rangle \text{ with } K_{ij} = \frac{h\gamma_i\gamma_j}{4\pi^2} \qquad \textbf{(63)}$$

Written under this simplified form, $S_{ij}^{s\ \mathrm{or}\ r}$ is the local order parameter for the enantiotopic internuclear vectors, r_{ij}, ($r_{ij}^{s} = r_{ij}^{r}$) while the K_{ij} parameter ($K_{ij}^{s} = K_{ij}^{r}$) depends on the nuclear isotopes involved. The brackets denote an (ensemble or time) average over molecular tumbling and internal motions.

As seen from **Eq. 63** the magnitude of RDCs is strongly dependent of the K_{ij} parameter. Thus for ^{13}C-^{13}C, ^{19}F-^{13}C, ^{1}H-^{13}C, ^{19}F-^{1}H, ^{1}H-^{1}H interacting nuclear pairs, the K_{ij} values are equal to 7 590, 28 400, 30 190, 112 960, 120 070 kHz.Å^{-3}, respectively.[28] Regarding K_{ij} values, the most attractive nuclear pairs in terms of sensitivity are clearly

^{1}H-^{1}H and ^{19}F-^{1}H ones. However due to the magnitude of long-range dipolar couplings, extraction of one-bond dipolar and scalar couplings associated to enantiotopic directions is usually not trivial on proton or fluorine 1D-NMR spectra, although various selective spin-spin edition strategies as SERF[131] or GET-SERF[132] experiments were successfully developed and can be easily implemented. Spectral analyses in weakly ordering solvents of ^{13}C-^{1}H pairs are often quite appealing for two reasons: (i) the one-bond C-H dipolar contribution, $^{1}D_{C\text{-}H}$, is generally small in comparison to $^{1}J_{CH}$; (ii) the long-range $^{n}D_{C\text{-}H}$ are usually small compared to $^{1}D_{CH}$.[133] Here again, various 2D-NMR approaches involving spectral edition were designed to extract sets of ^{13}C-^{1}H heteronuclear couplings.[134,135,136]

For a given value of S_{ij}, the spectral discrimination of enantiotopic elements in CLC originating from order symmetry breaking using RDCs is often much more difficult to reveal/observe than on NMR spectra dominated by RQCs. Four practical reasons explain this occurence: (i) the magnitude of RDCs is strongly dependent of K_{ij} by nature (see above) and significantly decreases when the distance between interacting internuclei increases (see **Eq. 63**). Thus in weakly aligning media, the magnitude of ^{13}C-^{1}H RDCs exceeds rarely some tens of Hz; (ii) compared to differences within *r* and *s* RQCs, the difference between RDC(*r*) and RDC(*s*) is generally small, and do not exceed 30% of the RDC magnitude; (iii) the small differences of RDCs can lead to weakly resolved, complex spectral patterns in particular when long-range dipolar couplings broaden the lines or obscure the signals; (iv) the presence of RDCs (added to *J*) can also generate second order effects. Note, however, that second-order effects in those solvents may be qualified as small ones when comparing with effect observed in thermotropic solvents.

For simple prochiral molecules, spectral enantiodiscriminations on methylene groups could be simply revealed using proton coupled ^{13}C spectra recorded in CLC. Thus, difference of ^{13}C-^{1}H or ^{13}C-^{2}H RDCs leads to second-order ^{13}C spectral pattern of type AXX' or AXY (A being ^{13}C) instead of AX_2 obtained in ALC (see **Table 4**). An illustrative experimental example has already been given in cases of **ethanol** and **ethanol-**

d_6 dissolved in PBLG/chloroform system (see **Figure 13b**). In that solvent, ^{13}C signals of the methylene group can be analysed as an AXX' and AXX'K_3 spin system, respectively. Interestingly, the structure of those spectral patterns is strongly dependent of the sign of ^{1}H-^{1}H and/or ^{1}H-^{13}C RDCs as demonstrated in the case of ethanol. Inversion of signs of RDCs induces dramatic change in peak frequencies.[50,51]

Finally, when isotopically normal ethanol is dissolved in PBCLL/$CDCl_3$ (see **Figure 25a**), the ^{1}H-^{1}H dipolar interaction between the methyl and methylene hydrogens becomes conspicuous and the methylene proton coupled ^{13}C signal has to be analysed as

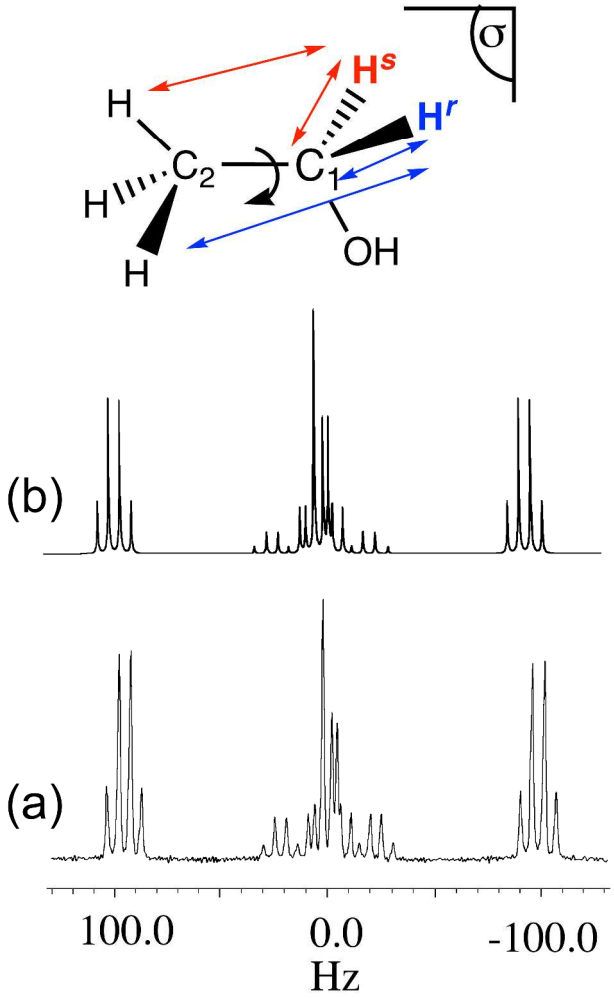

Fig. 25. (a) Experimental ^{13}C 1D spectrum (100.1 MHz) of the C-1 carbon in isotopically normal ethanol dissolved in CLC (PBCLL/$CDCl_3$). (b) Simulated spectrum of an $ABXK_3$ spin system obtained when $^{1}D_{AX} \neq {}^{1}D_{BX}$ and $^{3}D_{AK} \neq {}^{3}D_{BX}$. Figure adapted from ref. **51**.

an $AXYK_3$ spin system where $^1D_{AX} \neq {}^1D_{AY}$ and $^3D_{XK} \neq {}^3D_{YK}$. In this example, the simulation of spectrum (see **Figure 25b**) revealed also a tiny difference of ^1H CSA (1 Hz) between the two enantiotopic hydrogens of methylene as theoretically expected, but not directly observable.[51] The numerical analysis of spectrum has shown that not only dipolar interaction between the two methylene hydrogens and the methylene carbon are different, but also those between the methylene hydrogens and the methyl group hydrogens, thus reflecting enantiotopic edges (see also **Section 11**).[51]

Another noticeable experimental case of enantiodiscrimination revealed by a difference of ^{13}C-^1H RDCs was observed in **malononitrile,** a model for CH_2X_2 molecules where H-X directions are enantiotopic (see **Figure 7**). Contrarily to ethanol, the enantiotopic ^{13}C-^1H internuclear directions do not involve the prostereogenic carbon but enantiotopic two-bonds ^{13}C-^1H edges (see **Section 8.2.3**). As discussed below the successful spectral differenciation of enantiotopic ^{13}C-^1H internuclear vectors in **malononitrile** of C_{2v} symmetry (and without prostereogenic nuclear center) raises a fundamental question about the "universal" definition of the term "prochirality".

8. Definition of the prochirality concept

According to IUPAC nomenclature, a simple definition (generally used by organic chemists) states that an achiral molecule, or a part of it considered on its own is called prochiral when becoming chiral in a one-step reaction by the replacement of an existing atom (or group) by a different one (usually isotopic substitution). In other words, the prochirality can be seen as the property of an achiral object (or spatial arrangement of atoms or groups) able to be transformed into a chiral one through a single desymmetrisation step (chemioselective chiral process). By extension, an achiral object which is capable of becoming chiral in two desymmetrization steps is sometimes described as proprochiral. According to this idea, **malononitrile** can be seen a proprochiral molecule since it does not possess any prostereogenic tetrahedral center

whereas two desymmetrisations are necessary to obtain a chiral molecule of C_1 symmetry.

The possibility to discriminate enantiotopic directions in **malononitrile** when interacting with a CLC suggests that this molecule can also be said to be prochiral.[51] Hence, it is legitimate to define whether this type of compounds can be considered as a prochiral entity in isolation even though it does not possess a prostereogenic tetrahedral center. The previous rules defining the prochirality concept prevent considering such types of C_{2v} molecule as prochiral. This is mainly because to date the substitution or symmetry criterions employed as a test for the definition of prochirality involve only atoms (or groups),[1,2] but never intramolecular internuclear directions.

The key question is to establish if it is worthy, based upon experimental evidences, to qualify prochiral a Xggii-type molecule (where X is a tetrahedral atom, g and i are X-bonded ligands) exhibiting enantiotopic g-i directions that are discriminated in CLC as, in the same way all Xggij molecules (which contain g enantiotopic groups and subsequently X-g one-bond enantiotopic directions) are from theoretical definition denoted prochiral. Trivially it should be noticed that at this stage one stands on the borderline of the prochirality definition, and maybe it could be fruitful to look on this concept from a different point of view. In other words, should it be possible to extend the concept of prochirality to compounds having no prostereogenic tetrahedral center but non-bonded enantiotopic directions? This problem of definition has already been conceptually discussed by Fujita in 1990, who considers that ìthe compounds (CX_2Y_2) can be regarded as prochirals, since the four edges (X-Y) construct an enantiospheric $C_{2V}(C_1)$ orbit.[137,138,139] The results obtained with **malononitrile** in a CLC validates therefore experimentally this extended concept of prochirality, and also illustrates for the first time the purposes of Raban and Mislow who predicted in 1967, in the case of CH_2F_2, that the homotopic protons (resp. homotopic fluorine nuclei) would become anisogamous in a chiral solvent.[2]

9. Assignment of the absolute configuration of enantiotopic NMR signals

9.1 Problem and solutions

One of the most challenging problem relative to the analysis of NMR spectra of prochiral molecules dissolved in CLC is the possibility to assign the absolute configuration (*r*/*s*) of experimental NMR signals (^{1}H, ^{13}C, ^{2}H, …) originating from enantiotopic elements (nuclei, internuclear directions, groups or faces). The central question could be defined as another way: could we assign the absolute configuration of enantiotopic NMR signals by calculating the molecular ordering tensor assuming an "ideal" molecular structure and two sets of "infinitely accurate" experimental anisotropic observables? Actually, similarly to enantiomeric pairs, such spectral assignment of the absolute configuration is theoretically not possible. This fundamental problem has been addressed in a recent paper published in 2012 in the case of enantiomeric pairs, but the same arguments can be extended to enantiotopic elements in prochiral molecules.[140] Thus, for a (*R*/*S*) isomeric pairs of chiral molecules (with a single stereogenic center) where the coordinate vectors for each internuclear vector, $\vec{r}_{ij}$, in the *R* and *S* enantiomer can be related by inversion $\vec{r}_{ij}(R) = -\vec{r}_{ij}(S)$, the choice of the right dataset of experimental anisotropic observables, Obs$^{R/S}$, (dipolar coupling ($D^{\exp}$(*R* or *S*) or quadrupolar couplings ($\Delta\nu_{Q}^{\exp}$(*R* or *S*)) to the corresponding enantiomer (*R* or *S*) cannot be properly done on the simple basis of criteria such as the Cornilescu quality factor, *Q*, that can be defined as for a *R*/*S* pair:

$$Q_{AB} = \sqrt{\sum_{i}\left(\mathrm{Obs}_{Ai}^{\exp} - \mathrm{Obs}_{Bi}^{\mathrm{fit}}\right)^{2} / \sum_{i}\left(\mathrm{Obs}_{Ai}^{\exp}\right)^{2}} \qquad \textbf{(64)}$$

where A and B notation stand for *R* and *S*, while Obs$^{\mathrm{fit}}$ are back-calculated observables as a function of the ordering matrix elements. Thus Q_{RR} corresponds to the quality factor

obtained when fitting the experimental observable for the "*R*-enantiomer" to the *R*-isomer and Q_{RS} for fitting the same experimental observable data set to *S*-isomer. Since for a rigid molecule, all vectors in the two enantiomers fulfill $\vec{r}_{ij}(R) = -\vec{r}_{ij}(S)$, Q_{RR} (resp. Q_{SS}) and Q_{RS} (resp. Q_{SR}) are ideally (theoretically) equal to zero. Experimentally, the unaccuracy of experimental observables produces Q factors different from zero but also different non-zero values for all possible Q_{AA} and Q_{AB} factors. Those differences are meaningless, and cannot be used to assign the absolute configuration of observable datasets. As a consequence, the assignment of absolute configuration of experimental NMR signals of enantiomers (in case of racemic mixture) is not possible from RQC's or RDC's when they have strictly identical enantiomorphous 3D objects.

Obviously same inconsistency exists for the assignment of the absolute configuration of NMR signals related to enantiotopic elements in particular for C_s symmetry prochiral molecules. Here the two prostereogenic faces of a prochiral molecule can be defined as enantiomorphous structures. As a consequence, the determination of the stereodescriptor (*Re* or *Si* face) is here again impossible. That is the reason why during the analysis of NAD spectra of norbornen in CLC (see **Section 4.3.2**), it has been possible to group all RQC's for each of prostereogenic faces of the molecule, but not to associate the corresponding *Re*/*Si* stereodescriptors.[51] To solve this problem, an empirical approach based on spectral comparisons can be proposed as explained below.

8.2 Empirical method

Diphenyl methanol (**DPM**) is a C_s symmetry molecule in average, but compared to ethanol the molecule possesses now two enantiotopic aromatic groups instead of C-H enantiotopic directions (see **Figure 26a**). Due to their fast rotation, the two *ortho* and *meta* ^{13}C atoms in each aromatic ring atoms are equivalent (homotopic position), and hence only three inequivalent ^{13}C sites leading to six (2×3) ^{13}C resonances are observed on the ^{13}C-{^{1}H} 1D-NMR spectrum recorded in a CLC.[141] Such a spectral

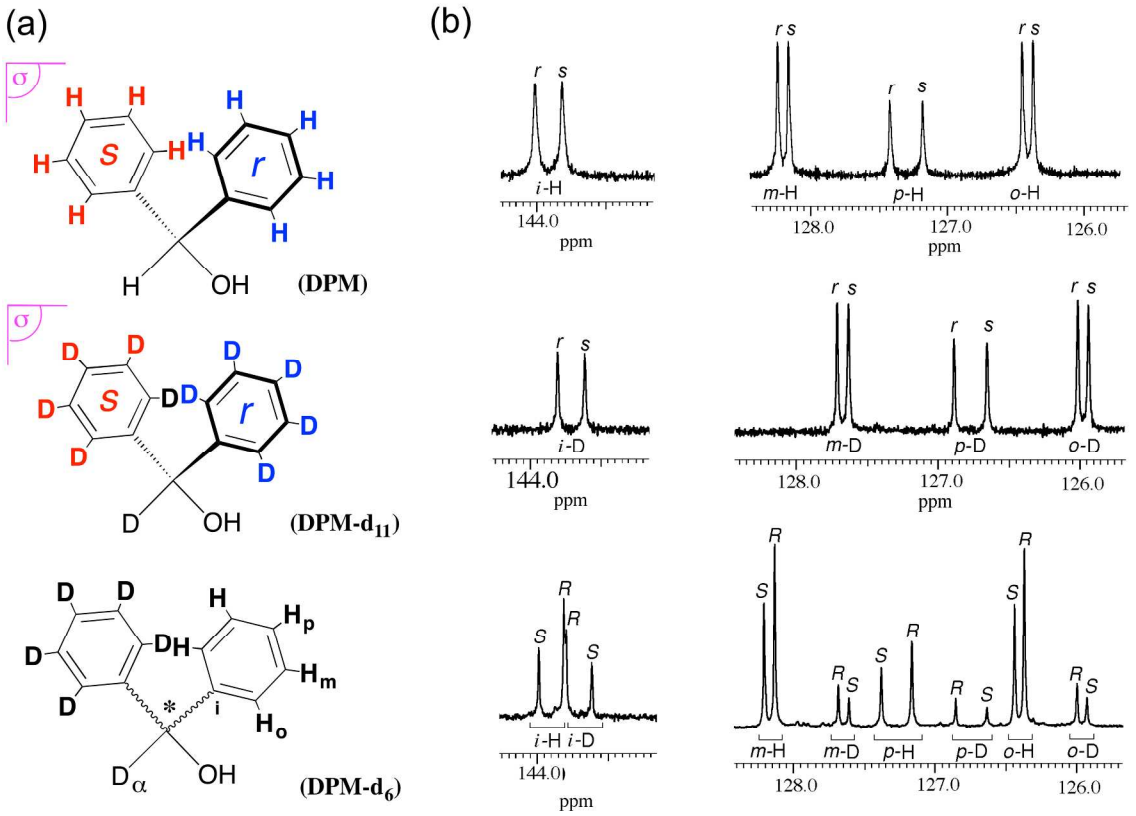

Fig. 26. (a) Structure and atomic numbering of **DPM** (top), **DPM-d$_{11}$** (middle) and **DPM-d$_6$** (bottom). The notation (*a*, *i*, *o*, *m*, *p*) defines both the deuterium and the carbon atoms. (b) Associated aromatic regions of the ^{13}C-{^{1}H, ^{2}H} 1D-NMR spectra (61.4 MHz) of three isotopologues recorded in the PBLG/CHCl$_3$ phase. All 1D -NMR spectra were recorded using the same experimental conditions. Figure adapted from ref. **141**.

enantiodiscrimination is observed both in protonated and perdeuterated derivatives (**DPM** and **DPM-d$_{11}$**) as seen on ^{13}C spectra of **Figure 26** (top and middle). The systematic upfield shielding of ^{13}C resonances observed on the ^{13}C-{^{2}H} spectrum of **DPM-d$_8$** (compared to ^{13}C-{^{1}H} spectrum of **DPM**) originates from ^{2}H isotope effect on ^{13}C, this effect being effective both in isotropic and anisotropic solvents.[73,142,143] Unfortunately in both examples, the assignment of absolute configuration (*r*/*s*) for each ^{13}C resonance cannot directly be deduced from the relative position of ^{13}C resonance on the anisotropic spectrum. Actually, such assignment reported in spectra of **DPM** and **DPM-d$_8$** has been deduced from the comparison of ^{13}C-{^{1}H} spectrum of a *R*-enriched mixture (20% *ee*) of the chiral isotopologues (**DPM-d$_4$**) of **DPM** and **DPM-d$_8$**.[142,143,144] ^{13}C-{^{1}H}

spectrum is displayed in **Figure 26b** (bottom). As seen, the *R*/*S* assignment of ^{13}C resonances associated with protonated aromatic ring of **DPM-d$_5$** seems to be inverted compared to the *r*/*s* assignment of **DPM**. Actually, it has been demonstrated that the relative positions (shielded/deshielded) of a given aromatic ^{13}C signal in the deuterated aromatic ring for the *R*- and *S*-enantiomers of **DPM-d$_6$** are opposite to that observed for the protonated one, and this result is general.[141] In other words, the assignment of ^{13}C signals of two substituents chemically differentiated by the isotope substitution in a chiral molecule is always inverted compared to the prochiral parent molecules. This situation is possible because the molecular order parameters for enantiomers of a molecule chiral by virtue of the isotopic substitution and their corresponding prochiral molecule are the same, and hence same ^{13}C-{^{1}H, ^{2}H} spectrum are expected to be observed for both types of molecule.

Recently, an empirical approach also based on comparison with homoguous chiral derivatives for which the absolute configuration of signals could be unambiguously assigned was applied to determine the stereoconfiguration of small chiral molecule having a single stereogenic center.[145]

10. Panel of chiral mesophases

Since the two last decades, and the renewed interest of using RDCs for structure determinations in biomolecules from 1997,[146] several types of weakly aligning media have been discovered and reported in literature. Without being exhaustive, we can cite: the homopolypeptide liquid-crystalline media, the filamentuous phage and bicelle (DMPC, DHPC) suspensions, membrane fragments, but also compressed polyacrylamide (charged, uncharged) or stretched collagen-based gelatin or collagen. Numerous articles or reviews on the subject can be found in literature.[33,34,35,36,37,38,39,40,41,100,146,147,148,149,150] Discussing all these systems is out the scope of this review, and below we will briefly

present the main chiral aligning media in which spectral enantiotopic discriminations have been experimentally observed by NMR spectroscopy.

10.1 The homopolypeptide CLCs

The main results discussed in this review involve lyotropic systems made of a single homopolypeptide (PBLG, PCBLL) dissolved in organic solvents.[42,43,44,45] Due to the large range of possible organic solvents, from weakly polar ($CHCl_3$, CH_2Cl_2) to polar ones (DMF, pyridine, …), these aligning systems dissolved a large collection of organic molecules and are very efficient for revealing enantiomeric and enantiotopic discriminations of almost all organic compounds ((a)polar, apolar, complexes, …).[42,59] The great flexibility on the choice of homopolypeptides and/or organic co-solvents do guarantee generally the possibility to reveal enantiotopic discriminations in these media, as seen in the case of **ethylbenzene-d_{10}** for which only ^{2}H NMR in PCBLL systems has permitted the discrimination of enantiotopic C-D directions.[151] Other optically active homopolypeptides such as poly-γ-ethyl-*L*-glutamate (PELG) provide also interesting chiral lyomesogens.[43,44,51] Another alternative consists of preparing a mixtures of two chiral homopolypeptides (such as PBLG and PCBLL, for instance) with rather close degree of polymerisation.[45] Using concentrations in polymer (12 -20 %w/w) similar to those used for a single homopolypeptide, chiral homogeneous mesophases are obtained where the degree of orientation of the solutes and the efficiency of enantiotopic and enantiomeric discriminations depend on the relative molar concentration of both polypeptides. This dependency is nicely illustrated in **Figure 27** in case of benzylic alcohol. More recently, chiral systems made of cross-linked helically PBLG have been also described as enantiodiscriminating alignment solvents.[152]

For investigating organic prochiral molecules, polypeptide helical polymers can be seen as the best enantiodiscriminating orienting media, however, they are by nature inadequate for water-compatible solutes. Modified homopolypeptides systems by mean

of additives (such as DMSO) have been proposed to investigate highly polar solutes, thus extending their analytical possibilities.[153] Although valuable, this solution has never been applied for specific analytical applications, so far.

Another approach consisting in diblock polymers composed of PBLG as the hydrophobic component and poly(ethylene oxide) (PEO) as the hydrophilic component could provide a possible alternative for water-compatible molecule guests. [154]

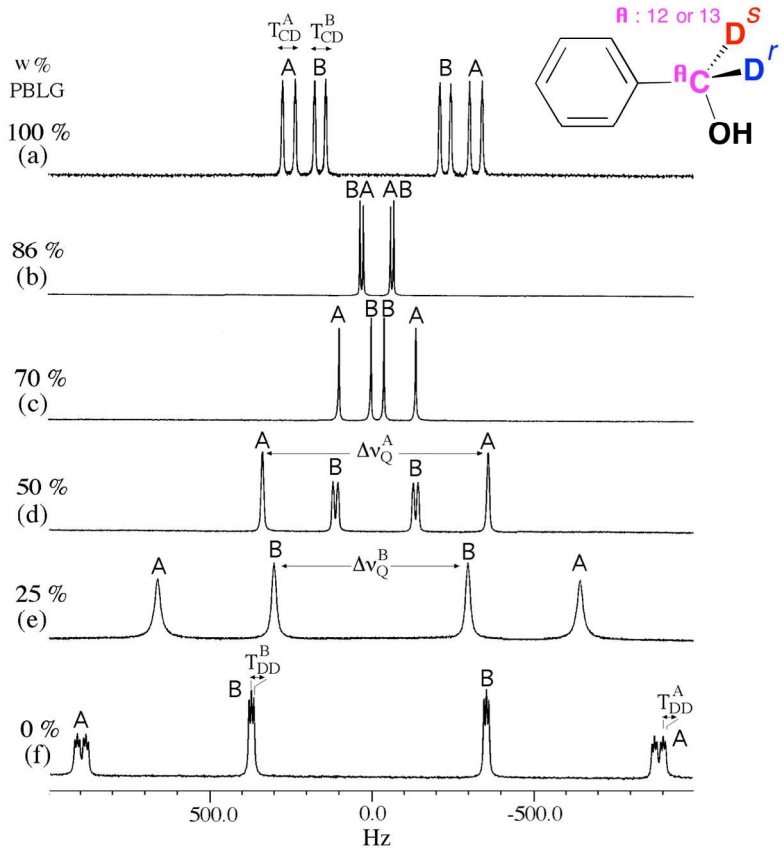

Fig. 27. Variation of ^{2}H-{^{1}H} 1D spectra (61.4 MHz) of **BZA-d$_2$** recorded at 300 K in a PBLG-PBCLL mixture in $CHCl_3$ as a function of the w/w(%) of PBLG. Note that the methylene group of the solute dissolved in mixtures made with 0, 50 and 100% of PBLG is also isotopically enriched in ^{13}C, and hence the ^{1}H-^{13}C total couplings (J and D) are visible on spectra a, d, and f. Figure adapted from ref. **45**.

10.2 The polynucleotide CLCs

From the end of 80's, DNA helices (double strands) in water at sufficient concentration (about 200 mg/ml) are known to form cholesteric mesophases (here again

weakly aligning) under magnetic constraints.[155,156] If this system was used for structure determinations of proteins by NMR,[157] its first application as enantiodiscriminating aqueous media has only been reported in 2009 by Ramanthan.[40] From this pionnering work, other studies involving ^{2}H NMR were achieved and shown fragmented-DNA based CLC in water (pH 6-7) reveals to be an efficient systems to resolve the ^{2}H signals of deuterated enantiomers of wide variety of natural α-AA, such as **alanine**, **valine** or **serine**, for instance.[41] In terms of enantiotopic discriminations, this water compatible helical system allowed the spectral differentiation by difference of ^{2}H RQCs of enantiotopic C-D directions of **glycine-d$_2$** as well as the enantiotopic deuterated methyl groups of **DMSO-d$_6$** (see **Figure 28**). Interestingly, the comparison of both examples shows large differences (a factor of ≈20) in the range of RQCs, while the sample composition and sample temperatures (*e.g.* 305 and 320 K) are rather similar.[41] Two distinct but combined effects may explain this large difference of RQC magnitude for both solutes: (i) an important difference of molecular mobility of the guest solutes; (ii) the averaging of ^{2}H RQCs associated to each C-D direction of methyl of **DMSO** due to its free rotation around the S-CH$_3$ bond. At a given Temperature, the difference of mobility between both solutes is mainly related to the strength of their various electrostatic interactions with DNA, and in particular their ability to form strong hydrogen bonding with DNA. Weaker hydrogen bondings are *a priori* expected for **DMSO-d$_6$**, thus decreasing the global alignment of solute and thereby the magnitude of the RQCs.[159] Interestingly as enantiodiscrimination mechanisms can be seen as short-range interactions, stronger the solute-solvent interactions are, more efficient the enantiorecognition mechanisms are. This occurrence can partly explains the large difference of RQC(*r*) and RQC(*s*) in case of glycine. On the other hand, the fast rotation of the methyle groups of **DMSO-d6** averages the order parameters associated with the methyl C-D bonds, leading to an average order parameter for the methyl group three times smaller (-1/3) than that of the C-S bond direction.[28]

Interestingly, it could be noted that ^{2}H NMR in DNA CLC has been proposed to monitor *in situ* and real-time the interconversion of chiral solute by an enzymatic racemization.[158]

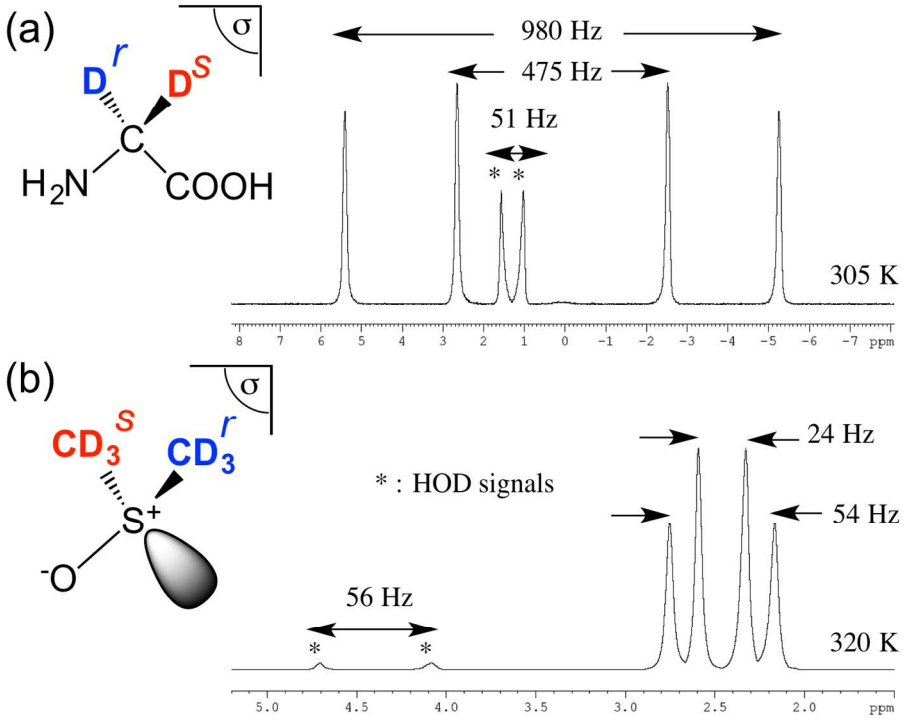

Fig. 28. ^{2}H-{^{1}H} 1D spectra (92.1 MHz) of (a) **glycine-d_2** (305 K) and (b) **DMSO-d_6** (320 K) recorded in DNA/water oriented system (73 mg of DNA/380 mL of buffer). Note the difference of magnitude of RQC's between both solutes. Figure adapted from ref. **41**.

10.3 The stretched chiral oriented gels

Starting in 2002, chiral oriented gels in water were introduced as alternatives to aqueous lyotropic CLC's.[34] The earlier systems consisted of collagen-based (polypeptides or small proteins) gelatins. Unlike in the classical aligning media (lyotropic and thermotropic liquid crystals) the anisotropy in these systems is introduced either by mechanical stretching[150,160] or allowing to swell (in a suitable solvent, such as water or DMSO within the NMR tube.[34,161]

10.3.1 The gelatin-based mesophases. Covalently cross-linked gelatin based alignment media (swallen in water or DMSO or a mixture of both) provide interesting chiral oriented

systems able to discriminate enantiotopic directions in prochiral solutes as seen in **Figure 29a**.[162] The cross-linking is obtained by irradiated cooled gelatin hydrogels with (accelerated-electron) irradiation dose ranging from 60–480 kGy and leads to highly homogeneous gels. The degree of alignment of sample can be easily controlled by modifying the extension factor, Ξ, of stretched e-gelatin swollen. Ξ is defined as the difference in length btween the streched and unstreched gel divide by the lenght of the unstreched gel.[163] This mechanical possibility affords a new adjustment parameter both on the magnitudes and the differences of RQCs (or RDCs) that does not exist with conventional CLC.[161] In these examples, a factor Ξ around 0.45 leads to the best spectral situation in terms of enantiodiscrimination efficiency since two QD are clearly observed. Note that in absence of gel stretching, the solute environment remains isotropic as in liquids.

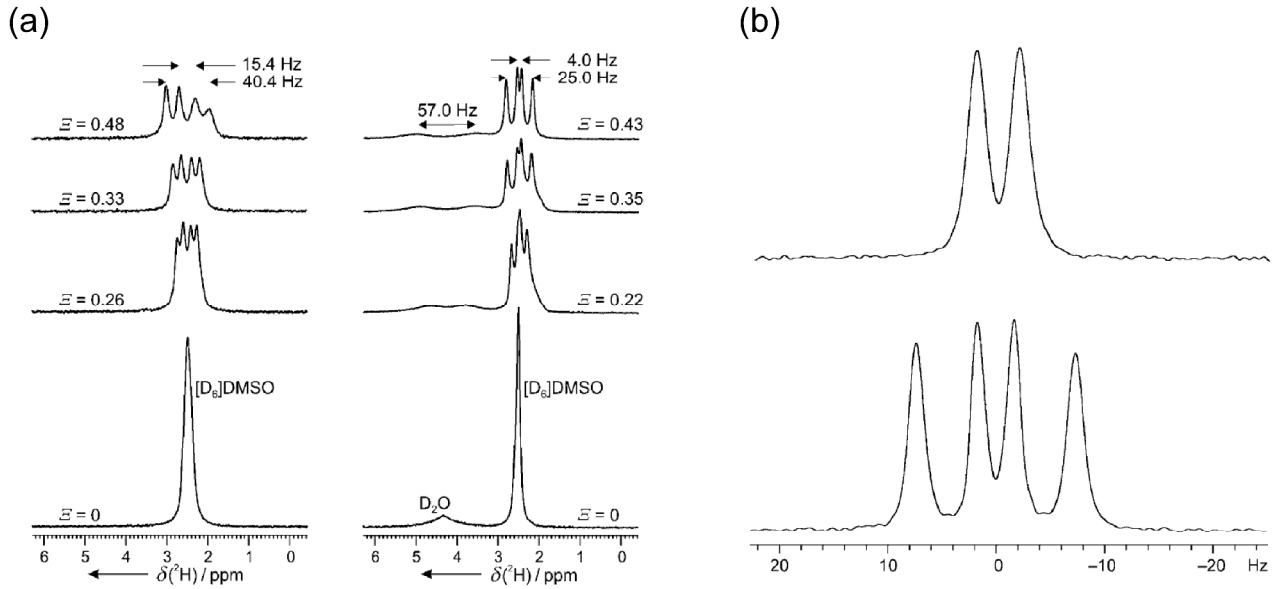

Fig. 29. (a) Series of ^{2}H NMR 1D spectra (38.4 MHz, 333 K) of **DMSO-d_6** *versus* the extension factor, Ξ, of stretched e-gelatin swollen in (left) pure **DMSO-d_6** and (right) **DMSO-d_6**/D_2O (4:1). (b) ^{2}H NMR (61.4 MHz, 288 K) spectra of 3% **DMSO-d_6** (v/v) in (top) stretched *k*-carrageenan gel (5.1% w/v, 143.3 mm NaCl) and (bottom) stretched *i*-carrageenan gel (5% w/v, 143.3 mm NaCl). Figures adapted from refs. **162** and **165** with permission.

10.3.2. The polysacharride mesophases. As another possible alternative to polypeptide and polynucleotide CLCs, polysacharride-based chiral aligning media have also been proposed for discriminating enantiomers of water-compatible chiral polar guests. Thus weakly aligning, mixtures of alkylpolyglucosides (mono and diglucosides) dissolved in hexanol/water system shown enantiodiscriminating properties in the case of chiral α-amino acids (AAs) but no example of enantiotopic discrimination has been reported.[164]

More recently, Kuchel *et* al. has described two chiral polysaccharide-based anisotropic gels that can be reversibly adjusted (just like e-gelatin system), but need much lower gel concentrations. These commercially available polysaccharides systems are prepared from seaweed: ι- and κ-carrageenan (3-10% v/v).[160] Unlike polypeptide systems, but similar to gelatin-based samples (see above), it is necessary to mechanically stretch (or compress) the gel to adequately tune the alignment of guest molecules.[160] While κ-carrageenan-based aqueous systems have been able to discriminate between enantiomers of alanine using ^{13}C NMR, only the ι-carrageenan solvent provided a suitable solution to spectrally separate the enantiotopic methyl ^{2}H NMR signals of **DMSO-d_6** (see **Figure 29b**). Here again the small magnitude of RQCs of **DMSO-d_6** reflects the rapid tumbling of the molecule combined with the free rotation of C-D directions in each methyl group.

11. Analytical Applications

In the previous sections of this review, we have discussed the origin of spectral discrimination of enantiotopic directions in rigid and flexible prochiral molecules when CLC is used as NMR solvent. Selected examples were described to illustrate the theory. In the following sections are described several applications of interest showing how NMR spectroscopy in CLC can provide analytical solutions to solve problems to (bio)chemists when molecular enantiotopic directions are involved. Two important experimental achievements are presented below.

11.1 Assignment of NMR signals in *meso*/*threo* mixtures

^{2}H-{^{1}H} NMR in chiral oriented media of labelled analytes can be a powerful tool when investigating reaction pathways or mechanisms.[83,165,166,167] This assessment was nicely demonstrated in the case of the SmI_2-mediated 3-*exo*-trig-cyclisation reaction of δ-halogeno-α,β-unsaturated. In this particular example, the cyclisation mechanism leading to cyclopropane compounds was remained misundertood for a while.[168] This cyclisation could theoretically produce in addition to a *meso* compound (denoted ***meso***) either a racemic or an enantioenriched mixture of enantiomers (denoted **x** and ***ent*-x**) according to the anticipated pathway of the reaction (see **Figure 30a**). Indeed if the ring opening of compound B to form A is slower than the reduction B can undergone to form C, no racemisation is possible. Thus the key question, both from a synthetic viewpoint and for a better understanding of the mechanisms, was to determine whether a homochiral γ-substituted substrate (δ-iodo benzylic esters) would retain or not its enantiomeric purity during the cyclisation process.

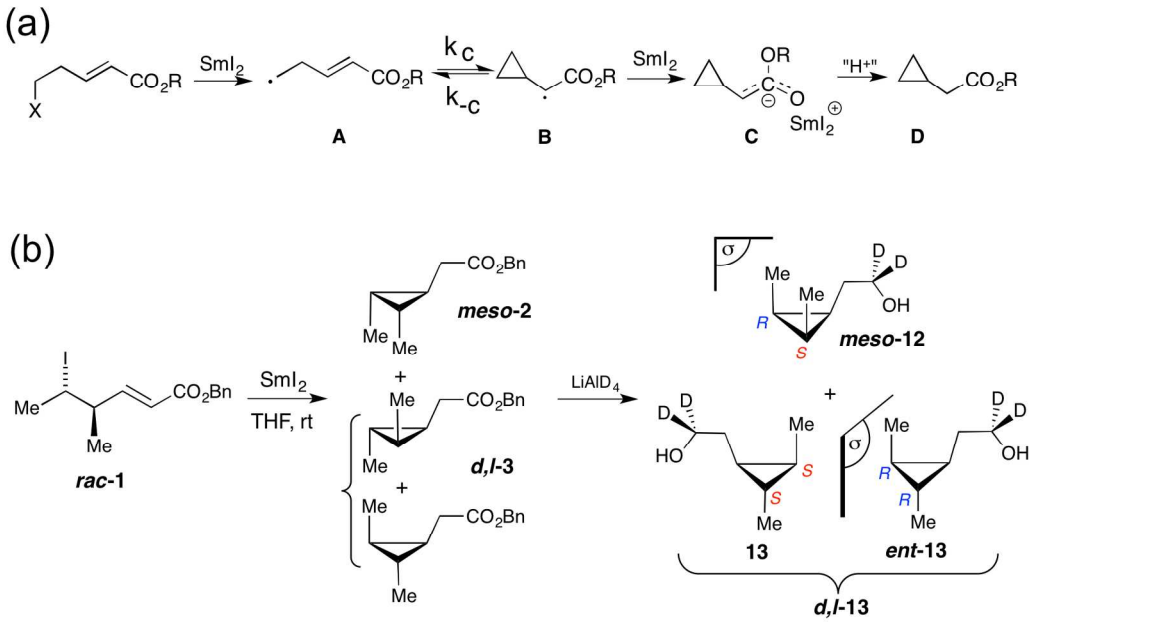

Fig. 30. (a) SmI_2 promoted cyclization process. **(b)** Example of cyclisation from the "*anti*" benzyl 4-methyl-5-iodohex-2-enoate (**1**) leading to *meso* (*meso*-**2**) and *d,l*-cyclopropanes (**3** and *ent*-**3**), then to dideuterated hydoxylated compound using for the NMR study. Figure adapted from refs. **169**.

To accomplish this task, the analytical strategy chosen was based on chemically positionning a -CD_2 group as stereochemical probe of the isomers produced, without modifying the composition of the initial mixture.[169] This quantitative chemical step was easily overcome by reducing the mixture using $LiAlD_4$ (see **Figure 30b**): following this reaction compound ***meso*-12** arises from ***meso-2***, **13** from enantiomer **3**, and ***ent*-13** from ***ent*-3**, respectively. To allow to identify and assign, and finally quantify each stereoisomer of the mixture, ^2H NMR in CLC was explored to spectrally discriminate: (i) enantiomers, here **3** and ***ent*-3**; (ii) enantiotopic D-groups of *meso* compound, here **12**, and reveal the presence of nonzero DD gem couplings within each of stereoisomers. In this perspective two samples were prepared: the experimental mixture of **12**, **13**, and ***ent*-13** was dissolved in the same conditions of concentrations using first a CLC, made of PBLG/$CHCl_3$ mixture (sample I), and then an ALC made of PBG/$CHCl_3$ mixture (sample II). In both cases, the ^2H-^2H COSY-45 2D-NMR experiment was run to group ^2H signals originating from the same isomer. The analytical strategy is summed up in **Figure 31**.

On the one hand, in the ALC (sample II), enantiotopic deuterons within the *meso* compound show a single QD, while diastereotopic deuterons in enantiomers show two QDs. To identify and assign the ^2H NMR signals belonging to the *meso* form, denoted $M_1 + M_2$, it is therefore sufficient to detect the lines which are autocorrelated, showing that they belong to the same QDs, but that do not present any cross correlation connecting that components to others NMR lines (see **Figure 32b**). Once identified, measuring the magnitude of $M_1 + M_2$ becomes straightforward and components correlated do belong to enantiomers. On the other hand, in the CLC (sample I, **Figure 32a**), a different situation occurs. In the *meso* compound, each enantiotopic deuteron will present its own QD, M_1 and M_2, that previously merged in a single ^2H signal in the ALC. Components of M_1 (resp. M_2) obviously show autocorrelation peaks between lines constituting the same QD, but they do also exhibit cross correlation peaks with components of M_2 (resp. M_1) on the COSY-45 map. These later peaks allow us to identify the two *meso* doublets, M_1 and M_2,

and to measure their RQCs. As concentrations in samples I and II are the same, there is a unique relationship between the magnitude of the doublet $M_1 + M_2$ (in PBG/$CHCl_3$) and the doublet M_1 and doublet M_2 (in PBLG/$CHCl_3$): $|\Delta\nu_Q(M_1 + M_2)| = |\Delta\nu_Q(M_1) + \Delta\nu_Q(M_2)|/2$. This equation allows to achieve the assignment of the *meso* compound.

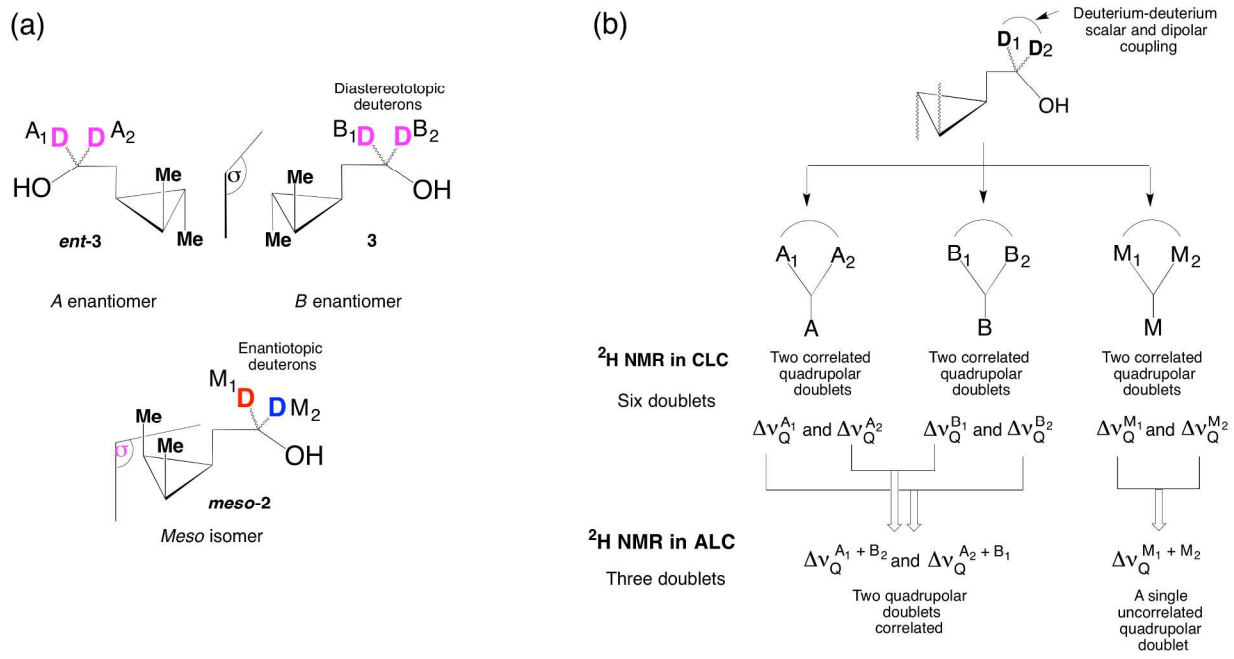

Fig. 31. (a) Structure of *meso* (***meso*-2**) and active forms (**3** and ***ent*-3**) of isotopically labelled cyclopropanic derivatives. The enantiotopic deuterons in *meso* are referred to as M_1 and M_2. The diastereotopic deuterons are referred to as $A_1(B_1)$ and $A_2(B_2)$ in the A(B) enantiomer. Deuterons $A_1(A_2)$ and $B_2(B_1)$ are mirror image. Note that the numbering A,B and 1,2 is arbitrarily chosen. (b) Spectroscopic principle for grouping of the various QDs observed in dideuterated mixture in the CLC and ALC. Only coupling correlations are expected between QDs originating from deuterons belonging to the same isomer. Figure adapted from **169**.

From the couple of enantiomers **13** and **ent-13** viewpoint, the picture is a bit more complicated, but again can be simply resolved by analyzing the COSY-45 map in both CLC and ALC, and using some symmetry considerations. In each optically active molecule, both deuterons are diastereotopic. Therefore, each deuteron of each enantiomer will exhibit its own QD in CLC whereas they do merge in ALC following some symmetry relationship and therefore sharing a unique relationship as illustrated in **Figure 32**. Here NMR signals of B_1 in **13** (resp. B_2) and A_2 in ***ent*-13** (resp. A_1) merge. Hence,

this means also that $|\Delta\nu_Q(A_1 + B_2)| = |\Delta\nu_Q(A_1) + \Delta\nu_Q(B_2)|/2$ and $|\Delta\nu_Q(B_1 + A_2)| = |\Delta\nu_Q(B_1) + \Delta\nu_Q(A_2)|/2$ that will allow to finalise the assignment of the optically active compounds. As in the case of the *meso* compound, identifiying the deuterons belonging to the same molecule can be easily performed using the COSY-type cross correlations between doublets of deuterons due to their non-zero *gem* D-D total coupling in the chiral as in the achiral solvent. Actually, this later result can be checked back once the QD corresponding to the *meso* compound $M_1 + M_2$ identified, as the two remaining doublets in the achiral solvent do mandatorily belong to the enantiomers.

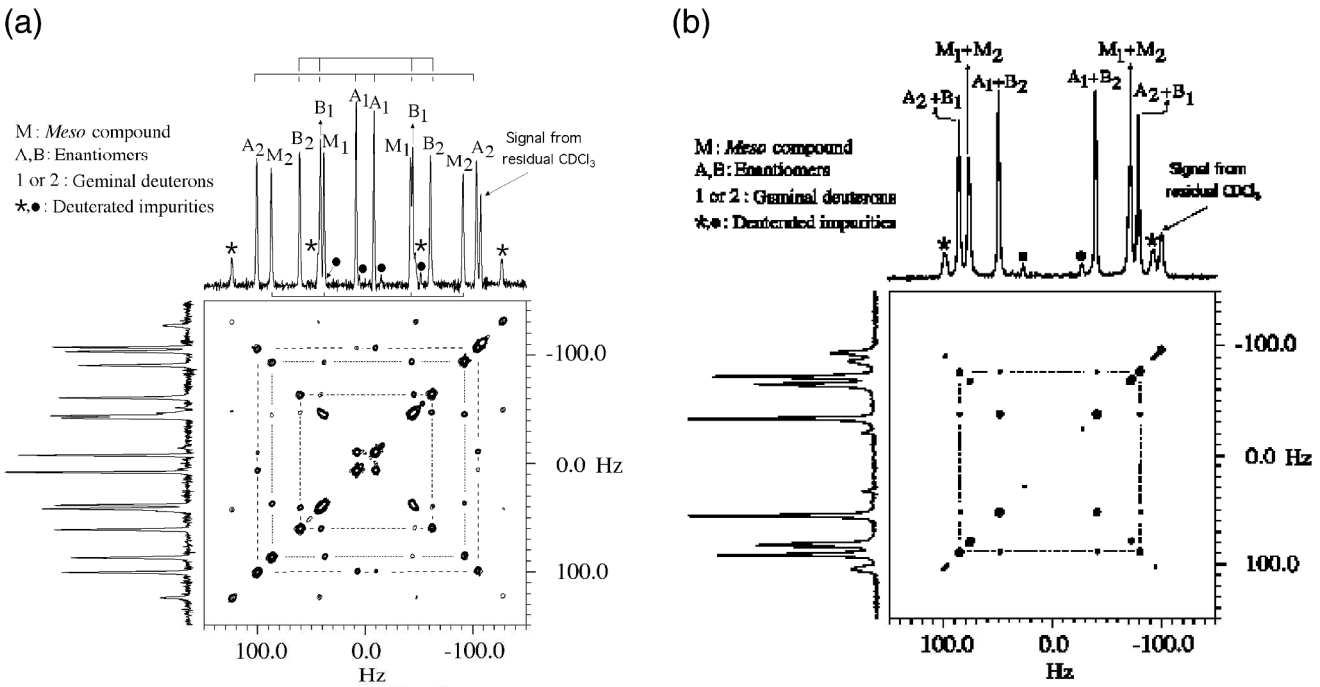

Fig. 32. (a) Proton-decoupled ^{2}H-^{2}H COSY-45 map (61.4 MHz) of *d,l*/*meso* mixture recorded in the CLC. (b) Same experiment recorded in the ALC. The QDs due to each type of deuteron are labelled M_1/M_2, A_1/A_2 and B_1/B_2. Note that in each case, the attribution of 1 and 2 is arbitrary. Figure adapted from ref. **169**.

In this specific example, the two deuterons are bonded to the same prostereogenic carbon atom, but the approach proposed has been also envisaged for studying *meso* and *d*/*l*-structures where deuterons are distant in the structure. This occurence can be found with dideuterated *para* and *meta* disubstituted aromatic compounds, for instance (see **Figure 33a**).[170] ^{2}H homonuclear 2D experiments involving either homo or heteronuclear

transfert polarizations ($D\rightarrow(H)_n\rightarrow D$ and $D\rightarrow(C)_n\rightarrow D$) for correlating deuterium atoms belonging to the *d*/*l*-compounds in the ALC and CLC were proposed as described in **Figure 33b**. The designed multiple pulse 2D-NMR sequences were derived from the DECADECY-INEPT or DECADECY-DEPT schemes proposed to correlate the ^{2}H signals of two geminal deuterons in prochiral molecules, and then adapted according to the desired transfer schemes.[170] Also as ^{13}C signatures for enantiomerically related (*RR*, *SS*) and *meso* (*RS*, *SR*) compounds are different in ALC and CLC, strategies involving ^{2}H-^{13}C heteronuclear 2D experiments were also designed.[170] In both cases, it appeared that the possibility to generate efficient heteronuclear polarization transfers to separate the useful ^{2}H NMR information proved to be heavily system dependent.

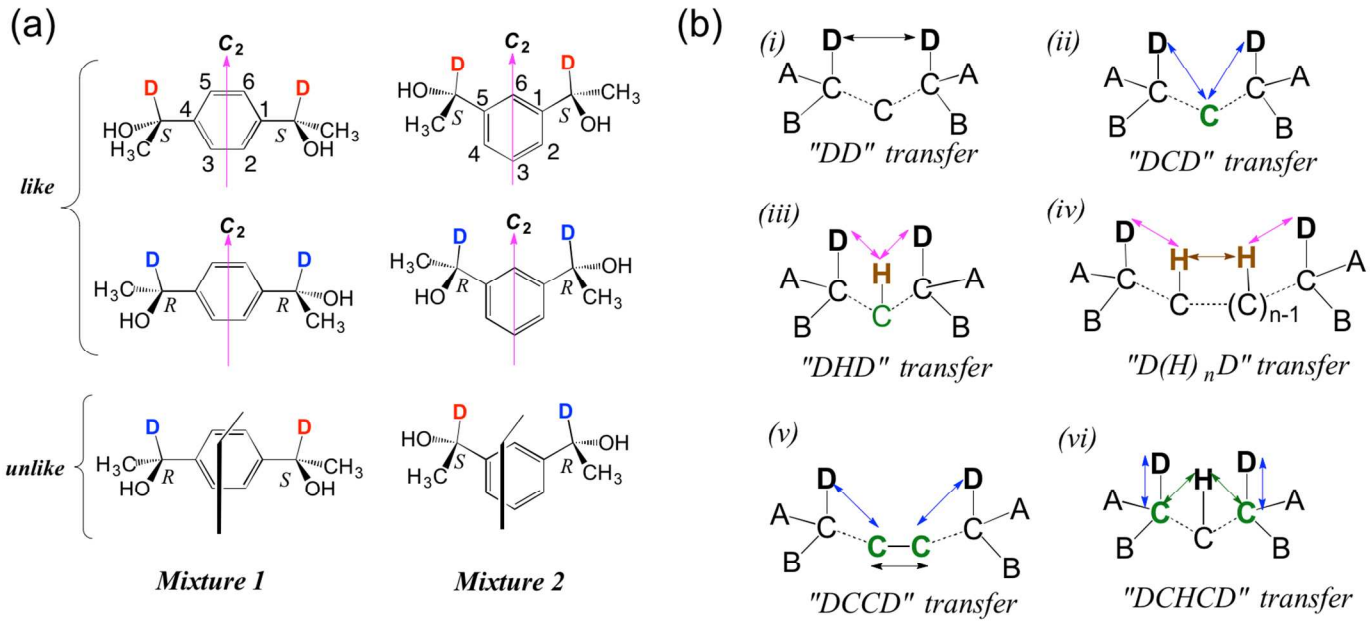

Fig. 33. (a) *Unlike/like (meso/RR,SS)* mixtures of disubstituted aromatic compounds with two remote deuterated stereogenic centers. (b) Examples of (i to vi) deuterium homonuclear NMR strategies to analyse the mixtures **1** and **2**, and using no (i), two (ii-iii) or more (iv-vi) heteronuclear polarization transfer(s). Figure adapted from ref. **170**.

11.2 ($^{2}H/^{1}H$) isotope fractionation in biocompounds

The measurement of deuterium/hydrogen ratio at a given site i, $(^{2}H/^{1}H)_i$, by quantitative ^{2}H NMR spectroscopy is a method of choice for the analysis of site-specific

natural isotope fraction (SNIF). This approach intensively developed by Martin and co-workers at late 70's is well-known as SNIF-NMR™.[172] Remarkably, the determination of the isotope profile of natural compounds leads to crucial information on: (i) the evaluation of kinetic isotopic effects (KIEs) associated with enzyme-catalyzed reactions; (ii) the biosynthetic pathway of bio-products such as fatty acids; (iii) the geographical (country, region, elevation), temporal parameters (year) or botanical origins (plants, microoriganisms) of natural compounds such as ethanol, for instance.[172,173,174,175] It is also a powerful method for traceability studying of natural compounds, fighting against counterfeiting (alduteration or denaturation) of food as well as alcoholic or non-alcoholic beverages.[176,177,178,179]

The site-specific $(^2H/^1H)_i$ ratios (in ppm) are calculated from evaluation of peaks surface in isotropic ^2H-$\{^1H\}$ 1D-NMR spectra in presence of an internal chemical reference as follows:[172,175]

$$\left(\frac{^2\mathrm{H}}{^1\mathrm{H}}\right)_{\mathrm{i}}^{\mathrm{iso}} = \frac{P_{\mathrm{ref}} \times m_{\mathrm{ref}} \times M_{\mathrm{s}} \times A_{\mathrm{i}}}{P_{\mathrm{i}} \times m_{\mathrm{s}} \times M_{\mathrm{ref}} \times A_{\mathrm{ref}}} \times \left(\frac{^2\mathrm{H}}{^1\mathrm{H}}\right)_{\mathrm{ref}}^{\mathrm{iso}} \quad \textbf{(65)}$$

where P_i and P_{ref} are the stoichiometric numbers of hydrogen at site *i* and in the reference, A_i and A_{ref} are the areas of the signals at site i and reference, and M_S, m_S and M_{ref}, m_{ref} are the molecular weights and masses of the sample and the reference, respectively.

Experimentally, the efficiency of the current isotropic ^2H-$\{^1H\}$ NMR is intrinsically limited by the rather small ^2H chemical shift dispersion in Hertz (6.5 lower than for ^1H), that can complexify spectra or even worth reduce the number of available information of $(^2H/^1H)$ ratios, in particular for large analytes. Increasing the strength of magnetic field could partly overcome this basic limitation of ^2H NMR, but this solution is expensive! More upseting, the use of isotopic achiral solvents prevents the enantiotopic deuterons in prochiral molecules to be spectrally discriminated, hence precluding the specific quantification of isotopic fractionation for each site on methylene prostereogenic sites while

the pro-*R*/pro-*S* hydrogens incorporated during the enzymatic process may originate from different sources or involve distinct incorporation mechanisms.

Compared to isotropic SNIF-NMR™ protocol, the NAD 2D-NMR in homopolypeptide CLC revealed to be a powerful analytical tool in complement of the classical approach for four pertinent reasons:[180,181] (i) the spectral differentiation of all non-equivalent ^2H sites (associated to monodeuterated isotopomers) can be achieved both on the basis of their chemical shifts and the RQCs, thus enhancing the spectral dispersion of ^2H signals; (ii) the enantiotopic C-H directions in prostereogenic CH_2 groups of prochiral molecules are expected to be non-equivalent in CLC, and can be spectrally differentiated using NAD NMR; (iii) a rather simple spectral analysis is possible using NMR 2D maps (such as *Q*-COSY Fz experiments); (iv) the adaptability and flexibility of the technique through the optimization of the chiral mesophase parameters (nature of polypeptide, polarity of co-solvent, component concentration, temperature) to each case studied.

From a practical viewpoint, recording anisotropic NAD spectra with quantitative conditions ($T_R = 5T_1(^2H)$) deuterium can be achieved with smaller recycling delay (T_R) between two scans of the 2D experiment, due to the smaller deuterium longitudinal relaxation times, $T_1(^2H)$ in anisotropic solvents compared to isotropic liquids. Besides, the large amount of analyte generally dissolved in polypeptide lyomesophases compensates (up to 100 mg): (i) the presence of two components for the deuterium signals (instead of a single resonance in liquids) (see **Figure 3**): (ii) the detection of enantio-isotopomers, and larger ^2H linewidths due to the viscosity of aligning solvents. Finally, the use of high-field NMR spectrometer (better when equipped with cryogenically cooled probes) allows the acquisition of anisotropic NAD 2D-NMR spectra with sufficient S/N ratio to provide robust evalution of (D/H) ratios, with reasonable experimental acquistion times (15-16 hours) for a large panel of molecules. Using 14.1 T spectrometer equipped with a slecteive ^2H cryogenic probe, the minimal concentration of ^2H enantio-isotopomers requested to record analytically exploitable NAD 2D-NMR spectra was evaluated at about 8 µmol/l.

Obviously, the use of highest magnetic fields (800-1000 MHz) in combination with modern electronic and the last generation of NMR cryoprobes should significantly decrease this value.[182] Concommitantly, the achievement of new NMR data acquisition (NUS method) available on recent NMR hardward coupled to post-acquisition data process (Covariance, CST) will allow also an noticeable acceleration of NAD NMR experiments.[183,184]

11.2.1 Prochiral unsaturated fatty acids. The potentials and the analytical interests for biochemical studies of NAD NMR in CLC was first experimentally demonstrated in the case of 1,1'-bis(phenylthio)hexane (**BPTH**) derived by cleavage from the methyl linoleate of safflower (*Carthamus tinctorius*), a prochiral fatty acid methyl ester (FAME) in 2004 using a 9.4 T NMR spectrometer equipped with conventional ^{2}H selective probe.[180] The method was then successfully extended to the case of complete mono or poly unsaturated FAMEs (PUFA) such as **MO**, **ML**, **MLN**, …,[180,181,185] and then applied to the complexe case saturated FAMEs (SAFA) such as **MS** (see **Figure 34**), both using a 14.1 T NMR spectrometer equipped with selective ^{2}H cryogenic probe.[42,185] The diversity in the classes of fatty acids (or corresponding methyl ester derivatives noted FAMEs) that are essential metabolites both as active molecules in a number of biological processes or as structural components of cell membranes is due to the large number of enzymatic modifications of their chain (introduction of double bond, conjugated double bond, epoxidation, ….) as seen in scheme of **Figure 34**. Such reactions are known to involve small changes in the activity of enzymes of the same family (the Fatty Acid Desaturase (FAD) superfamily) for which the mechanisms are not completely elucidated or are still unknown.[174,186,187]

As illustrative example, **Figure 35c** shows the series of NAD 1D sub-spectra (extracted from *Q*-COSY Fz map) of **ML** (a central, essential FAME precursors of various other FAMEs) dissolved in PBLG/pyridine mesophase at 305 K.[188] Contrarily to isotropic NAD 1D spectra (**Figure 35b**) where only 30% of deuterium signals (8/26 of

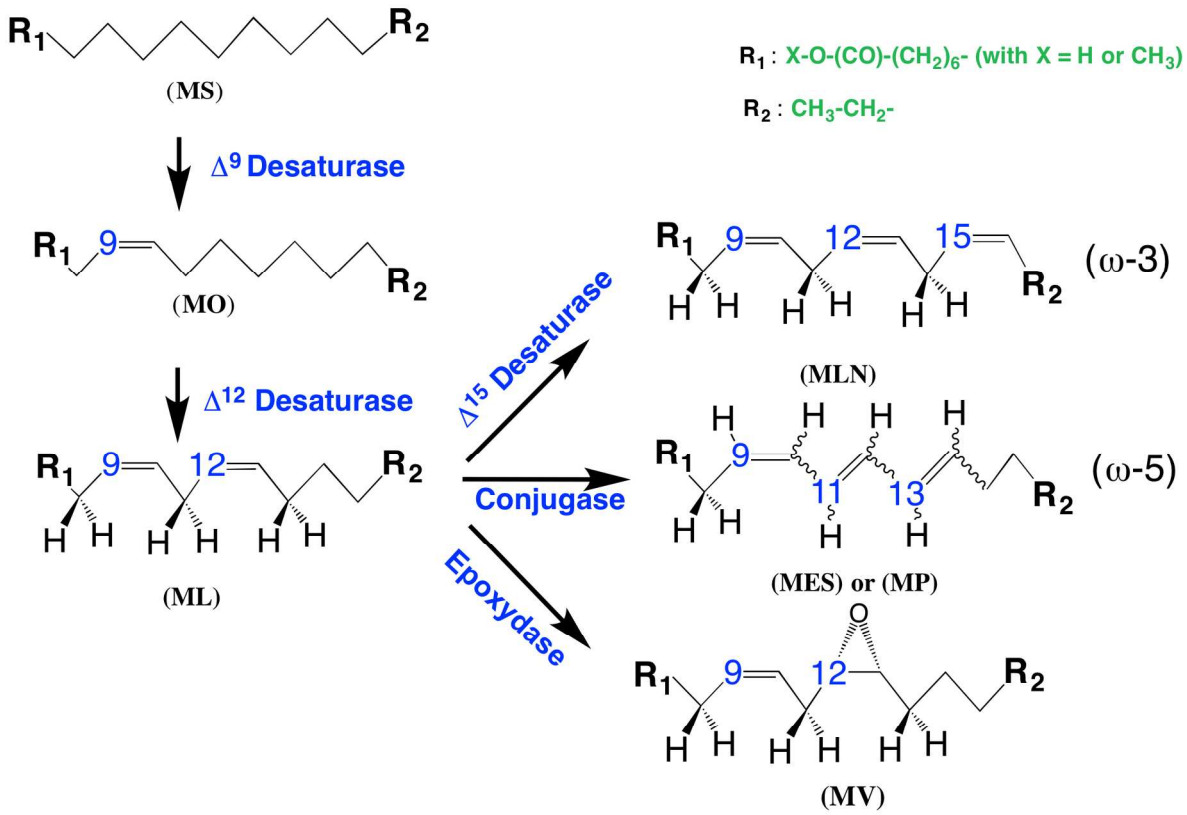

Fig. 34. Biochemical pathway leading to ω-5 PUFAs (MLN: (9*Z*, 12*Z*, 15*Z*)-methyl linolenate, MES: (9*Z*, 11*E*, 13*E*)-methyl eleosterate, MPU: (9*Z*, 11*E*, 13*Z*)-methyl punicate, MV: (12*R*,13*S*)-methyl vernoleate) biosynthesized from the methyl stearate (MS) through the (9*Z*)-methyl methyl oleate (MO), an then the (9*Z*, 12*E*)-methyl linoleate (ML). X corresponds to coenzyme A (CoA) or acyl-carrier-protein (ACP) in the plant or micro-organism cells and methyl group for the NMR analysis. Figure adapted from ref. 188.

inequivalent ^{2}H sites) are clearly observable with no specific data for the ethylenic groups (broad peak), all monodeuterated isotopomers and enantio-isotopomers (corresponding to the various inequivalent hydrogen sites) of the mixture are now spectrally discriminated. This also includes the deuterium signals of methylene group 11 (see **Figure 35a**) that had not been discriminated in the PBLG mesophase using a weakly polar organic co-solvent ($CHCl_3$).[180] For the first time the possibility of measuring the (^{2}H/^{1}H) ratio at ethylenic positions as well as the (^{2}H/^{1}H)^r and (^{2}H/^{1}H)^s ratios (at the same methylene position along of the fatty acid chain were experimentally demonstrated using a single NAD 2D-NMR experiment and without requiring any molecular cleavage (susceptible to modify the natural isotope profile).

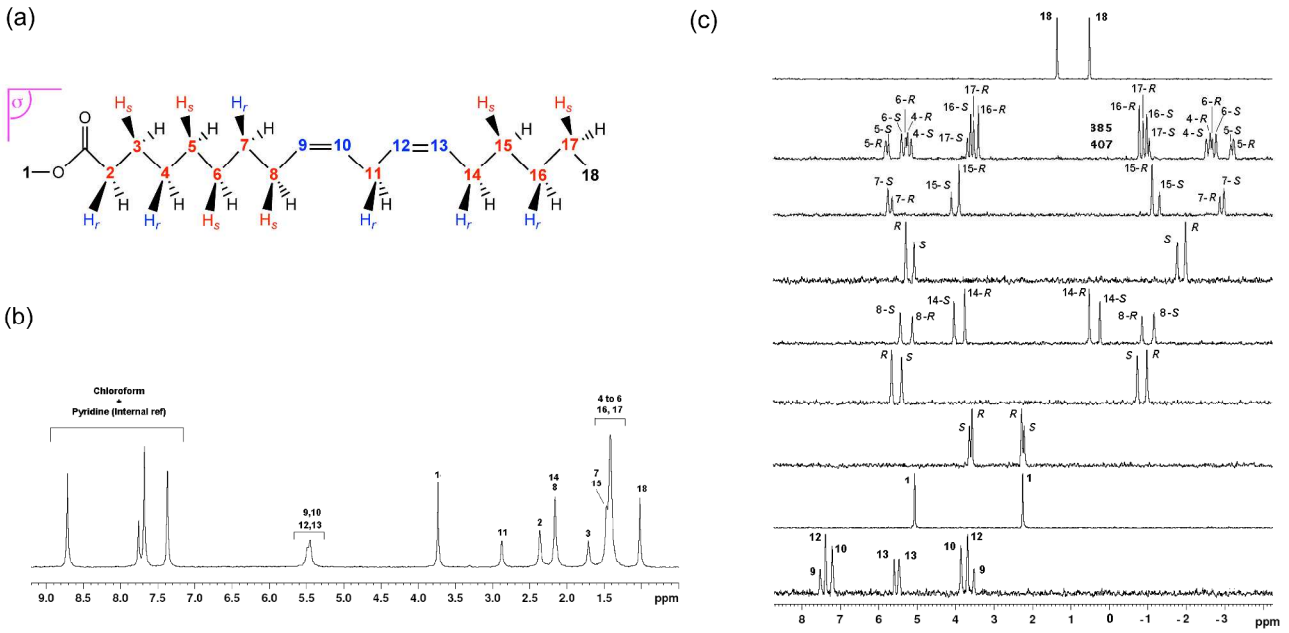

Fig. 35. Structure and atomic numbering of **ML** along with the stereosecriptors for each hydrogen site. Here only the stereodescriptors (*r*,*s*) of hydrogens in front of the symmetry plane are shown. (b) Isotropic SNIF-NMR™ spectrum (92.1 MHz) of **ML** (chloroform with pyridine used as internal reference for quantification). (c) Series of 92.1 MHz NAD 1D-NMR subspectra extracted from the tilted *Q*-COSY Fz map recorded in PBLG/Py. For each CH_2 site, the absolute configuration of the natural, major enantio-isotopomer (CIP rules applied to **ML)** is given. Figure adapted from ref. **188**.

As no calibrated internal reference (such as TMU) is added in the anisotropic samples, the $(^2H/^1H)_i$ ratios measured in PBLG, denoted $(^2H/^1H)_i^{aniso}$, can be safely derived from $(^2H/^1H)_i$ ratios determined by isotropic quantitative NAD NMR $(^2H/^1H)_i^{iso}$, following **Eq. 64**:

$$\left(\frac{^2H}{^1H}\right)_i^{aniso} = \left[\frac{(\%area)}{100} \times n \times \left(\frac{^2H}{^1H}\right)_i^{iso}\right] \qquad \textbf{(66)}$$

where n is the number of equivalent deuterons contributing to the ^2H isotropic signal. This two-steps approach is possible when the source of analyte studied is used to determine the values of $\left(^2H/^1H\right)_i^{aniso}$ and $\left(^2H/^1H\right)_i^{iso}$ ratio is obviously the same.[189]

The variation of pairs of $(^2H/^1H)^R$ and $(^2H/^1H)^S$ ratios (expressed in ppm) *versus* each methylene site of **ML** is shown on column plot of **Figure 36a**. As it can be seen, the $(^2H/^1H)$ ratios for each hydrogen site differ significantly from the V-SMOW value (Vienna Standard Mean Ocean Water) used as reference (V-SMOW = 155 ppm), besides the difference between the enantiotopic sites in methylene groups varies between 4 ppm (site 2) and 91 ppm (site 15).

The stereodescriptors, *R*/*S*, given in **Figure 35c** and also in **Figure 36** are associated with each enantio-isotopomers of mixture. They were assigned by combining the analysis of ^2H NMR spectra of regio- and enantioselectively deuterated BPTH compared to its NAD spectrum, both recorded in CLC with same conditions,[180,190] and considering that the FAS enzyme acts identically at each elongation cycle of the fatty acid.[188,189] As the **BPTH** and **ML** have the same botanical origin (*Carthamus tinctorius*), the isotopic fractionation relative to methylene sites 4 and 5 in BPTH was therefore the same as for sites 16 and 17 in **MS**, and hence in **ML**, allowing to confidently predict that the $(^2H/^1H)^s$ ratio is always smaller than the $(^2H/^1H)^r$ ratio at each odd and even methylene (15 to 2) as in case of **BPTH**. Formally, this argument is only valid in the case of **MS** where the stereochemistry of deuterium sites located in front of the molecular symmetry plane (see **Figure 29a**) is always the same along the chain, according to the CIP rules (as in **BPTH**) (see **Figure 30**). For **ML** this stereochemical characteristic is not true since for methylene groups noted 6, 7 and 8, the stereochemistry of deuterium sites located in front of the plane of symmetry is inverted compared with in **MS** due to the presence of the double bond in position 9-10. Except for sites 6-8 in **MS**, the stereodescriptors, *R/S*, (associated to the corresponding enantio-isotopomer) were assigned to the highest- and lowest-intensity doublets displayed on NAD 1D sub-spectra.

Concommittantly to determination of $(^2H/^1H)$ ratios for each hydrogen site, it is possible to evaluate the value of enantio-isotopomeric excess (*eie* =

$\left|\left(^2\mathrm{H}/^1\mathrm{H}\right)_i^R - \left(^2\mathrm{H}/^1\mathrm{H}\right)_i^S\right| / \left[\left(^2\mathrm{H}/^1\mathrm{H}\right)_i^R + \left(^2\mathrm{H}/^1\mathrm{H}\right)_i^S\right]$ measured for each CH_2 group. For FAMES, it was shown that *eie* at odd CH_2 positions are larger than those measured at even CH_2 groups all along the chain. This observation was explained by the incorporation way of hydrogens into the chain during the elongation of fatty acids (*via* the FAS enzyme). In fact, at odd sites, hydrogen are incorporated by the action of two different reductases which use NAD(P)H as co-factor whereas at even CH_2 groups both hydrogens are incorporated into the chain mainly from cell water by exchange and only for a small part by acetate.[191,192,193,194] Thus, except for site 2, the variation at all even sites remains unchanged at around 10 ± 2 % which is probably submitted to further exchange due to the acidity of both hydrogen at this position (a to the carbonyl group).

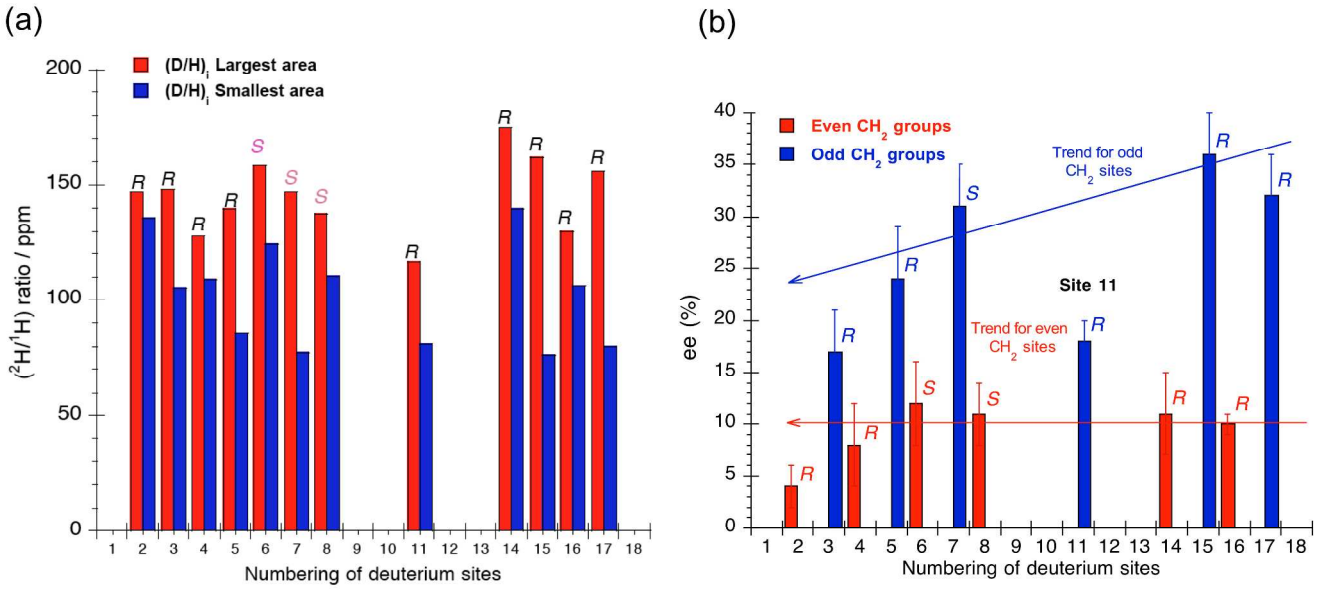

Fig. 36. (a) Variation of (H/H) ratios all along the methylenic groups of ML. (b) Variation of the *eie's*. For each CH_2 site, the absolute configuration of the major enantio-isotopomer is given (in agreement with CIP rules). Figure adapted from ref. 188.

Also the higher *eie* values observed at even sites are compatible with a different normal primary KIE occurring for hydride transfer from the co-factor to the fatty acid chain during reduction steps. Since the *R*-enantiomers (CIP rule applied to stearate) are in excess, hydride transfer to the pro-*S* position is subjected to the stronger primary KIE as

shown previously in the case of methyl linoleate isolated from *F. lateritium* (fungus).[191] As seen here, the first measurements of the *eie* values at natural abundance level of deuterium at all CH_2 groups have provided novel information (unknown so far), concerning the ^2H distribution in enantiotopic position all along a fatty acid chain.

In a second stage, the NAD 2D-NMR in CLC was applied to analyse ω-3 unconjugated FAME such as **MLN** or conjugated **PUFA** such as **MES** or **MPU** (see **Figure 34**). Here the method allowed all important deuterium sites of those molecules to be spectrally discriminated, namely the deuterons located on the ethylenic fragments and the enantiotopic sites at methylene groups located in α-position of double bonds.[42] Such a situation is ideal to analyze and understand the possible changes of ($^2H/^1H$) isotope ratios between the susbtrate **(ML)** and the final products, either the **MLN** or **MES** or **MPU** under the action of Δ^{15}-desaturase or conjugase, respectively.

11.2.2 Prochiral saturated fatty acids. Depending on the type of solutes and strongly of their polarity, the choice of organic co-solvent used to prepare the PBLG ot PCBLL CLC is an important parameter for optimizing both the quality of NAD spectra (linewidth) and the difference of enantiodiscriminations. In case of **ML**, pyridine ($\mu = 2.21$ D) has proved to be a better co-solvent (compared to $CHCl_3$, $\mu = 1.04$ D) to increase the number and the magnitude of enantiodiscriminations at methylene groups,[4] and subsequently, PBLG/pyridine mesophase has been mainly used for investigating SAFA and triglyceride. From a more theoretical viewpoint, it is remarkable that the best spectral discriminations were obtained with mesophases prepared with co-solvents of higher polarity. If the role of co-solvent polarity in the global ordering mechanisms is not fully elucidated yet, the trend observed here shows clearly that intermolecular potentials depend on the dielectric constants of their environment.

Compared to PUFA's, SAFA's are featured by the absence of double bonds, which significantly reduces the ^2H chemical shift dispersion for the central methylene groups

Thus isotropic NAD spectrum of **MS** (see **Figure 37b**) shows a single broad resonance that is the sum of all NAD signals associated to sites 4 to 17. The isotropic SNIF-NMR™ at 14.1 T appears therefore to be of low interest since only 27% of all possible inequivalent ^{2}H sites of **MS** are resolved achiral in a liquid solvent. Unfortunately, the strong pseudo-isochrony of methylene groups, no better resolution of resonance has been obtained even recording the spectrum using a 21 T magnetic field.[185] Additionally, the SAFA's cannot be easily chemically cleaved in smaller fragments, in order to reduce the overlap of ^{2}H signals of CH_2 groups as in cases of PUFA's. Under these circumstances, only the use of non-invasive method such as NAD 2D-NMR in oriented media appears to be the most suitable, simplest analytical solution.

For illustrating the purpose, the series of NAD 1D sub-spectra associated to methylene groups of **MS** dissolved in PBLG/pyridine mesophase is given in **Figure 37c**. The presence of two doublets in place of a single one observed in the ALC (PBG/pyr) indicates that numerous enantiotopic sites are spectrally discriminated. Here, about 80% of ^{2}H sites (expected to be inequivalent in a CLC) are spectrally resolved. Similar results have been obtained for methyl myristate and palmitate, two homoguous derivatives with a shorter alkyl chain. The discrimination is easily visible on extreme methylene sites of the chain, in particular the sites 2 and 3, as well as 16 and 17. As other FAME, difference of intensity (area) between resonances of enantiotopic pairs originates from natural isotope fractionation. A spectacular effect of enrichment/depletion in deuterium at methylene groups 16 and 17 can be noticed. Analogous effects for these two sites can be seen on **ML** (see **Figure 37**), which is successively biosynthetised from **MS** and **MO**. The similarity in isotopic profile at terminal sites can be explained, considering that Δ^9 and then Δ^{12} desaturases should significantly affect the isotopic fractionation of methylene groups reduced by these enzymes. As a consequence, the (^{2}H/^{1}H) ratios for enantiotopic

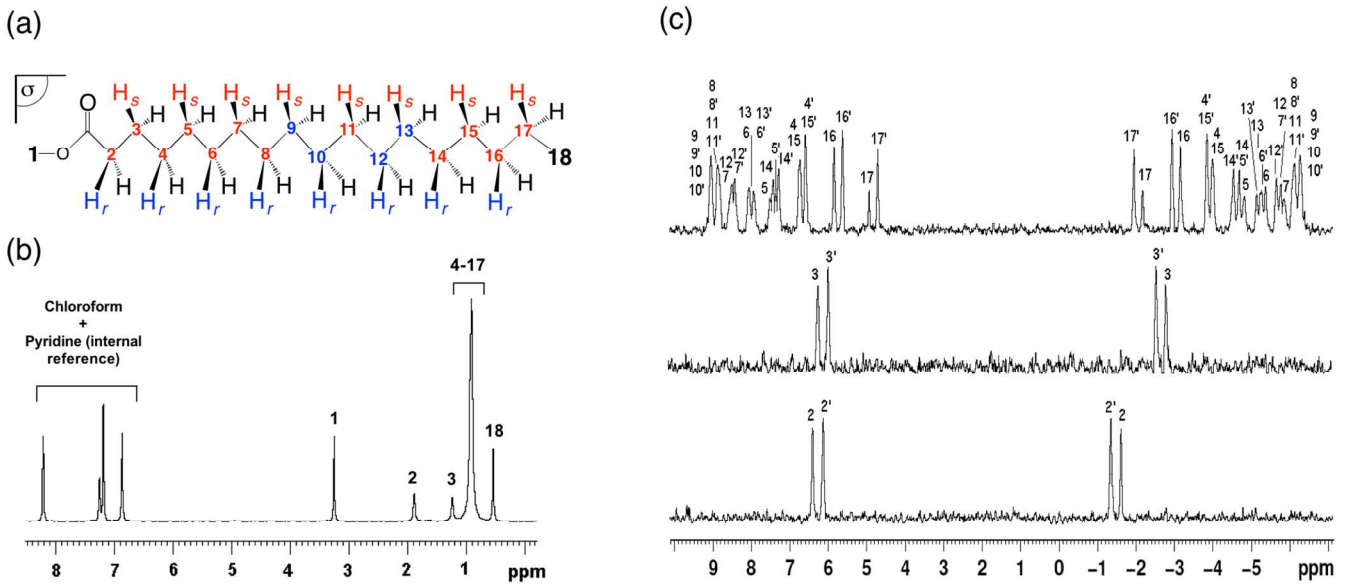

Fig. 37. Structure, atomic numbering and (*r*,*s*)-stereodecriptors (front of the symmetry plane) of **MS**. (b) NAD isotropic SNIF-NMR^{TM} spectrum (92.1 MHz) of **MS** (chloroform with pyridine used as internal reference for quantification). (c) Series of NAD 1D subspectra extracted from the tilted *Q*-COSY Fz map (92.1 MHz) recorded in PBLG/Py. Figure dapted from ref. **185**.

directions in CH_2 groups far from doublet bond is very similar to the ratios measured on the precursors.

Contrary to **ML** or other PUFA's, the assignments of quadrupolar doublets on NAD spectrum of **MS** in CLC is a very challenging task in particular if the analysis only lies on the ^2H chemical shifts. Here the experimental assignment of QDs combining various sources of information (isotope odd/even effect specific to FAME, knowledge gained from the analysis of PUFA, regioselective deutration of **ML**, …) were also supported with a theoretical prediction of RQCs along the chain using new modeling tool, which combines the conformational sampling of solutes with the prediction of their RQCs in an homopolypeptide ALCs.[185] Computational calculations based on a model dominated by steric repulsions between SAFA and the polypeptide (modeled as solid rod-like) were able to well reproduce the experimental trends of RQCs, thus providing new propects to understand the mechanisms for the orientational order of SAFA's.

11.2.3 Analysis of homogeneous triglycerides. The use of NAD 2D-NMR in CLC to potentially investigate the natural isotope fractionation of FAMEs was successively tested on PUFAs and then on C-14 to C-18 SAFAs before to be applied to a much more complex class of lipids: the homogeneous saturated triglycerides (**TG**) with short and long chain such as tributyrin (**TB**) (see **Figure 38**) and trimyristin (**TM**), respectively.[194] Recording anisotropic NAD spectra of **TG** afford the possibility of determining the isotopic profile along the alkyl chain without any transesterification step transforming the triglyceride into glycerol and the corresponding FAME.

According to Altmann's definition,[78] homogeneous, saturated **TG** are flexible molecules of C_s symmetry (*i.e* containing a plane of symmetry, σ) on average, but the various stereochemical relationships between the various hydrogens sites in the triglyceryl part and flexible chains (see **Figure 38a)**. They leads to very complex NAD spectrum that can be only analyzed using QUOSY experiments. As an example **Figure 38c** shows the series of 1D-NMR subspectra extracted from NAD *Q*-COSY Fz map recorded in the CLC (PBLG/Py) that can be compared to isotropic NAD 1D spectrum (see **Figures 38b)**. For **TB**, it has been shown that almost all inequivalent ^{2}H sites (19/20 QDs) are spectrally discriminated in the CLC. The comparision with NMR spectra recorded in the ALC allows a simple assignment of doublets.

For **TB**, the NMR results are fully consistent with the idea that the molecule behaves as a C_s symmetry molecular object on average in the CLC. This behavior is reasonable whether the 3D volumes (corresponding to maximal conformational space) explored by the lateral chains is sufficiently different from that of the central chain ($V_{a/c} \neq V_b$). For **TM**, the deceptively simple NAD spectra suggest that molecule behave as a C_{3v} symmetry molecular object on average, as expected when those volumes of chains are identical ($V_{a/c} = V_b$). This situation illustrates clearly the limits of the efficiency/sensitivity of shape molecular recognition mechanisms of when difference of

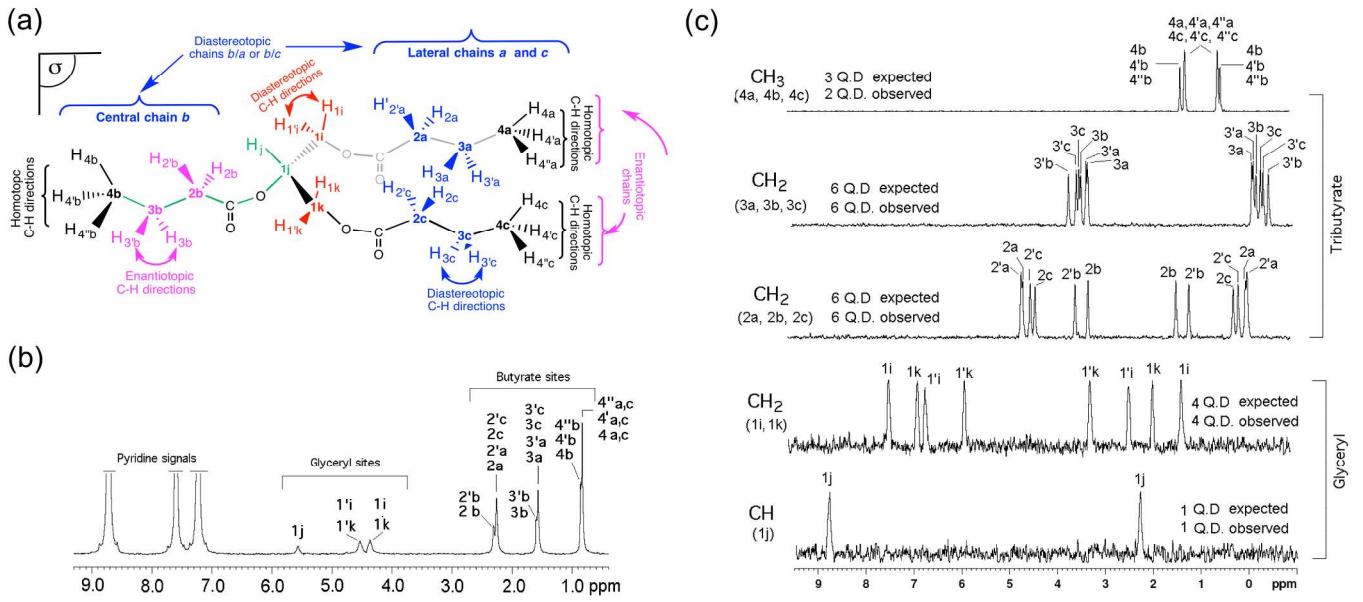

Fig. 38. (a) Atomic numbering and Stereochemical relationships between the various hydrogens sites of the glyceryl part (sites i, j, k) and methylene (2 and 3) and methyl (4) groups in the three hydrocarbon chains (*a*, *b* and *c*) of **TB**. (b) Proton-decoupled NAD 1D-NMR spectrum (92.1 MHz) recorded using quantitative conditions ($T_R = 5T_1$) in pyridine. (c) Series of 1D-NMR subspectra extracted from the tilted NAD Q-COSY Fz map (92.1 MHz) recorded in PBLG/Py. The assignment of QDs relative to diastero- and enantiotopic C-H directions in CH_2 groups is arbitrary. Figure adapted from ref. **194**.

volumes between substituents around a central atom is not enough large to be differenciated.[194]

11.2.4 Tools for biochemical studies. Applying this approach, the origin of hydrogen atoms during fatty acid biosynthesis by the oleaginous fungus *Fusarium lateritium* has been quantified from isotope tracking close to natural abundance.[191] In practice **ML** was isolated from *F. lateritium* grown in natural abundance medium (reference), or in medium slightly enriched with labeled precursors, namely either ^2H_2O, or [6,6-$^2H_2$]glucose or [1-^{2}H]glucose or [2-$^2H_3$]acetate. The analysis ($^2H/^1H$) ratio at each *r*- and *s*-hydrogen position of the CH_2 groups along the chain allowed the isotope redistribution coefficients (a_{ij}) that characterize the specific source of each hydrogen atom to be related to the non-exchangeable hydrogen atoms in glucose and to the medium water. More interestingly, the stereoselectivity which operates during the introduction or removal of hydrogen atoms

along the fatty acid chain was deduced. This study yielded to important results on enzymatic mechanisms: (i) at even CH_2 positions, the *s*-hydrogen comes only from water by protonation while the *r*-hydrogen is introduced partly *via* acetate but principally from water due to "post malonate" exchange; (ii) the non-exchangeable hydrogens of glucose (at least positions 6,6H and 1H) are shown to be introduced to the odd CH_2 positions via the NAD(P)H pool, these cofactors being used by both reductases involved in the elongation steps of the fatty acids chain; (iii) all hydrogens removed at sites 9,10 and 12,13 during desaturation by Δ^9- and Δ^{12}-desaturases are *r* (pro-*R*), and that during both these desaturations, a-secondary kinetic isotope effects occur at the 9 and 12 positions during Δ^9- and Δ^{12}-desaturation respectively.[191]

In a more recent study, NAD 2D-NMR in CLC was applied to probe possible difference in the biosynthesis of vernoleic acid from linoleic acid (see **Figure 28**) in two plants from different families, *Euphorbia lagascae* (Euphorbiaceae) and *Vernonia galamensis* (Asteraceae). In this application work, the relative variations in the site-specific natural distribution of ^2H using was determined to ascertain whether distinct features of the reaction center could be recorded in the $(^2H/^1H)_i$ isotopic ratios of the substrate and product.[195] Although *E. lagascae* and *V. galamensis* use different enzymes to carry out the Δ^{12}-epoxidation of linoleate to vernoleate: a cytochrome P450 monooxygenase in the former and a di-iron dioxygenase in the latter, it was evidenced that the linoleate and vernoleate isolated from the seed oils of the two plants show remarkably similar isotope profiles, with selection against ^2H in the positions around the Δ^{12}-epoxidation site. Such similarity was interpreted as indicating that the dominant feature of the reaction mechanism is the involvement of the activated Fe, while the architecture of the active site is less important.[195]

12. Conclusion and perspectives

NMR using weakly aligning CLC as solvent is a powerful analytical method for the investigation of the enantiotopicity relationships (between nuclei, groups of atoms, directions or faces) in prochiral molecules. In this review we provide to readers the most recent, overview on this topic covering: i) the understanding of the spectral enantiodiscriminations mechanisms both in rigid prochiral molecules and flexible solutes; ii) the analysis of experimental illustrative results for various symmetry groups impacted by the chirality of the mesophase in terms of symmetrical and antisymmetrical matrix decomposition; iii) the presentation of the most pertinent achievements and application of the method proposed to chemists and biochemists.

The sum of successful results summarized in this compendium indicates clearly that NMR in CLC is a unique, general tool currently available to distinguish between signals of enantiotopic elements in prochiral molecules. Compared to isotropic NMR methods, its main analytical advantage lies on the unnecessity of reactive groups in the molecules under investigation, thus covering a wide range of prochiral analytes, from rigid apolar molecules to flexible organic complexes. Conclusively, compared to method involving chiral-selective twisting of the electronic structure of the solute, mechanisms based on orientational ordering of molecules reveals to be much efficient and general from NMR viewpoint.

Among new developments or prospects of NMR in CLC for analyzing prochiral molecules, two important exciting challenges should be accomplished in futur. The first one concerns the possibility to experimentally evidence a possible difference in the concentration of enantiomeric conformers that could exist for flexible prochiral molecules in CLC. Hitherto, the mechanism of enantiodiscrimination proposed postulates a difference of orientational ordering and equal concentration of the interchanging mirror-image isomers. Such a difference could provide new insights on the possible influence of the chiral mesophase on the conformational dynamic of solute.[52]

The second fascinating challenge associated with the analysis of enantiotopic elements in prochiral molecules interacting with CLC is obviously the determination of the absolute configuration of enantiotopic signals observed on anisotropic NMR spectra. Absolute stereochemical descriptor assignments made on the exclusive basis of calculation of ordering matrix elements from anisotropic data, without any others stereochemical information are not possible, and hitherto only empirical approaches based on a comparative strategy has provided a possible solution to this fundamental problem. Actually, the use of computational calculations (molecular dynamics or modeling) based on robust interactional models to mimic the experimental spectra could be the unique way to reach this aim.[196,197,198,199]

Finally, considering the results obtained using NMR in CLC, a conceptual question about the prochirality definition has been re-opened in **Section 8**. Indeed, organic chemists are generally more interested in the chemical reactivity of the compounds rather than its molecular symmetry, contrarily to spectroscopists. Therefore they pay more attention on the precise denomination of functional groups and absolute configuration of (pro)stereogenic centers or bonds generating the chemical reactivity, and subsequently, on the definition of the stereodescriptors associated with these sites of reactivity. As a result, the notion of prochirality is commonly related for the organic chemists to the possibility for a molecule to become chiral (by virtue of isotopic labelling or a single-step organic synthesis), leading as a consequence to the determination within the molecular structure of its enantiotopic elements involved in stereoselective syntheses.

As effective molecular symmetry governs the structure of NMR spectra, spectroscopists from, a different viewpoint, use to start from the notion of (hetero or homo)topicity including enantiotopicity that refers exclusively to symmetry arguments, and is *a priori* defined independently of any organic reactivity clue. As a side effect, topicity evidences allow to finally define if the solute considered is either prochiral or not.

Therefore the possibility to unify the chemistry-based and symmetry-based definitions into a global concept would be an interesting challenge, as both approaches are not fully equivalent. In that process the definition of an adequate stereochemical nomenclature should be primarily addressed in order to open a discussion upon (new) enantiotopicity-based stereodescriptors. Currently, various types of stereodescriptors exist concerning molecules possessing prostereogenic elements[1]: i) pro-*R*/pro-*S* for molecules having (at least) one prostereogenic center; ii) *Re*/*Si* for molecules having prostereogenic faces (both of them being of C_s symmetry); iii) no (clear) notations for C_{2v}, D_{2d} or S_4 symmetry molecules where no prostereogenic faces or sites can be defined whereas enantiotopic sites or directions do exist. In these later cases, quadrants defined within the intersection of the two molecular planes of symmetry, as for **NBD**, or prostereogenic surfaces defined through the rotation-reflection axis, as for **TMCOT**, would probably be more pertinent to stereodescribe the enantiotopic groups of these type of solutes. The unification of all stereodescriptors into a (surprisingly) simple notation such as *R/L (Right/Left)* could simplify the problem and could be matched both with the definition of prochirality used by (organic) chemists concerned by chemical reactivity and spectroscopists looking rather at the symmetry arguments.

13. Abbreviations and notations

- ALC: Achiral Liquid Crystal
- CDCOM: Carbon and Deuterium Correlation in Oriented Medium
- CLC: Chiral Liquid Crystal
- CST: Compressed Sensing Theory
- DNA: Desoxyribo Nucleic Acid
- $\Delta\nu_Q$: Quadrupolar splitting (in Hz)
- *eie*: Enantio-isotopomeric excess
- FT: Fourier Transformation
- FAME: Fatty Acid Methyl Ester
- NAD: Natural Abundance Deuterium
- NASDAC: Natural Abundance Spectroscopy for Deuterium And Carbon

- NMR: Nuclear Magnetic Resonance
- NUS: Non Uniform Sampling
- PAS: Principle Axis System
- PBLG: Poly-γ-Benzyl-*L*-Glutamate
- PBDG: Poly-γ-Benzyl-*D*-Glutamate
- PCBLL: Poly-ε-Carbobenzyloxy-*L*-Lysine
- PELG : Poly-γ-ethyl-*L*-Glutamate
- PUFA : SAturated Fatty Acid
- QD: Quadrupolar Doublet
- QUOSY: QUadrupole Ordered SpectroscopY
- *Q*-COSY: Quadrupolar COrrelation SpectroscopY
- *Q*-COSY Fz: Quadrupolar COrrelation SpectroscopY with z- gradient filter
- SAFA: SAturated Fatty Acid
- RDC: Residual Dipolar Coupling
- RQC: Residual Quadrupolar Coupling
- T_1: Longitudinal relaxation
- T_R: Recycling delay
- V-SMOW: Vienna Standard Means Ocean Water

14. Acknowledgments

P.L. and C.A thanks CNRS for continuous funding and also thanks all other contributors of work reported in this review. Z.L. acknowledges the historic generosity of the Harold Perlman Family to the Weizmann Institute.

15. References and notes

(1) E. E. Eliel and S. H. Wilen in "*Stereochemistry of Organic Compounds*", J. Wiley & Sons, Wiley-Interscience, (1994).
(2) K. Mislow and M. Raban, *Top. Stereochem.,* 1967, **1**, 1-38.
(3) For a highly exhaustive review on the subject (1668 references), see: T. Wenzel in "*Discrimination of Chiral Compounds using NMR Spectroscopy*", John Wiley & Sons, INC publication, Wiley-Interscience, (2007).
(4) W. H. Pirkle and C. W. Boeder, *J. Org. Chem*., 1977, **42**, 3697-3700.
(5) T. J. Wenzel and R. E. Sievers, *Anal. Chem*., 1981, **53**, 393-399.
(6) T. J. Wenzel and R. E. Sievers, *J. Am. Chem. Soc.,* 1982, **104**, 382-388.
(7) W. Offermann, A. Mannschreck, *Org. Magn. Reson.*, 1984, **22**, 355-363.

(8) K. Wypchlo and H. Duddeck, *Tetrahedron: Asymmetry*, 1994, **5**, 27-30.
(9) J. M. Buriak and J. A. Osborn, *Chem. Commun*., 1995, 689-690.
(10) D. Parker, *Chem. Rev*., 1991, **91**, 1441-1457.
(11) To find out more informations, an entire issue of *Chemical Review* (1998, **98**, 1741-2076) was devoted to cyclodextrins. See the articles of: (i) J. Szejtli, *Chem. Rev*., pp**.**1741-1754; (ii) H.-J. Schneider, F. Hacket, V. Rüdiger and H. Ikeda, pp. 1755-1786; (iii) W. Saenger, J. Jacob, K. Gessler, T. Steiner, D. Hoffmann, H.Sanbe, Kyoko Koizumi, S. M. Smith and T. Takaha, pp. 1787-1802.
(12) P. Schreier, A. Bernreuther and M. Huffer in "*Analysis of Chiral Organic Molecules*", Ed. Walter de Gruyter & Co., Berlin, 1995.
(13) R. Rothchild, *Enantiomer*, 2000, **5**, 457-471.
(14) For an overview of the use of chiral platinium(II) complexes, see: G. Uccello-Barretta, R. Bernardini, F. Balzano and P. Salvadori, *Chirality*, 2002, **14**, 484-489.
(15) T. J. Wenzel and C. D. Chisholm, *Prog. in NMR Spectrosc*., 2011, **59**, 1-63.
(16) T. J. Wenzel and C. D. Chisholm, *Chirality*, 2011, **23**, 190-214.
(17) R. Sachin, R. Chaudhari and N. Suryaprakash, *Org. Biomol. Chem.,* 2012, **10**, 6410-6419.
(18) G. Bian, H. Fan, S. Yang, H. Yue, H. Huang, H. Zong and L. Song, *J. Org. Chem.*, 2013, **78**, 9137-9142.
(19) D. Kumari, P. Bandyopadhyay and N.Suryaprakash, *J. Org. Chem*, 2013, **78**, 2373-2378.
(20) J. Labuta, S. Ishihara, T. Šikorský, Z. K Futera, At. Shundo, L. Hanyková, J. V. Burda, K. Ariga and J. P. Hill, *Nature Chemistry*, 2013, **4**, 2188/1-8.
(21) R. R. Fraser, M. A. Petit and M. Miskow, *J. Am. Chem. Soc.,* 1972, **94**, 3253-3254.
(22) R. W. Lang and H. J. Hansen, *Helv. Chem. Acta,* 1979, **62**, 1458-1465.
(23) A. Bilz, T. Stork and G. Helmchen, *Tetrahedron: Asymmetry,* 1997, **8**, 3999-4002.
(24) J. Huskens, R. Goddard and M. T. Reetz, *J. Am. Chem. Soc.,* 1998, **120**, 6617-6618.
(25) E. Sackmann, S. Meiboom and L. C. Snyder, *J. Am. Chem. Soc*., 1968, **90**, 2183-2184.
(26) J. W. Emsley, J. C. Lindon in "*NMR Spectroscopy Using Liquid Crystal Solvents*", Chapter 2, Pergamon press, Oxford, (1975).
(27) R. Y. Dong in "*NMR of Ordered Liquids*", Chapter 16, Kluwer Academic Publishers, Drodrecht, 2003.
(28) M. Sarfati, P. Lesot, D. Merlet and J. Courtieu. *Chem. Commun*. 2000, 2069-2081, and references therein.
(29) E. Lafontaine, J.-P. Bayle and J. Courtieu, *J. Am. Chem. Soc*., 1989, **111**, 8294-8296.
(30) I. Canet, J. Løvshall and J. Courtieu, *Liquid Crystals*, 1994, **16**, 405-412.
(31) K. Czarniecka and E. T. Samulski, *Mol. Cryst. Liq. Cryst*., 1981, **63**, 205-214.

(32) J.-P. Bayle, J. Courtieu, E. Gabetti, A. Loewenstein and J.-M. Péchiné, *New J. Chem*., 1992, **16**, 837-838.
(33) C.-M. Thiele, W. C. Pomerantz, N. L. Abbott and S. H. Gellman, *Chem. Commun.*, 2011, **47**, 502-504.
(34) K. Kobzar, H. Kessler and B. Luy, *Angew. Chem. Int. Ed.*, 2005, **44**, 3145-3147.
(35) C. Naumann and P.W. Kuchel, *Chem. Eur. J.*, 2009, **15**, 12189-12191.
(36) U. Venkateswara Reddy and N. Suryaprakash, *Chem. Commun.*, 2011, **47**, 8364-8366.
(37) N.-C. Meyer, A Krupp, V. Schmidts, C.-M. Thiele and M. Reggelin, *Angew. Chem. Int. Ed.*, 2012, **51**, 8334-8338.
(38) M. Dama and S. Berger, *Tet. Lett.*, 2012, **53**, 6439-6442.
(39) L. Arnold, A. Marx, C.-M. Thiele and Reggelin, *Chem. Eur. J.*, 2010, **16**, 10342-10346.
(40) S. P. Sau and K. V. Ramanathan, *J. Phys. Chem. B*, 2009, **113**, 1530-1532.
(41) P. Lesot, U. Venkateswara Reddy and N. Suryaprakash, *Chem. Commun*. 2011, **47***,* 11736-11738.
(42) P. Lesot, Z. Serhan and I. Billault, *Anal. Bioanal. Chem.*, 2011, **399**, 1187-1200.
(43) C.-M. Thiele, *J. Org. Chem*., 2004, **69**, 7403-7413.
(44) T. Montag and C.-M. Thiele, *Chem. Eur. J.*, 2013, **19**, 2271-2274.
(45) P. Lesot, C. Aroulanda, O. Lafon and R. Dong, *Chem. Eur. J.,* 2008, **14**, 4082-4092.
(46) C. Canlet, D. Merlet, P. Lesot, A. Meddour, A. Loewenstein and J. Courtieu*, Tetrahedron: Asymmetry,* 2000, **11**, 1911-18.
(47) P. Lesot, D. Merlet, Y. Gounelle and J. Courtieu, *J. Phys. Chem. A*., 1995, **99**, 14871-14875.
(48) Lesot, D. Merlet, J. Courtieu, J. W. Emsley, T. T. Rantala and J. Jokisaari. *J. Phys. Chem. A*, 1997, **101**, 5719-5724.
(49) J. W. Emsley, P. Lesot and D. Merlet, *Phys. Chem. Chem. Phys*., 2004, **6**, 522-530, (2004).
(50) D. Merlet, A. Loewenstein, W. Smadja, J. Courtieu and P. Lesot, *J. Am. Chem. Soc*., 1998, **120**, 963-969.
(51) C. Aroulanda, D. Merlet, J. Courtieu and P. Lesot, *J. Am. Chem. Soc*., 2001, **123**, 12059-12066.
(52) J .W. Emsley, P. Lesot, J. Courtieu and D. Merlet, *Phys. Chem. Chem. Phys*., 2004, **6**, 5331-5337.
(53) D. Merlet, J. W. Emsley, P. Lesot and J. Courtieu, *J. Chem. Phys*., 1999, **111**, 6890-6896.
(54) P. Lesot, C. Aroulanda *and Z. Luz, J. Chem. Phys.,* 2009, **131**, 104501/1-16.
(55) In fact, molecules with cubic symmetry often exhibit splitting due to anisotropic vibrational and rotational modes in the axial potential of theliquid crystal. Such effects are ignored in the present paper: J. G. Snijders, C. A. de Lange and E. E.

Burnell, *J. Chem. Phys*., 1983, **79**, 2964-2969.

(56) Note that in the source **Table 3** in ref. **3000,** the entries "Enantiotopic forbidden" and "Enantiotopic allowed" were mistyped as "Enantiomeric forbidden" and "Enantiomeric allowed". In the same ref. in the second equation 26, the term T^{k}_{aa} in the definition of T^{k}(anti) should be changed to 0.

(57) I. Canet, J. Courtieu. A. Loewenstein, A Meddour and J.-M. Péchiné, *J. Am. Chem. Soc*., 1995, **117**, 6520-6526.

(58) P. Lesot, D. Merlet, A. Loewenstein and J. Courtieu, *Tetrahedron: Asymmetry*, 1998, **9**, 1871-1881.

(59) P. Lesot, M. Sarfati and J. Courtieu, *Chem. Eur. J.,* 2003, **9**, 1724-1745.

(60) P. Lesot and J. Courtieu, *Prog. Nucl. Magn. Reson., Spectrosc*., 2009, **55***,* 128-159.

(61) P. Lesot and C. Aroulanda in "*NMR Spectroscopy of Liquid Crystals"*, 1st Print Edition, Ed. R.Y. Dong, World Scientific Publishing Co. Pte. Ltd, Chap. I, pp. 37-78, (2010)

(62) P. Lesot in "*Deuterium NMR of Liquid-crystalline Samples at Natural abundance*" in *Encyclopedia of Magnetic Resonance (eMagRes)*, Vol. 2(3), pp. 315–334, DOI: 10.1002/9780470034590.emrstm1318, Eds R. K. Harris and R. E. Wasylishen, John Wiley & Sons, Chichester. Posted online 15th October **2013**.

(63) In ref. 49, the ratio used was $(\Delta\nu_{Q}^{C\text{-}D^{i}} / {}^{1}D_{C\text{-}H^{i}})$ instead of $(2\Delta\nu_{Q}^{C\text{-}D^{i}} / {}^{1}D_{C\text{-}H^{i}})$. This is dependent of the definition used for $\Delta\nu_{Q}^{i}$.

(64) D. Merlet, B. Ancian, J. Courtieu and P. Lesot, *J. Am. Chem. Soc.*, 1999, **121**, 5249-5258.

(65) O. Lafon, P. Lesot, D. Merlet and J. Courtieu, *J. Magn. Reson.,* 2004, **171**, 135-142.

(66) O. Lafon, P. Lesot, *Chem. Phys. Lett.,* 2005, **404**, 90-94.

(67) P. Lesot, O. Lafon, *Chem. Phys. Lett*., 2008, **458**, 219-222.

(68) D. Merlet, M. Sarfati, B. Ancian, J. Courtieu, P. Lesot, *Phys. Chem. Chem. Phys.,* 2000, **2**, 2283-2290.

(69) P. Lesot, O. Lafon, P. Berdagué, *Magn. Reson. Chem*., 2014, DOI 10.10002/mrc.4110.

(70) P. Lesot, M. Sarfati, D. Merlet, B. Ancian, J. W. Emsley and B. A. Timimi, *J. Am. Chem. Soc.,* 2003, **125**, 7689-7695

(71) O. Lafon, P. Berdagué and P. Lesot, *Phys. Chem. Chem. Phys*., 2004, **6**, 1080-1084.

(72) P. Lesot and O. Lafon, *Anal. Chem.*, 2012, **84**, 4569-4573.

(73) P. E. Hansen, *Ann. Report NMR Spectrosc.* 1983, **15**, 105-231.

(74) A. Meddour. I. Canet, A. Loewenstein. J.-M. Péchiné and J. Courtieu, *J. Am. Chem. Soc*., 1994, **116**, 9652-9656.

(75) D. Merlet, J. W. Emsley, J. Jokisaari and J. Kaski*, Phys. Chem. Chem. Phys*., 2001, **3**, 4918-4925.

(76) C. Aroulanda, P. Lesot, D. Merlet and J. Courtieu, *J. Phys. Chem. A*, 2003, **107**, 10911-10918.

(77) C. Aroulanda, H. Zimmermann, Z. Luz and P. Lesot *J. Chem. Phys*., 2011, **134**, 134502-1/8.
(78) S. I. Altmann, *Proc. Roy. Soc.* A, 1967, **298**, 184-203.
(79) P. Lesot, D. Merlet, M. Sarfati, J. Courtieu, H. Zimmermann and Z. Luz, *J. Am. Chem. Soc.,* **2002**, *124*, 10071-10082.
(80) O. Lafon, P. Lesot, H. Zimmermann, R. Poupko and Z. Luz, *J. Phys. Chem. B,* 2007, **111**, 9453-9467.
(81) P. Lesot, C. Aroulanda, P. Berdagué, H. Zimmerman and Z. Luz, *J. Phys. Chem. B,* 2011*,* **115**, 11793-11804.
(82) H. Zimmermann, R. Poupko and Z. Luz, *Tetrahedron*, 1988, **44**, 277-279.
(83) D.O'Hagan, R. J. M. Goss A. Meddour and J. Courtieu, *J. Am. Chem. Soc.,* 2003, **125**, 379-387
(84) C. A. Fan, B. Ferber, H.B. Kagan, O. Lafon and P. Lesot, *Tetrahedron: Asymmetry*, 2008, **19**, 2666-2677.
(85) M. Sarfati, C. Aroulanda, J. Courtieu and P. Lesot, *Tetrahedron: Asymmetry*, 2001*,* **12**, 737-744.
(86) C. Aroulanda, O. Lafon and P. Lesot, *J. Phys. Chem. B,* 2009, **113***,* 10628-10640.
(87) G. Szalontai, *Magn*. *Reson*. *Chem*., 2000, **38**, 872-876.
(88) D. K. Dalling, D. M Grant and L. F Johnson, *J*. *Am*. *Chem*. *Soc*., 1971, **93**, 3678-3682.
(89) D. K. Dalling, D. M. Grant and E. G Paul, *J*. *Am*. *Chem*. *Soc*., 1973, **95**, 3719-3724.
(90) C. Boeffel, Z. Luz, R. Poupko and H. Zimmermann, *J*. *Am*. *Chem*. *Soc*., 1990, **112**, 7158-7163.
(91) P. Lesot, O. Lafon, H. B. Kagan and C. A. Fan, *Chem. Commun.*, 2006, 389-391.
(92) O. Lafon, P. Lesot, C. A. Fan and H. B. Kagan *Chem. Eur. J.,* 2007, **13**, 3772-3786.
(93) Z. Luz and S. Meiboom, *J. Chem. Phys.,* 1973, **59**, 1077-1092.
(94) F. A. L. Anet, *J. Am. Chem. Soc.,* 1962, **84**, 671-672.
(95) R. Naor and Z. Luz, *J. Chem. Phys*., 1982, **76**, 5662-5664.
(96) F. A. Cotton in "*Chemical Applications of Group Theory*" John Wiley & Sons, New York, 3rd addition, 1990, pp. 58.
(97) C. Avitabile, P. Ganis and V. Petracconi, *J. Phys. Chem*., 1969, **73**, 2378-2381.
(98) P. Ganis, A. Musco and P. A. Temussi, *J. Phys. Chem*., 1969, **73**, 3201-3204.
(99) N. L. Allinger, J. T. Sprague and C. J. Finder, *Tetrahedron*, 1973, **29**, 2519-2523.
(100) N. Tanjdra and A. Bax, *Science,* 1997, **278**, 1111-1114.
(101) M. Blackledge, *Prog. Nucl. Magn. Reson*, 2005, **45**, 24-61.
(102) B. Böttcher and C.-M. Thiele in "*Determining the Stereochemistry of Molecules from Residual Dipolar Couplings (RDCs)*, in Encyclopedia of Magnetic Resonance (*eMagRes*), DOI: 10.1002/9780470034590.emrstm1194. Eds R. K.

Harris and R. E. Wasylishen, John Wiley & Sons, Chichester. Posted online 15th March **2012**.
(103) F. A. L. Anet and A. J. R. Bourn, *J. Am. Chem. Soc*., 1965, **87**, 5250-5251.
(104) K. Wuthrich, *Accounts of Chemical Research*, 1989, **22**, 36-44.
(105) K. Wuthrich, *Angew. Chem. Int. Ed*., 2003, **42**, 3340-3363.
(106) F. Kramer, M. V. Deshmukh, H. Kessler and S. J. Glaser, *Concepts Magn. Reson. Part A,* 2004, *21A*, 10-21.
(107) C. Aroulanda, C. Celebre, G. De Luca, M. Longeri, *J. Phys. Chem. B*, 2006, **110**, 10485-1049.
(108) G. Celebre and M. Longeri, "NMR of Ordered Liquids", pp 305-325, Eds E. E. Burnell and C. A. de Lange, Kluwer Academic Publishers: Dordrecht, Boston, London, 2003, ISBN 1-4020-1343-4.
(109) M. E. Di Pietro, C. Aroulanda, D. Merlet, G. Celebre, G. De Luca, *J. Phys. Chem. B*, 2014, DOI: 10.1021/jp505084g.
(110) G. Celebre, G. De Luca, M. E. Di Pietro, *J. Phys. Chem. B* 2012, **116**, 2876-2885.
(111) G. Celebre, G. De Luca, M. Longeri, *Liq. Cryst.* 2010, **37**, 923-933.
(112) J. W. Emsley, G. R. Luckhurst, C. P. Stockley, *Proc. R. Soc. London, Ser. A,* 1982, **381**, 117-138.
(113) G. Celebre, G. De Luca, J. W. Emsley, E. K. Foord, M. Longeri, F. Lucchesini, G. Pileio, *J. Chem. Phys.* 2003, **118**, 6417-6426.
(114) C.-M. Thiele, A. Marx, R. Berger, J. Fischer, M. Biel and A. Giannis, *Angew. Chem. Int. Ed*., 2006, **45**, 4455-4460.
(115) V. Schmidts, M. Fredersdorf, T. Lübken, A. Porzel, N. Arnold, L. Wessjohann, C.-M. Thiele, *J. Nat. Prod*., 2013, **76**, 839-844.
(116) C.-M. Thiele, A. Maliniak, B. Stevensson, *J. Am. Chem. Soc.,* 2009, **131**, 12878-12879.
(117) R. R. Gil, *Angew. Chem. Int. Ed.*, 2011, **50**, 7222-7224.
(118) P. Trigo-Mourino, R. Sifuentes, A. Navarro-Vazquez, C. Gayathri, H. Maruenda and R. R. Gil, *Nat. Prod. Commun*., 2012, **7**, 735-738.
(119) B. Luy, A. Frank and H. Kessler, in "*Molecular Drug Properties: Measurement and Prediction*", Ed. R. Mannhold, Volume 37 of Methods and Principles in Medicinal Chemistry (Eds. R. Mannhold, H. Kubinyi, G. Volkers), pp. 207-254, (2008).
(120) G. Kummerlöwe and B. Luy, *Trends Anal. Chem*., 2009, **28**, 483-493.
(121) G. Kummerlöwe, B. Luy, *Annu. Rep. NMR Spectrosc,*. 2009, **68**, 193-232.
(122) B. Luy, A. Frank, H. Kessler in "*Conformational Analysis of Drugs by NMR Spectroscopy*", in "*Molecular Drug Properties: Measurement and Prediction*", Ed. R. Mannhold, volume 37 of Methods and Principles in Medicinal Chemistry, Eds. R. Mannhold, H. Kubinyi, G. Volkers, pp. 207-254, (2008).

(123) P. Trigo-Mourino, M. Carmen de la Fuente, R. R. Gil, V. M. Sanchez-Pedregal, and A. Navarro-Vazquez, *Chem. Eur. J*., 2013, **19**, 14989-14997.
(124) G. Kummerlöwe and B. Luy, *Annu. Rep. NMR Spectrosc*., 2009, **68**, 193-232.
(125) C. Aroulanda, V. Boucard, E. Guibé, J. Courtieu and D. Merlet, *Chem Eur. J*., 2003, **18**, 4536-4539.
(126) U. M. Reinscheid, M. Köck, C. Cychon, V. Schmidts, C.-M. Thiele and C. Griesinger, *Eur. J. Org. Chem.*, 2010, 6900-6903.
(127) M. Schmidt, H. Sun, P. Rogne, G. K. E. Scrib, C. Griesinger, L. T. Kuhn and U. M Reinscheid, *J. Am. Chem. Soc.,* 2012, **134**, 3080-3083.
(128) J. D. Snider, E. Troche-Pesqueira, S. R. Woodruff, C. Gayathri, N. V. Tsarevsky and R. R. Gil, *Magn. Reson. Chem*., 2012, **50**, S86-S91.
(129) A. Enthart, J. C. Freudenberger, J. Furrer, H. Kessler and B. Luy, *J. Magn. Reson.,* 2008, **192**, 314-322.
(130) T. Reinsperger and B. Luy, *J. Magn. Reson.,* 2014, **239**, 110-120.
(131) J. Farjon, D. Merlet, P. Lesot and J. Courtieu, *J. Magn. Reson.*, 2002, **158**, 169-172.
(132) M. E Di Pietro, C. Aroulanda and D. Merlet, *J. Magn. Reson.,* 2013, **234**, 101-105.
(133) P. Lesot, D. Merlet, A. Meddour, A. Loewenstein and J. Courtieu, *J. Chem. Soc.*, *Faraday Trans*., 1995, **91**, 1371-1375.
(134) J. Farjon, J.-P. Baltaze, P. Lesot, D. Merlet and J. Courtieu, *Magn. Res. Chem.*, 2004, **42**, 594-599.
(135) N. Nath, Nilamoni, B. Baishya, N. Suryaprakash, *J. Magn Reson.*, 2009, **200**, 101-108.
(136) U. R. Prabhu, S. R Chaudhari and N. Suryaprakash, *Chem. Phys. Lett.*, 2010, **500**, 334-341.
(137) S. Fujita, *J. Am. Chem. Soc*., 1990, **112**, 3390-3397.
(138) S. Fujita, *Tetrahedron,* 1991, **47**, 31-46.
(139) S. Fujita, *Tetrahedron,* 2000, **56**, 735-740.
(140) R. Berger, J. Courtieu, R.R. Gil, C. Griesinger, M. Köck, P. Lesot, B. Luy, D. Merlet, A. Navarro-Vazquez, M. Reggelin and U.M. Reinscheid, *Angew. Chemie, Int. Ed.,* 2012*,* **51**, 2-5.
(141) P. Lesot, O. Lafon, J. Courtieu and P. Berdagué, *Chem. Eur. J.,* 2004, **10**, 3741-3746.
(142) P. E. Hansen, *Prog. in NMR Spectrosc.*, 1988, **20**, 207-257.
(143) S. Berger in "*Isotope Effects in NMR Spectroscopy", NMR Basic Principles and Progress"*, 1990, **22**, 1-29, Springer-Verlag, Berlin.
(144) R. H. Newman-Evans, R. J. Simon and B. K. Carpenter, *J. Org. Chem.*, 1990, **55**, 695-711.
(145) L. Ziani, P. Lesot, A. Meddour and J. Courtieu, *Chem. Commun.*, 2007, 4737-4739.
(146) A. G. Kummerloewe and B. Luy, *Trends Anal. Chem.*, 2009, **28**, 483-493.

(147) N.-C. Meyer, A. Krupp, V. Schmidts, C. M. Thiele and M. Reggelin, *Angew. Chem. Int. Ed*., 2012, **51**, 8334-8338.
(148) G. Kummerlöwe, E. F. McCord, S. F. Cheatham, S. Niss, R.W. Schnell and B. Luy, *Chem. Eur. J*., 2010, **16**, 7087-7089.
(149) S. S. D. Büchler, G. Kummerlöwe and B. Luy, *Int. J. Artif. Organs*, 2011, **34**, 134-138.
(150) C. Merle, G. Kummerloewe, J. C. Freudenberger, F. Halbach, W. Stoewer, Wolfgang, C.L. von Gostomski, C. Lierse, J. Hoepfner, T. Beskers, M. Wilhelm and B. Luy, *Angew. Chem. Int. Ed*., 2013, **52**, 10309-10312.
(151) C. Aroulanda, M. Sarfati, J. Courtieu and P. Lesot, *Enantiomer*, 2001, **6**, 281-287.
(152) T. Montag and C.-M. Thiele, *Chem. Eur. J.*, 2013, **19**, 2271-2274.
(153) M. A. Böttcher and C.-M. Thiele, *Chem. Eur. J.*, 2010, **16**, 1656-1663.
(154) C.-S. Cho, J.W. Nah, Y.I. Jeong, J.-B. Cheon, S. Asayma, H. Ise and T. Akaike, *Polymer*, 1999, **40**, 6769-6775.
(155) T. E. Strzelecka and R. L. Rill, *J. Am. Chem. Soc.,* 1987, **109**, 4513-4518.
(156) R. Brandes and D. R. Kearns, *Biochemistry,* 1986, **25**, 5890-5885.
(157) S. M. Douglas, J. J. Chou and W.M. Shih*, PNAS,* 2007*,* **104**, 6644-6648.
(158) M. Chan-Huot, P. Lesot, P. Pelupessy, L. Duma, G. Bodenhausen, P. Duchambon, M. D. Toney, U. V. Reddy and N. Suryaprakash, *Anal. Chem.,* 2013, **85**, 4694-4697.
(159) S. Protti, A. Mezzetti, J.-P. Cornard, C. Lapouge and M. Fagnoni, *Chem. Phys. Lett*., 2008, **467**, 88-93.
(160) P. W. Kuchel, B. E. Chapman, N. Mueller, W. A. Bubb, D. J. Philp and A. M. Torres, *J. Magn. Reson.*, 2006, **180**, 256-265.
(161) U. Eliav and G. Navon, *J. Am. Chem. Soc.*, 2006, **128**, 15956-15957.
(162) G. Kummerlöwe, M. Udaya Kiran, B. Luy, *Chem. Eur. J.,* 2009, **15**, 12192-12195.
(163) C. Naumann, W.A. Bubb, B.E. Chapman, P.W. Kuchel, *J. Am. Chem. Soc*., 2007, **129**, 5340-5341.
(164) A. Solgadi, A. Meddour and J. Courtieu, *Tetrahedron: Asymmetry*, 2004, **15**, 315-1318.
(165) J.-L. Canet, A. Fadel, J. Salaün, I. Canet-Fresse and J. Courtieu, *Tetrahedron Asymmetry*, 1993, **4**, 31-34.
(166) I. Canet, A. Meddour, J. Courtieu, J.-L. Canet and J. Salaün, J., *J. Am. Chem. Soc.*, 1994, **116**, 2155-2156.
(167) A. Martine, A. Meddour, J.-C. Fiaud and J.-Y. Legros, *Tetrahedron: Asymmetry*, 2010, **21** 1701-1708.
(168) H. David, C. Afonso, M. Bonin, G. Doisneau, M.-G. Guillerez and F. Guibé, *Tetrahedron Lett*., 1999, **40**, 8557-8561.
(169) H. Villar, F. Guibé, C. Aroulanda and P. Lesot, *Tetrahedron: Asymmetry*, 2002, **13**, 1465-1475.

(170) K. Benali, O. Lafon, H. Zimmermann, E. Guittet and P. Lesot, *J. Magn. Reson.,* 2005*,* **187**, 205-215.
(171) O. Lafon and P. Lesot, *J. Magn. Reson*., 2005, **174**, 254-264.
(172) G. J. Martin and M. Martin, *Tet. Lett.*, 1981, **22**, 3525-3528.
(173) S. Kellya, K. Heaton and Hoogewerff, *Trends in Food Science & Technology* 2005, **16**, 555–567.
(174) B. Behrouzian and P. H. Buist, *Phytochem. Rev.,* 2003, **2**, 103-111.
(175) G. Martin, B.-L. Zhang, N. Naulet and M. Martin, *J. Am. Chem. Soc.*, 1986, **108**, 5116-5122.
(176) C.W. Hsieh, P.H. Li, Po-Hsien, J.-Y. Cheng and J.-T. Ma, *Ind. Crops & Prod.,* 2013, **50**, 904-908.
(177) A. Gregrova, H. Cizkova, J. Mazac and M. Voldrich, *J. of Food & Nutr. Res*., 2012, **51**, 123-131.
(178) G. S. Remaud, Y. L. Martin, G. G. Martin and G. J. Martin, *J. of Agr & Food Chem*., 1997, **45**, 859-866.
(179) J. Kidric, *Ann. Rep. NMR Spectrosc*., 2008, **64,** 161-171.
(180) P. Lesot, C. Aroulanda and I. Billault, *Anal. Chem.*, 2004*,* **76**, 2827-2835.
(181) P. Lesot, V. Baillif and I. Billault, *Anal. Chem.*, 2008, **80**, 2963-2972.
(182) H. Kovacs, D. Moskau and M. Spraul, *Prog. Nucl. Magn. Reson. Spectrosc*., 2005, **46**, 131-155.
(183) O. Lafon, B. Hu, J.-P. Amoureux and P. Lesot, *Chem. Eur. J.*, 2011, **17**, 6716–6724.
(184) K. Kazimierczuk, O. Lafon and P. Lesot, *Analyst,* 2014, **139**, 2702-2713.
(185) Z. Serhan, I. Billault, A. Borgogno, A. Ferrarini and P. Lesot, *Chem. Eur. J.,* 2012, **18**, 117-126.
(186) P. H. Buist, *Tetrahedron: Asymmetry,* 2004, **15**, 2779-2785.
(187) D. W. Reed, C. K. Savile, X. Qiu, P. H. Buist, and P. S. Covello, *Eur. J. Biochem.,* 2002, **269**, 5024-5023.
(188) Z. Serhan, L. Martel, I. Billault and P. Lesot, *Chem. Commun.,* 2010, **46**, 6599-6601.
(189) I. Billault, S. Guiet, F. Mabon and R. J. Robins, *ChemBioChem,* 2001, **2**, 425-431.
(190) V. Baillif, R. J. Robins, I. Billault and P. Lesot, *J. Am. Chem. Soc*. 2006, **128**, 11180-11187.
(191) V. Baillif, R. J. Robins, S. Le Feunten, P. Lesot and I. Billault, *J. Biol. Chem.*, 2009, **284**, 10783-10792.
(192) P. Buist and B. Behrouzian, *J. Am. Chem. Soc.*, 1998, **120**, 871-876.
(193) B. Behrouzian, P. Buist and J. Shanklin, *Chem. Commun*., 2001, **5**, 401-402.
(194) P. Lesot, Z. Serhan, C. Aroulanda and I. Billault, *Magn. Reson. Chem.*, 2012, **50**, S2-S11*,* and corrigendum, idem, 2013, **51**, 444-445.
(195) I. Billault, A. Ledru, M. Ouetrani, Z. Serhan, P. Lesot and R. J. Robins, *Anal. Bioanal. Chem.*, 2012, **402**, 2985-2998.

(196) E. Elvira, J. Breton, J. Plata and C. Girardet, *J. Chem. Phys*., 1991, **155**, 7-18.
(197) J. Helfrich, R. Hentschke and U. M. Apel, *Macromolecules*, 1994, **27**, 472-482.
(198) G. Celebre, *J. Chem*. *Phys*., 2001, **115**, 9552-9556.
(199) J. Helfrich and R. Hentschke, *Macromolecules*, 1995, **28**, 3831-3841.

Tables

Table 1. Definition of the various terms of the spin Hamiltonian in **Eqs. 1** and **2**.[a]

H^k	H_i^Z	H_i^σ	H_{ij}^J	H_{ij}^D	H_i^Q
Type of interaction	Zeeman[c] energy	Electronic[c] shielding	Indirect (scalar) coupling	Direct (dipolar) coupling	Quadrupolar coupling
A^k	$(0, 0, B_0)$	$(0, 0, B_0)$	(I_{iX}, I_{iY}, I_{iZ})	(I_{iX}, I_{iY}, I_{iZ})	(I_{iX}, I_{iY}, I_{iZ})
B^k	(I_{iX}, I_{iY}, I_{iZ})	(I_{iX}, I_{iY}, I_{iZ})	(I_{jX}, I_{jY}, I_{jZ})	(I_{jX}, I_{jY}, I_{jZ})	(I_{iX}, I_{iY}, I_{iZ})
l^k	$-\gamma_i h = -\nu_{0i}/B_0$	$\gamma_i h \sigma_i^{iso} = \nu_{0i} \sigma_i^{iso}/B_0$	J_{ij}^{iso}	0	0
$T_{zz}^{k\,b}$	0	$\gamma_i h \sigma_{izz} = \nu_{0i} \sigma_{izz}/B_0$	J_{ijzz}	$-\gamma_i \gamma_j h/4\pi^2 r_{ij}^3$	$eQ_iV_{izz}/[2hI_i(2I_i\text{-}1)] = K_{C\text{-}Di}/2$

[a] Upper cases X, Y, Z are the laboratory-fixed axes with $Z \parallel B_0$. Lower cases x, y, z, refer to the principal axes of the corresponding k-tensor.

[b] The zz components (in Hz) of T^k in the principal coordinate system of H^k.

[c] The chemical shift Hamiltonian, H_i^{cs}, is defined as $H_i^{cs} = H_i^Z + H_i^\sigma$.

Table 2. The high-field equations for the various magnetic interactions in a solute dissolved in a nematic liquid crystal.[a]

k	H^k(iso)	H^k(aniso)
σ	$\nu_{0i}\sigma_i^{iso}I_{iZ}$	$\nu_{0i}\Delta\sigma_i I_{iZ}$
		$\Delta\sigma_i = \sigma_{i,aa}S_{aa}+\frac{1}{3}(\sigma_{i,bb}-\sigma_{i,cc})(S_{bb}-S_{cc})+ 4/3(\sigma_{i,ab}S_{ab} + \sigma_{i,ac}S_{ac} + \sigma_{i,bc}S_{bc})$
J	$j^{iso}_{ij}[I_{iZ}I_{jZ}$ $(I_{i+}I_{j-} + I_{i-}I_{j+})]\frac{1}{2}$ +	$-\Delta J_{ij}[I_{iZ}I_{jZ} -\frac{1}{4}(I_{i+}I_{j-} + I_{i-}I_{j+})]$ [a] $\Delta J_{ij} = J_{ij,aa}S_{aa} + \frac{1}{3}(J_{ij,bb}- j_{ij,cc})(S_{bb}-S_{cc})+ 4/3(J_{ij,ab}S_{ab} + J_{ij,ac}S_{ac} + J_{ij,bc}S_{bc})$
D	0	$-2D_{ij}[I_{iZ}I_{jZ} - \frac{1}{4}(I_{i+}I_{j-} + I_{i-}I_{j+})]$ [a]
		$D_{ij} = -(K_{ij}/r_{ij}^3)[\frac{1}{2}(3\cos^2\theta_{ij}^a - 1)S_{aa}+\frac{1}{2}(\cos^2\theta_{ij}^b - \cos^2\theta_{ij}^c)(S_{bb}-S_{cc})$ $+ 2(\cos\theta_{ij}^a\cos\theta_{ij}^b\ S_{ab} + \cos\theta_{ij}^a\cos\theta_{ij}^c\ S_{ac} + \cos\theta_{ij}^b\cos\theta_{ij}^c\ S_{bc})]$ [b]
Q	0	$\Delta\nu_Q^i[I_{iZ}^2 - I_i(I_i+1)/3]$
		$\Delta\nu_Q^i = q_{i,aa}S_{aa} + \frac{1}{3}(q_{i,bb}-q_{i,cc})(S_{bb}-S_{cc})$ $+ 4/3(q_{i,ab}S_{ab} + q_{i,ac}S_{ac} + q_{i,bc}S_{bc})]$ [c]

[a] The operator $(I_{i+}I_{j-} + I_{i-}I_{j+})$ applies to homonuclei i, j, pairs and can be deleted for heteronuclei pairs.

[b] $K_{ij} = \gamma_i\gamma_j h/4\pi^2$; θ_{ij}^{α} is the angle between the internuclear direction, r_{ij}, and the molecular frame axis α.

[c] $q_{i,zz} = \frac{3}{4}QCC_i$, where QCC = $eV_{zz}Q$ is the quadrupolar coupling constant along the main principal axis, z, of the interaction. For deuterons in C-D bonds, the QCC's are assumed to be axially symmetric are approximately 175 kHz and 185 kHz for sp^3 and sp^2 types of bonds, respectively.

Table 3. Characteristics of the Saupe ordering matrix and of the magnetic interactions for molecules with non-cubic improper symmetries.[a]

	Enantiotopic "forbidden"					**Enantiotopic "allowed"**			
	Axial		**Non axial**						
Improper group	C_{nh} C_{nv},S_{2n} n ≥ 3	D_{nh} D_{nd} n ≥ 3	C_i	C_{2h}	D_{2h}	C_s	C_{2v}	D_{2d}	S_4
No. of $S_{\alpha\beta}$ in $S_{\alpha\beta}$(sym)	1	1	5	3	2	3	2	1	1
$S_{\alpha\beta}$(sym)	S_{aa}	S_{aa}	S_{aa} S_{bb-cc} S_{ab} S_{ac} S_{bc}	S_{aa} S_{bb-cc} S_{bc}	S_{aa}, S_{bb-cc}	S_{aa} S_{bb-cc} S_{bc}	S_{aa} S_{bb-cc}	S_{aa}	S_{aa}
Proper subgroup	C_n	D_n	C_1	C_2	D_2	C_1	C_2	D_2	C_2
No. of $S_{\alpha\beta}$ in subgroup	1	1	5	3	2	5	3	2	3
$S_{\alpha\beta}$(anti)	0	0	0	0	0	S_{ab} S_{ac}	S_{bc}	S_{bb-cc}	S_{bb-cc} S_{bc}
$T^{r,s}_{\alpha\beta}$**(anti)**[b] **Enantiotopic**	0	0	0	0	0	$T^r_{ab} = -T^s_{ab}$ $T^r_{ac} = -T^s_{ac}$	$T^r_{bc} = -T^s_{bc}$	$T^r_{bb-cc} = -T^s_{bb-cc}$	$T^r_{bb-cc} = -T^s_{bb-cc}$ $T^r_{bc} = -T^s_{bc}$
$T^{h}_{\alpha\beta}$**(anti)**[c] **Homotopic**	0	0	0	0	0	$T^h_{ab} = 0$ $T^h_{ac} = 0$	$T^h_{bc} = 0$	$T^h_{bb-cc} = 0$	$T^h_{bb-cc} = 0$ $T^h_{bc} = 0$

[a] Definitions: S(sym) = S^{ALC}, namely the ordering matrix of the solute in ALC; S^{CLC}: the ordering matrix of the solute in CLC; S(anti) = $S^{CLC} - S^{ALC}$; For shortening notation, we use $S_{bb-cc} = S_{bb} - S_{cc}$ and $T_{bb-cc} = T_{bb} - T_{cc}$.

[b] Symmetry relations between elements of the antisymmetric magnetic interaction tensor, T^k, belonging to enantiotopic pairs, *r*, *s*.

[c] Symmetry properties between elements of the antisymmetric magnetic interaction tensor, T^k, belonging to homotopic pairs, h, or to diastereotopic sites. Note that in the source Table III in ref. **54**, the entries "Enantiotopic forbidden" and "Enantiotopic allowed" were mistyped as "Enantiomeric forbidden" and "Enantiomeric allowed". In the same ref. in the second Eq. 26, the term T^k_{aa} should be changed to 0.

Table 4. Calculated peak position and intensities of the A spin for AX_2 and AXX' spin systems (I_A, I_X = ½).[a,b]

Lines description	Line position in AX_2	Line intensity in AX_2	Line position in AXX'	Line intensity in AXX'
Central peak	ν_0	2	ν_0	~2
Inner doublet	$\nu_0 \pm 2D_{C\text{-}H}$	1	$\sim\nu_0 \pm (D_{C\text{-}H} + D_{C\text{-}H'})$	~1
Outer doublet	-	-	$\sim\nu_0 \pm ({}^2J_{H\text{-}H'} - D_{H\text{-}H'})$	$\sim(D_{C\text{-}H} - D_{C\text{-}H'})^2/({}^2J_{H\text{-}H'} - D_{H\text{-}H'})^2$

[a] Neglecting $^2J_{AX}$

[b] Assuming $(D_{AX} - D_{AX'})^2 << ({}^2J_{XX'} - D_{XX'})^2$ and calculated by 2nd order perturbation theory.

End of the article